Progress in Polymer Science 81 (2018) 80–113

Contents lists available at ScienceDirect

Progress in Polymer Science

journal homepage: www.elsevier.com/locate/ppolysci

From nano to micro to macro: Electrospun hierarchically structured polymeric fibers for biomedical applications

Guang Yang[a,b], Xilin Li[a], Yang He[a], Junkai Ma[a], Guoli Ni[a], Shaobing Zhou[a,*]

[a] School of Materials Science and Engineering, Key Laboratory of Advanced Technologies of Material, Minister of Education, Southwest Jiaotong University, Chengdu 610031, Sichuan, PR China
[b] College of Medicine, Southwest Jiaotong University, Chengdu 610031, Sichuan, PR China

ARTICLE INFO

Article history:
Received 13 January 2017
Received in revised form 16 October 2017
Accepted 28 December 2017
Available online 30 December 2017

Keywords:
Hierarchical structures
Biomaterials
Drug delivery
Tissue engineering
Electrospinning
Three-dimension

ABSTRACT

Hierarchically structured polymer fibers encompassing 1-D, 2-D, and 3-D structures with at least one dimension nano- to micro-meters in size have recently received an increasing amount of attention due to their vast potential in such applications as sensing, medicine, energy storage. This review summarizes advancements in the last ten years in the design and fabrication of hierarchically structured polymer fibers *via* electrospinning technologies, including a diversity of electrospinning devices and electrospinning parameters using various polymers. These well-defined, multilevel structures enable the fibers to be used more effectively in applications in the biomedical field, such as drug delivery, tissue engineering, and diagnostics. This review can provide a better understanding of the relationships between the structure and functionality of polymer fibers for further biomedical applications.

© 2017 Elsevier B.V. All rights reserved.

Contents

1. Introduction 81
2. Electrospinning process and available biomaterials 81
   2.1. Process and parameters 81
   2.2. Available biomaterials 83
   2.3. Developments 83
3. Structural diversity of electrospun fibers 85
   3.1. Structural diversity of individual electrospun fibers 85
      3.1.1. Core-shell fibers 85
      3.1.2. Beaded fibers 85
      3.1.3. Porous fibers 89
      3.1.4. Ribbon fibers 89
      3.1.5. Other fibers 89
   3.2. Structural diversity of electrospun fiber mats 90

Abbreviations: 0-D, zero dimensional; 1-D, one dimensional; 2-D, two dimensional; 3-D, three dimensional; anti-EpCAM, anti-epithelial cell adhesion molecule; bFGF, basic fibroblast growth factor; BSHFs, bead-on-string heterostructured fibers; CFU, Colony-Forming Units; CTCs, circulating tumor cells; DC, direct current; DCM, Dichloromethane; DEPA, delivery system on an electrospun pillar array; DGNs, dextran glassy nanoparticles; DMAc, Dimethylacetamide; DMF, N,N-Dimethylformamide; DMNs, dissolving microneedles; DRG, primary dorsal root ganglia; ECs, endothelial cells; FDM, fast-dissolving drug delivery membrane; HFIP, Hexafluoroisopropanol; IBU, ibuprofen; MWCNTs, multi-walled carbon nanotubes; PAA, poly(acrylic acid); PCL, Poly(ε-caprolactone); PDMS, poly (dimethylsiloxane); PE, polyethylene; PEG-PCL, poly(ethylene glycol)-poly(ε-caprolactone); PEI, poly(ether imide); PELA, poly(ethylene glycol)-co-poly(d,l-lactide); PEO, polyethylene oxide; PGA, poly(glycolic acid); PIPAAm, poly(N−isopropylacrylamide); PLA, poly(lactic acid); PLGA, poly(lactic-co-glycolic acid); PLLA, poly-L-lactic acid; PS, polystyrene; PS-PSMA, polystyrene-poly(styrene-co-maleic anhydride); PSNs, polystyrene nanoparticles; PU, polyurethane; PVA, polyvinyl alcohol; PVAc, polyvinyl acetate; PVD, physical vapor deposition; PVP, polyvinyl pyrrolidone; rBMSCs, rat bone marrow mesenchymal stem cells; TBT, titanium butoxide; TFE, Trifluoroethanol; THF, Tetrahydrofuran; WBC, white blood cell.

* Corresponding author.
E-mail address: shaobingzhou@swjtu.cn (S. Zhou).

https://doi.org/10.1016/j.progpolymsci.2017.12.003
0079-6700/© 2017 Elsevier B.V. All rights reserved.

3.2.1. Random fibers ... 90
3.2.2. Aligned fibers ... 90
3.2.3. Nanofiber yarns ... 90
3.2.4. Patterned fibers ... 90
3.2.5. 3-D nanofibrous macrostructures ... 91
4. Biomedical applications of electrospun polymeric fibers ... 92
4.1. Drug delivery ... 92
4.1.1. Controlled release mechanism of electrospun fibers ... 92
4.1.2. Oral drug delivery ... 96
4.1.3. Transdermal drug delivery ... 96
4.1.4. Implantable drug delivery systems ... 97
4.2. Tissue engineering and regenerative medicine ... 101
4.2.1. Wound dressing ... 101
4.2.2. Vascular tissue engineering ... 102
4.2.3. Muscle tissue engineering ... 103
4.2.4. Neural tissue engineering ... 103
4.2.5. Bone tissue engineering ... 104
4.2.6. Other applications ... 104
4.3. Diagnostics ... 104
4.3.1. Humoral diagnosis of cancer ... 104
4.3.2. Diagnostics for other diseases ... 105
4.4. Other applications in medicine ... 105
4.4.1. Mimicking the tumor microenvironment ... 105
4.4.2. Immobilization of enzyme ... 106
4.4.3. Protection and filtration ... 107
5. Conclusions and future challenges ... 107
Acknowledgments ... 107
References ... 107

1. Introduction

Hierarchically complex structures are observed in many biological systems [1–4], and these structures impart diverse functionalities to organisms, such as nanoscale viruses, microscale cells, and macroscale tissues. For example, bone tissues possess an unusal combination of remarkable strength and toughness, attributed to their precisely organized hierarchical structures: nanometer-sized hydroxyapatite crystals periodically deposit within the gap zones of collagen fibrils, leading to excellent nanomechanical heterogeneities and enabling a mechanism for high energy dissipation and resistance to fracture [3]. So far, various hierarchical structures (*e.g.,* zero dimensional (0-D) particles [5,6], one dimensional (1-D) fibers [7], two dimensional (2-D) substrates [8–10] and three dimensional (3-D) scaffolds [11]) have been developed for biomedicine and other applications. Among these structures, hierarchically structured fibers with diameters ranging from nano- to micrometers as well as wires and tubes, can be used as building blocks to assemble 1-D to 3-D structures. These hierarchically structured fibers represent an important category and have attracted a great deal of attention in the biomedical field and other scientific research fields (*e.g.,* electronics [12], optics [13], sensors [13,14], catalysis [15],energy storage [16–18], oil/water separation [19], and air filtration [20,21]), because they possess a larger specific area and additional heterogeneous interfaces, which may play an important role in enhancing the nanosize effect [22]. Numerous approaches have been developed for fabricating 1-D fibers in recent years [23–27]. However, very few review articles have specifically reported the progress in electrospun polymeric fibers with a hierarchical structure from 1-D to 2-D to 3-D and with fiber diameters from nano- to mico-meters.

In this review, we provide a comprehensive overview of recent research regarding the design and fabrication of electrospun hierarchically structured polymer fibers for biomedical applications including drug delivery, tissue engineering, diagnostics and others, as shown in Fig. 1. Electrospinning is a facile and multifunctional technique used to produce ultrafine, continuous fibers with controllable diameters in the range of nanometers to micrometers, from either organic or inorganic materials [28–31]. These electrospun fibers, possessing a large specific surface area, a high aspect ratio, a high porosity, a controllable small pore size and the ability to resemble an extracellular matrix's architecture, are widely used in a variety of fields, including filtration and adsorption, sensing, self-cleaning, catalysis, food engineering, nanofiber-reinforced composites, optoelectronics, energy storage and biomedical applications [22,32,33]. The electrospinning technique may be considered to be a variant of the electrospraying process [34,35], both of which use a high voltage to form a liquid jet. In the past ten years, various electrospun fibers with precisely controlled fiber morphology, diameter, and arrangement have been successfully obtained through tuning of the electrospinning parameters, which has broadened the application of electrospun fibers into the biomedical field. The aim of this review is to provide the 'state-of-the-art' and current guidelines in preparation of different structured electrospun polymeric fibers for the purpose of biomedical applications, including drug delivery, tissue engineering and regenerative medicine, diagnostics and other applications in medicine.

2. Electrospinning process and available biomaterials

2.1. Process and parameters

A typical setup for electrospinning is composed of several basic parts: a high voltage (usually direct current (DC)) power supplier, a spinneret (usually a stainless needle with a solution container), a syringe pump, and a grounded collector (usually aluminum foil). The spinneret, which contains the spinning solution or melt, is connected to one electrode of the high voltage power supplier and the grounded collector is placed directly below the outlet of the spinneret, located at a proper distance. During electrospinning, a small droplet (a Taylor cone) hangs at the outlet of the spinneret,

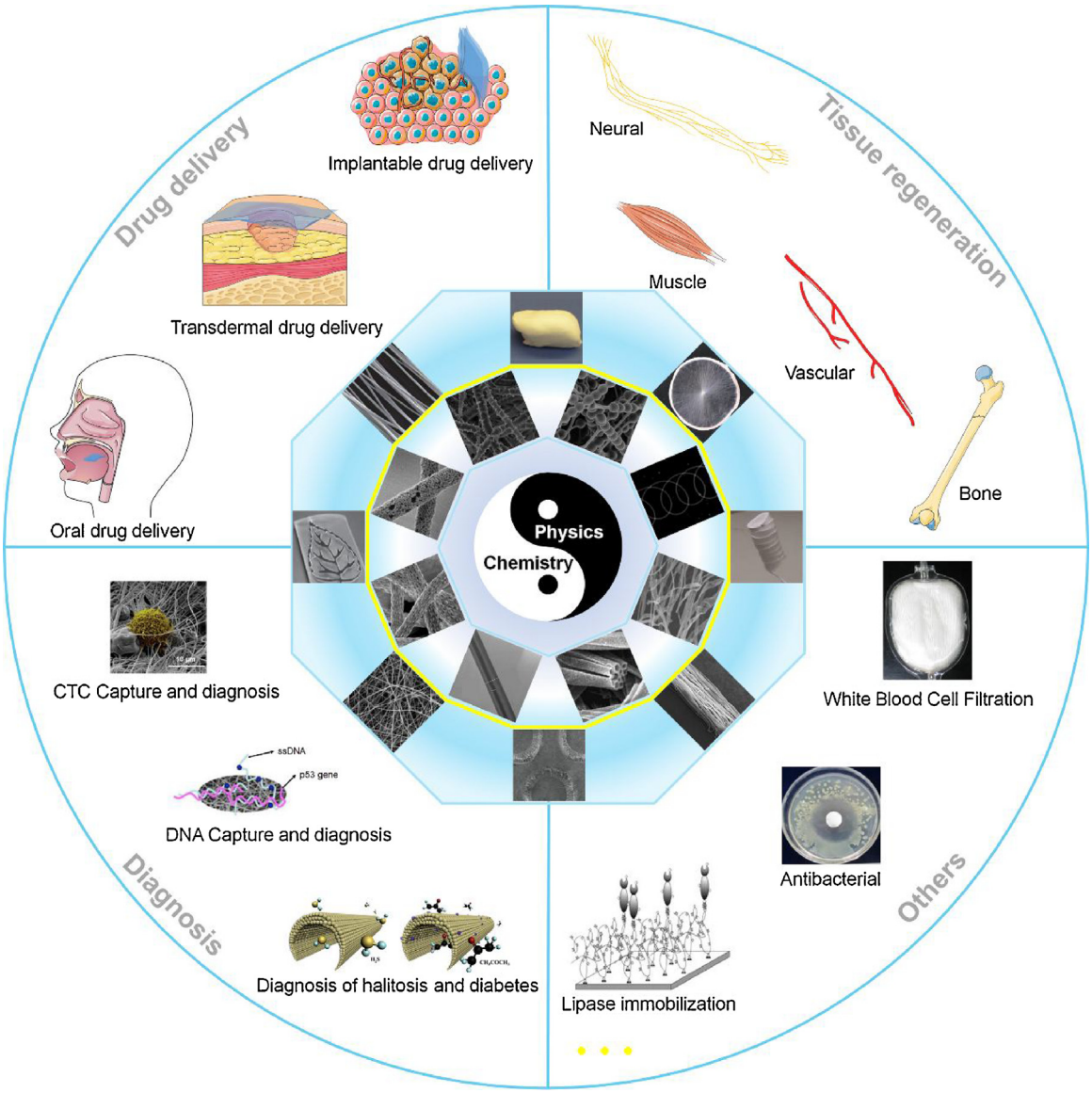

Fig. 1. Illustration of electrospun hierarchical structured one to three demensional polymeric fibers and their applications in biomedical field. Structural diversity of individual electrospun fiber and collection of electrospun fibers are presented within and outside the yellow hexadecagon, respectively. The biomedical applications of electrospun fibers are roughly classified into: drug delivery, tissue engineering, diagnosis and others. Partial images adapted from Ref. [112], Copyright 2007; [119], Copyright 2005; [155], Copyright 2016; [159], Copyright2012; [188], Copyright 2010; [334], Copyright 2012; [353], Copyright 2005. Reproduced with permission from Elsevier Ltd; [90], Copyright 2005; [103], Copyright 2017; [135], Copyright 2012; [140], Copyright 2001; [180], Copyright 2015; [327], Copyright 2016; [330], Copyright 2015; [355],Copyright 2012. Reproduced with permission from John Wiley & Sons Inc; [63],Copyright 2008; [138], Copyright 2012; [157], Copyright 2013; [323], Copyright 2010; [337], Copyright 2013. Reproduced with permission from the American Chemical Society; [213], Copyright 2014. Reproduced with permission from Springer Science + Business Media New York; [164], Copyright 2010, Reproduced with permission from Royal Society of Chemistry. (For interpretation of the references to colour in this figure legend, the reader is referred to the web version of this article.)

formed due to the extrusion of the precursor spinning solution by the syringe pump in the presence of an electric field. Then, the charged solution jets are ejected from the Taylor cone, followed by the fluid extending into uniform filaments. As this happens, bending instabilities result in vigorous whipping and/or splitting motions of the filament, accompanied by the evaporation of the solution solvent. Finally, the continuously spun fibers are solidified and deposited onto the collector, commonly forming a 2-D, non-woven web. The ordinary movement of the charged solution jet [30], shown in Fig. 2a, is rapid and complex in addition to having many instabilities [36–38]. Changing some of the process parameters, changes the jet track. For example, Xin et al. [39] used lithium chloride (LiCl) as salt to increase the conductivity of the polystyrene (PS) solution and investigated the jet movement during the electrospinning process. They found that at relatively high voltage, the jet of PS solution with salt firstly formed bending coils with small and slowly increasing diameters. Subsequently these small diameter coils were incorporated into a larger diameter bending instability coil, producing a complicated jet path, which was called a “garland” (Fig. 2b, c). The coils entangled and conglutinated in flight to form a fluffy network of fibers.

During this process, many factors would affect the jet movement and influence the final products, including the molecular structure of the polymers (molecular weight and architecture (branched or linear)), the solution properties (concentration, viscosity, surface tension and conductivity), voltage, flow rate, collecting distance, the diameter of the spinneret, and other ambient parameters (temperature, humidity, gas atmosphere, air flow and pressure, etc.) [40]. In different electrospinning systems, these parameters play different roles and may have larger or smaller effects on the final

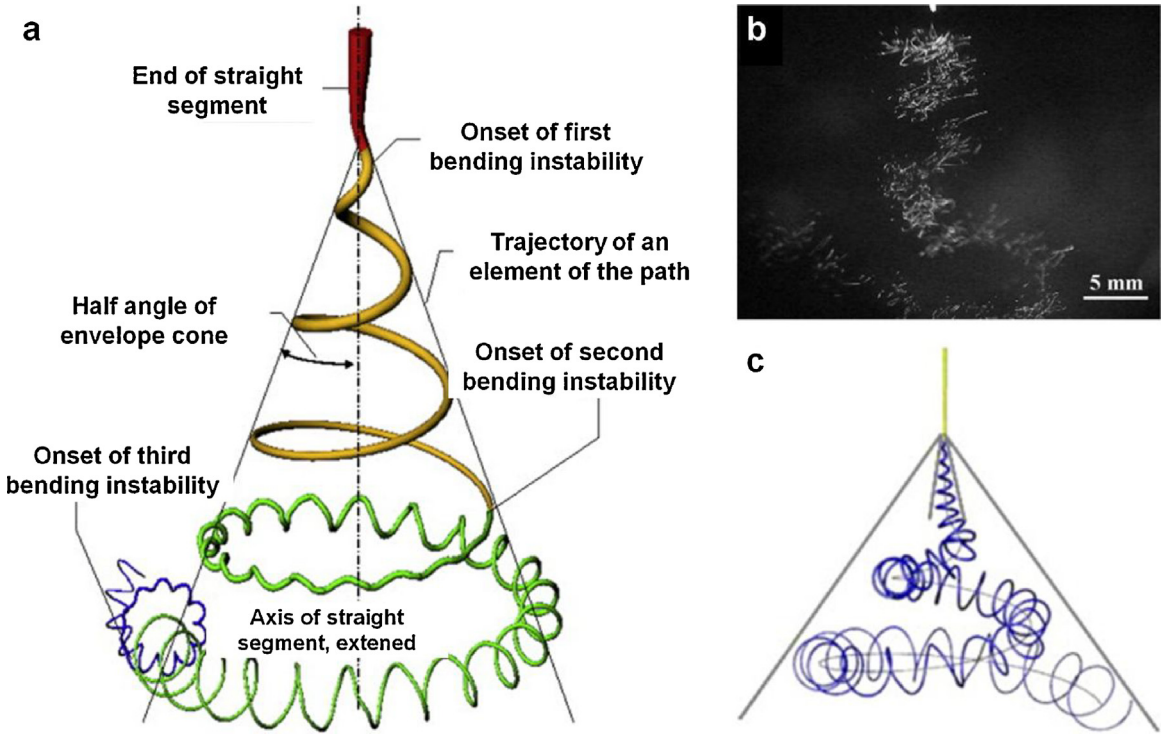

Fig. 2. a) The diagram showing the path of an ordinary electrospinning jet [30]. b, c) The path of garland-like electrospinning jet [39]. b) The image of garland formed during electrospinning of an 8 wt% PS solution in tetrahydrofuran (THF) with 2 wt% LiCl. c) The diagram of the formation of garland: a coil with a slender envelope cone developed first and this slender coil formed a larger bending coil with a more rapidly increasing diameter. The gray line inside the coils shows the centerline of the larger coil that forms a garland.

Sources:a) [30], Copyright 2008; b–c) [39], Copyright 2012. Reproduced with permission from Elsevier Ltd.

fibers, which creates difficulties for the large-scale electrospinning production processes. However, in recent studies, researchers have been able to use these parameters to their advantage in order to achieve effective control of fiber surface morphologies, diameters and arrangements [41–45].

2.2. Available biomaterials

Thus far, numerous polymers have been utilized for electrospinning, which can be roughly divided into natural polymers, synthetic polymers, multicomponent composite polymers and inorganic/organic composite materials. Table 1 summarizes the most commonly reported biomaterials used in electrospinning. Poly(ε-caprolactone) (PCL), poly(lactic acid) (PLA), poly(lactic-co-glycolic acid) (PLGA), poly(ethylene glycol)-co-poly(d,l-lactide) (PELA), poly(ethylene glycol)-poly(ε-caprolactone) (PEG-PCL), PS, polyurethane (PU) are the most commonly used synthetic biopolymers soluble in organic solvents, while polyvinyl alcohol (PVA), polyvinyl pyrrolidone (PVP) and polyethylene oxide (PEO) are commonly used synthetic water-soluble biopolymers. In addition, collagen, gelatin, silk fibroin, spider silk protein, chitosan and alginate are the most commonly used natural polymers for electrospinning. Notably, for many natural polymers which have a relatively poor solubility and a low molecular weight, electrospinning into fibers is difficult without mixing in synthetic polymers. So some synthetic polymers, such as PLA [46–48], PLGA [49,50], PCL [51], PEO [52], or PVA [53,54], are often co-electrospun with the aforementioned natural polymers as carrier polymers.

2.3. Developments

After the initial explorations of how the electrospinning process parameters affect the spinnability of different kinds of polymers, electrospinning techniques are currently being developed for more precise fabrication and for finer control of a diversity of fiber morphologies, diameters and arrangements of fibers. These developments can be roughly divided into two research efforts: (1) improving the traditional electrospinning devices; (2) combining electrospinning with other polymer processing techniques.

As shown in Fig. 3 , improvements made to the traditional electrospinning devices (Fig. 3a) (*e.g.,* a high voltage power supply, a spinneret, an injection pump and a fiber collector) were mainly focused on the spinneret and the fiber collector. In addition to the traditional single nozzle spinneret or needle, double-/multiple-nozzle spinnerets [84–87], coaxial/multiaxial spinnerets [88–91], side-by-side/multichannel spinnerets [92,93], the flat spinneret [94], and even the needleless spinneret (*e.g.,* the spiral coil spinneret [95,96], the rotary cone spinneret [97], the cylinder or disk spinneret [98,99]) have been developed to achieve electrospun fibers with a wide range of individual fiber structures (*e.g.,* core-shell structure, triaxial structure, multichannel structure and Janus fibers) or to achieve the mass production of micro-/nanofibers, as shown in Fig. 3b and c. Along with these improvements, variable air pressure [100,101] was also introduced in order to assist in the formation of the electrospinning jets.

In regards to the fiber collector, in addition to the traditional grounded conducting plate, many other collectors have been developed, including 3-D columnar collectors, which are used to fabricate fibrous tubes [102], helical spring-shaped collector (Fig. 3d) employed to fabricate 3-D nanofibrous construct [103], parallel electrodes (the horizontal parallel conductive substrates [104] or the dual collection rings [105]) that help fabricate aligned fibers (Fig. 3e, f), and patterned collection plates (more details in section 3.2.3). Various grounded rotators, which are employed to collect aligned fibers due to the work of applied mechanical force during the fiber collecting process, have also been developed, such

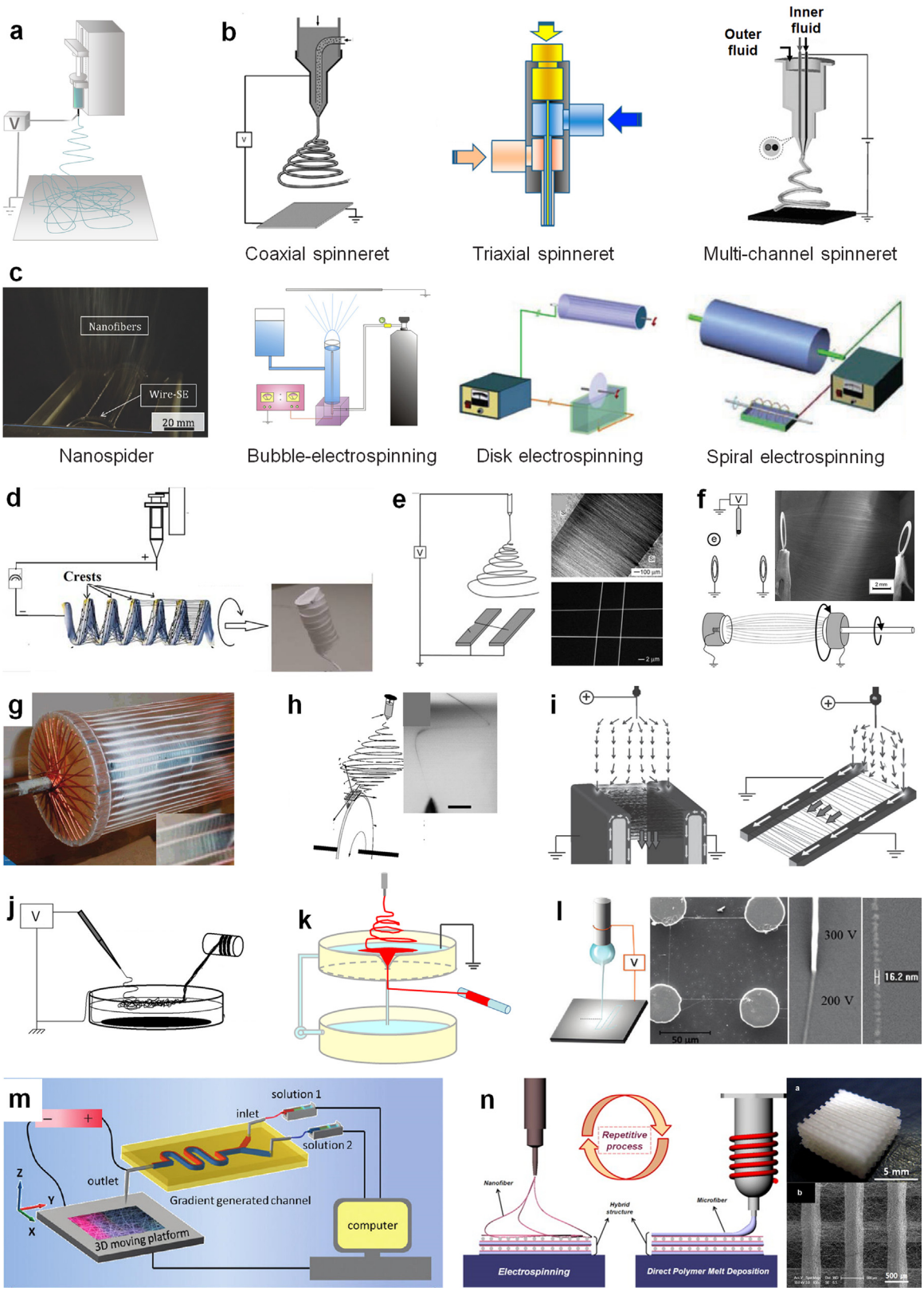

Fig. 3. a) The tranditional setups of electrospinning, including: a static high voltage power supply, a spinneret, a microflow pump and a collecting plate; b) different spinnerets, including coaxial spinneret [90], triaxial spinneret [88] and multi-channel spinneret [93]; c) the needleless electrospinning techniques: including the Nanospider with wire spinning electrode [98], bubble disturbing needleless electrospinning [100], disk needleless electrospinning [99] and spiral needleless electrospinning [96]; d) the helical spring collector [103]; e) the parallel electrodes and the collected aligned nanofibers [104]; f) the dual collection rings and the collected aligned nanofibers [105]; g) a rotating drum with parallel wires [108]; h) the rotating disk collector [109]; i) the automated parallel tracks [110]; j) the fiber collecting water bath [111]; k) a dynamic liquid support system for collecting nanofiber yarn [112]; l) The low-voltage near-field electrospinning [42]; m) a microfluidic assisted electrospinning [113]; n) Combination of 3D-printing and electrospinning [114].

Sources: h) [109], Copyright 2003. Reproduced with permission from AIP Publishing LLC; c) [100], Copyright 2009; f) [105], Copyright 2004; j) [111], Copyright 2005; k) [112], Copyright 2007; n) [114], Copyright 2008. Reproduced with permission from Elsevier Ltd; c) [96], Copyright 2012, an open access article. Reproduced with permission

as the rotating drum or stick [106,107], the rotating wire drum collector (Fig. 3g) [108] and the rotating disk collector (Fig. 3h) [109]. Furthermore, in order to acquire a more efficient collector, a few researchers have introduced additional useful devices such as automated parallel tracks (Fig. 3i) [110] or a water bath (Fig. 3j and k) [111,112]. Efforts have also been made to improve the other parts of the electrospinning setup. For example, in order to more precisely control fiber arrangement, Bisht [42] employed a very low voltage (200 V) as compared to the traditional voltage, generally 10 kV to 20 kV, to achieve low-voltage, near-field electrospinning, effectively inhibiting bending instabilities, increasing the control of the resulting polymer jet in the electrospinning process, and successfully freely suspending the individual polymeric nanofiber between microstructures of a 3-D carbon structure (Fig. 3l).

With other polymer processing technique developments, the combination of electrospinning and these processing techniques have attracted more and more attention. For example, Zhang et al. [113] presented a microfluidic-assisted electrospinning approach for producing electrospun nanofibers containing gradients in composition, nanoparticle content, and biomolecule concentration in order to study spatial differentiation in mesenchymal stem cells (Fig. 3m). Park et al. [114] used a hybrid process by combining a direct polymer melt deposition and electrospinning to make a 3-D scaffold with polycaprolactone/collagen nanofiber matrices inside (Fig. 3n). Jia et al. used a localized dissolution method by employing a piezoelectric printer to prepare various patterned electrospun fiber mats [115].

3. Structural diversity of electrospun fibers

3.1. Structural diversity of individual electrospun fibers

The normally desirable morphology of individual electrospun polymeric fibers involves a uniform diameter, a round cross-section, and a generally smooth appearance. However, to satisfy the requirements of all kinds of applications, electrospun polymeric fibers with various interesting and tunable secondary structures are being fabricated more often, usually by careful tuning of the electrospinning parameters.

3.1.1. Core-shell fibers

Electrospun core-shell fibers, which are quite useful in many applications, especially in biomedical applications, have been widely studied by many researchers. Both coaxial electrospinning and emulsion electrospinning are utilized to fabricate core-shell fibers. For coaxial electrospinning, a spinneret fabricated from two coaxial capillaries is required (Fig. 3b). These coaxial capillaries were first originated for coaxial electrospraying [116], then they were utilized in electrospinning [117] to fabricate core-shell nanofibers. During coaxial electrospinning, an outer and inner spinning solution are fed into the outer and inner capillary, respectively. Then, the outer and inner solutions join together to form a coaxial Taylor cone as a result of carefully tailored feeding rates, consequently forming a coaxial fluid jet in the high voltage electrostatic field [118]. Finally, core-shell fibers (Fig. 4a) with distinct inner and outer phases are produced due to the short confluence time and the low diffusion coefficient of polymers after electrospinning.

Because of their structures, electrospun core-shell fibers from coaxial electrospinning can delay the release of drugs when used as drug carriers, leading to a wide range of applications in controlled drug delivery, tissue engineering, and wound dressing and suture [119]. Additionally, coaxial electrospinning is able to fabricate nanofibers composed of polymers that are not electrospinnable or are difficult to process using conventional methods of spinning. For example, natural silk, a suitable material for producing tough biocompatible fibers, is hard to process due to its low elasticity at low concentration and its tendency to gel at high concentration [120]. Though the addition of some electrospinnable high molecular weight polymer (*e.g.,* PEO) or the use of caustic solvents (*e.g.,* formic acid and hexafluoro-2-propanol) can render the silk electrospinnable, the additives or caustic solvents may compromise the properties of the intended fibers (*e.g.* mechanical integrity and biocompatibility) Rutledge et al. reported the use of "two-fluid" electrospinning (coaxial electrospinning) to fabricate silk/PEO core-shell fibers [118,121]. After inducing the conformation transformation of silk from the random coil and/or silk I to predominantly β sheet (silk II) structure by treatment of high humidity or methanol, the silk core filament is insoluble and the PEO shell can be removed by water, resulting in a solid, crystallized silk fiber. Furthermore, fibers with special structures derived from an initial core-shell structure can also be produced by coaxial electrospinning or by a derived electrospinning technique. As an example, Li et al. [91] made hollow nanofibers (Fig. 4b) with walls made of inorganic/polymer composites or ceramics which were obtained by electrospinning two immiscible liquids through a coaxial spinneret, followed by the selective removal of the cores. Chen et al. [89] prepared core/shell ultrathin fibers with a nanowire-in-microtube structure (Fig. 4c), which was fabricated using a multifluidic coaxial electrospinning approach with an extra middle layer of fluid between the core and shell fluid layers present in traditional coaxial electrospinning. Zhao et al. [122] successfully fabricated tubes with two to five channels (Fig. 4d) through a multifluidic compound-jet electrospinning technique derived from a combination of coaxial electrospinning and dual nozzle side-by-side electrospinning [123,124].

In addition to coaxial electrospinning, emulsion electrospinning is an alternate method for fabricating electrospun core-shell nanofibers [125] or hollow fibers [126]. For emulsion electrospinning, the spinning solution consists of uniform emulsions, including either an oil-in-water emulsion [127] or a water-in-oil emulsion [128]. In contrast to coaxial electrospinning, emulsion electrospinning does not require a coaxial spinneret; consequently, researchers do not have to consider the coaxiality of the two capillaries in the spinneret or the feeding rate of the outer and inner fluids. However, the emulsion is not a stable electrospinning solution, and the ingredients of the emulsion must be chosen carefully, which limits the development and application of emulsion electrospinning.

3.1.2. Beaded fibers

Beaded fibers are commonly discovered during electrospinning, usually considered to be "by-products" of the process. Fong et al. [77] summarized that the formation of beaded fibers (Fig. 4e) may be due to the capillary breakup of the electrospun jets as a result of surface tension, altered by the presence of electrical forces. Further researches by Shin [129] and Hohman [38] revealed that the formation of beaded fibers was attributed to the axisymmetric instabilities in the fluid jet in the presence of an external electric field. The beads on the electrospun fibers were formerly thought of as a kind of structural defect during the electrospinning process; however, research developments in recent years relating to the application of electrospun fibers have informed the current under-

from Hindawi; b) [90], Copyright 2005; b) [93], Copyright 2010; c) [98], Copyright 2013; c) [99], Copyright 2009; d) [103], Copyright 2017; e) [104], Copyright 2004; i) [110], Copyright 2013. Reproduced with permission from John Wiley & Sons Inc; b) [88], Copyright 2013; g) [108], Copyright 2004; l) [42], Copyright 2011; m) [113], Copyright 2012. Reproduced with permission from the American Chemical Society.

Table 1
Some commonly polymers for electrospinning towards biomedical applications.

	Polymer	Molecular formula	Solvent	Method	Diameter	Highlight	Ref.
Synthetic polymers	PCL	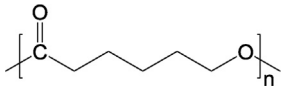	THF/DMF (1:1, w/w); DMF/DCM (1:1, w/w)	Normal electrospinning	250–700 nm; 100–1200 nm	PCL is a semi-crystalline poly-α-hydroxy aliphatic polyester well known for its slow biodegradability, high biocompatibility, and good drug permeability	[55–59]
	PLA	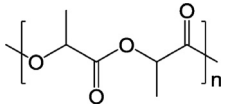	acetone; DCM; chloroform; dioxane; THF; DMF; DMAc	Normal electrospinning	210–1181 nm		[60,61]
	PLGA	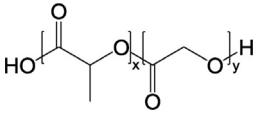	DCM; HFIP; THF; THF/DCM	Normal electrospinning		Increasing the percentage of glycolide to lactide in the copolymer increased the rate of degradation in vitro and in vivo.	[62–65]
	PELA	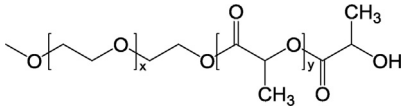	acetone	Normal electrospinning	610–1010 nm	PELA copolymer also displays a good biocompatibility in vivo, improved degradation rate, decreased acidity of the degradation products, and increased hydrophilicity compared to pure poly(d,l-lactic) and thus it exhibits good potential in formulating drug delivery systems.	[46]
	PEG-PCL	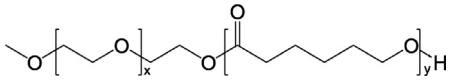	DMF/DCM (1:3, v/v)	Normal electrospinning	350–400 nm	The hydrophilic polyethylene glycol (PEG) co-polymerized with ε −caprolactone to improve the water wettability and degradation rate of PCL	[66]
	PS	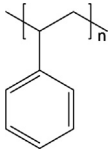	DMF; THF; DMF/THF (1:1, w/w)	Normal electrospinning	600–2760 nm		[67–69]
	Polyanhydride	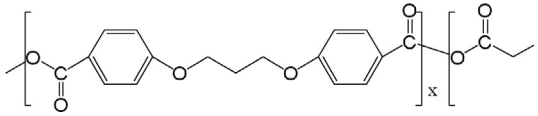	chloroform	Normal electrospinning	80–3200 nm	Polyanhydrides are believed to predominantly undergo surface erosion which is also termed heterogeneous erosion for hydrolytic instability of the anhydride bond and hydrophobicity, due to which the drug can be released by a steady speed from the polymer matrix.	[70]

	PU	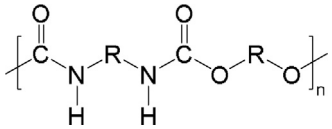	HFIP	Normal electrospinning	400–1400 nm	Biomechanical analysis and in vitro cell studies show that this polymer has satisfying biomechanical properties and that its degradation by-products are non-toxic. The polymer has a low degradation time, 10 times less than that of polylactic acid.	[71,72]
	PVA	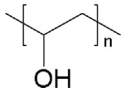	water; water/DMF (7:3, w/w)	Normal electrospinning	50–500 nm; 190–1500 nm	Poly(vinyl alcohol) (PVA) is a water-soluble polymer with chemical stability and excellent physical and mechanical properties	[73,74]
	PVP	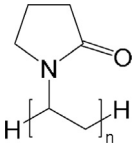	water;	Normal electrospinning			[75,76]
	PEO	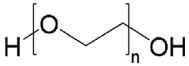	water	Normal electrospinning		Often be used as carrier polymers	[45,77]
Natural polymers	Collagen	–	HFIP	Normal electrospinning	100–1200 nm		[78]
	Gelatin	–	TFE; hot water	Normal electrospinning	100–340 nm		[79,80]
	Silk fibroin	–	formic acid	Normal electrospinning	30–120 nm		[81]
	spider silk protein	–	formic acid	Normal electrospinning			[82]
	Chitosan	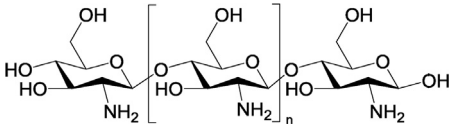					[83]
	Alginate/(PEO or PVA)	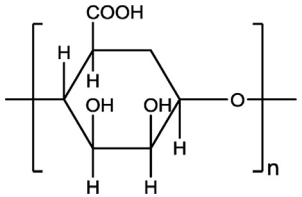	water	Co-electrospinning		Alginate, a naturally abundant linear anionic polysaccharide extracted from brown sea algae, has a similar structure to one of the major components of the ECM in human tissue, glycosaminoglycan (GAG), of particular interest for tissue scaffolds.	[54]

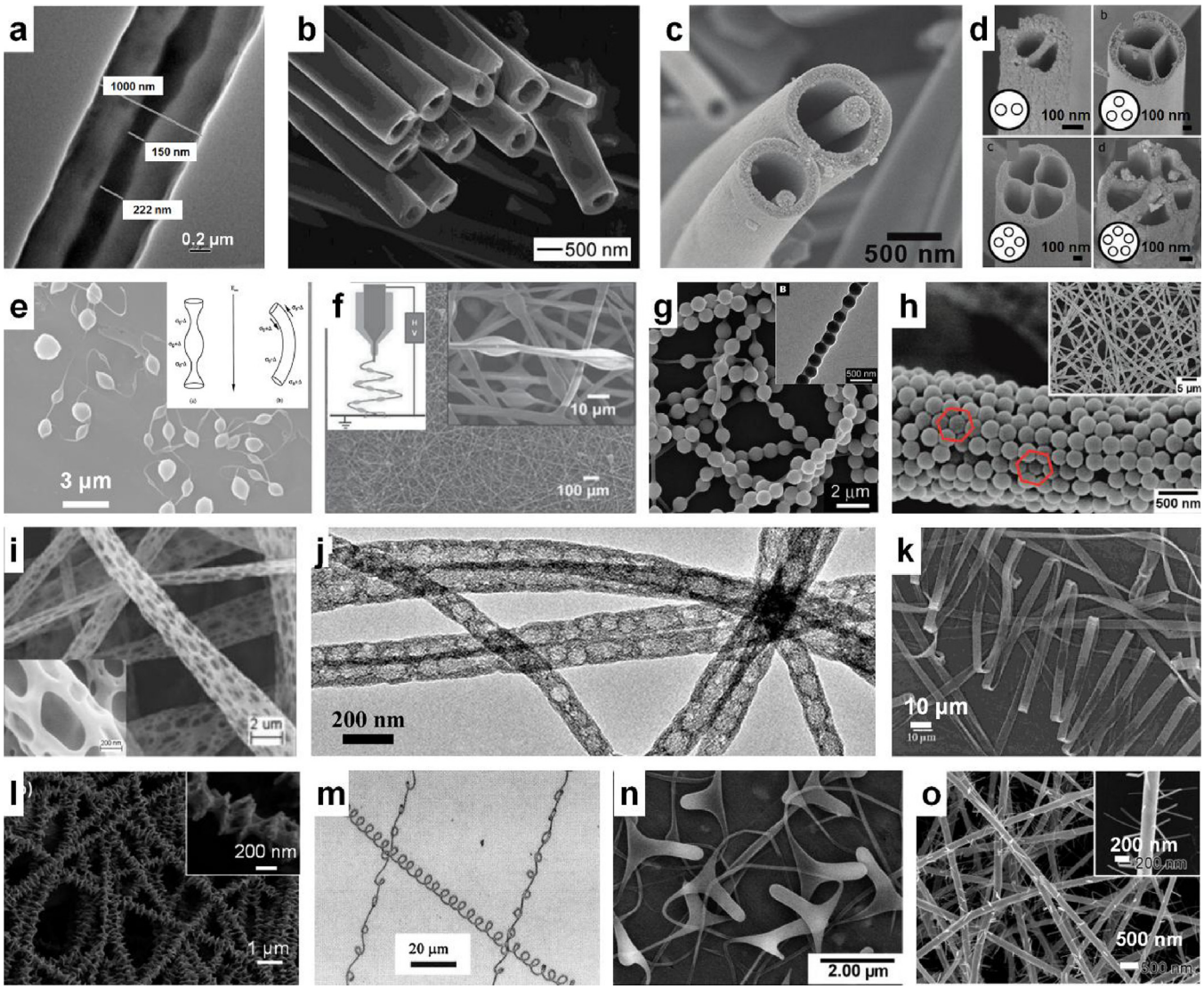

Fig. 4. Structural diversity of the individual electrospun fiber. a) core-shell fibers produced by coaxial electrospinning [117]; b) hollow fibers [91]; c) nanowire-in-microtube structured fibers [89]; d) multichannel microtube structured fibers [122]; e) beaded-fibers [77] produced by the axisymmetric instability during electrospinning, the inserted illustration shows two different instability occurred in the electrospinning process, including axisymmetric instability (*e.g.,* raleigh instability) and bending instability [129]; f) bead-on-string fibers produced by coaxial electrospinning [132]; g) beaded (necklace-llike) fibers produced from electrospinning of blend of SiO_2 particles and PVA solution [137]; h) colloidal fibers produced from electrospinning of blend of PS nanoparticles and PVA solution [138]; i) porous fibers [139]; j) bamboo-like nanofibers with internal cavities [147]; k) ribbon fibers [148]; l) nanofibers with a nanohybrid shish-kebab structure [156]; m) helical fibers [158]; n) barbed fibers produced from electrospinning of 3 wt% PVA solution [160]; o) barbed V_2O_5-TiO_2 nanofibers and the barbs comes from the growth of V_2O_5 crystals during the calcining of V_2O_5-TiO_2-Ta_2O_5 composite nanofibers [161].

Sources: m) [158], Copyright 2004. Reproduced with permission from AIP Publishing LLC; e) [77], Copyright 1999; e) [129], Copyright 2001. Reproducedwith permission from Elsevier Ltd; a) [117], Copyright 2003; f) [132],Copyright 2011; k) [148], Copyright 2001. Reproduced with permission from JohnWiley & Sons Inc; n) [160], Copyright 2008. Reproduced with permission fromSociety of Plastics Engineers; o) [161], Copyright 2006; b) [91], Copyright 2004; c) [89], Copyright 2010; d) [122], Copyright 2007; g) [137], Copyright 2010; h) [138], Copyright 2012; i) [139], Copyright 2007; j) [147], Copyright 2015; l) [156], Copyright 2013. Reproduced with permission from the American Chemical Society.

standing of this phenomenon. A greater amount of attention has been paid to the study of the production and application of these beaded fibers in novel ways. For example, Luo et al. [130] produced a series of beaded electrospun fibers with different sizes and varying densities of beads on the fibers by altering the concentration of the polymer solution, effectively controlling the surface nanoroughness of the resulting electrospun fiber mats. Furthermore, the researchers studied both the impact of surface nanoroughness on cellular behavior by culturing rat bone marrow mesenchymal stem cells (rBMSCs) on the beaded fibers, and the effect of surface nanoroughness on subcutaneous bone formation *in vivo*. Additionally, Ding et al. [131] studied the synergistic effects of releasing dexamethasone (a chemical signal) and surface nanoroughness (a physical cue) on mesenchymal stem cell differentiation. They found that the gradual release of dexamethasone into the culture medium played a dominant role in promoting rBMSCs' differentiation towards osteoblast-like cells, while the surface nanoroughness played a supporting role in the differentiation.

Based on the axisymmetric instabilities during electrospinning, the method for producing beaded electrospun fibers by controlling the concentration of polymer solution is simple and easy to operate. However, the beads on the fibers which are produced in this way are made of the same components as the fiber matrix, which may not fit all the requirements of a given application. To overcome these limitations, Tian et al. [132] fabricated "bead-on-string heterostructured fibers (BSHFs)" (Fig. 4f), in which hydrophilic

PEG beads are imprinted onto a hydrophobic PS string by using a sprayable outer fluid and a spinnable inner fluid in a coaxial electrospinning process. The occurrence of the spontaneous Rayleigh break-up of the outer fluid during the process was the key for successfully fabricating BSHFs. By carefully matching the viscosity, surface energy and feeding rate of the inner and outer fluids, nearly perfect bead-on-string heterostructures were produced. They also demonstrated that the BSHFs showed an interesting response to changes in environmental relative humidity because of their alternating hydrophilic and hydrophobic surface characteristics; specifically, the BSHFs demonstrated a segmented swelling and shrinking behavior in the "bead" parts whereas the "string" parts remained constant.

In addition to the aforementioned ways to produce beaded electrospun fibers, nano/microparticles [133–135] may also be introduced into polymer solutions, fabricating beaded or necklace-like fibers through a process known as colloid electrospinning [136]. Yu et al. [137] utilized PVA as a polymer matrix for fabricating necklace-like arrays of silica particles, as shown in Fig. 4g. They found that the diameters of the SiO_2 particles, the voltage, and the solution ingredients all influenced the final morphology of the electrospun fibers. Smaller SiO_2 particles (143 nm) tended to aggregate into bunches in the fibers, while bigger SiO_2 particles (265 nm and 910 nm) were more likely to align along the fibers one by one, forming necklace-like structures. Furthermore, the water content of the PVA/SiO_2/H_2O solution also played an important role in the diameter of the fibers and consequently determined the morphology, with too thin solutions leading to a blackberry-like structure and too condensed solutions being difficult to eject from the spinneret. Only the solution with a precisely tailored mixture of ingredients was able to produce necklace-like structured fibers. These researchers provided a set of references to other systems (such as work involving other polymers or particles) for the fabrication of necklace-like structures. For example, Yuan et al. [138] used 225 nm or 473 nm polystyrene nanoparticles (PSNs) to form necklace-like fibers and other fibers with interesting shapes such as uniform colloidal fibers (Fig. 4h).

3.1.3. Porous fibers

Porous structures on an electrospun fiber surface or through the entire fiber matrix, as shown in Fig. 4i, can increase the surface to volume or surface to weight ratio of fibers and broaden the range of applications for electrospun fibers [139,140].

Various organic or inorganic electrospun porous fibers have been reported in the past years. For organic electrospun porous fibers, the formation of pores primarily depends on the phase separation of the different components of the electrospinning solution, specifically, the separation between the polymers and solvents, the separation between the polymers and the nonsolvents or the phase separation of different polymer components. For example, Lin et al. [141] reported a direct approach for fabricating nanoporous polymer fibers *via* electrospinning in which the resulting PS fibers with micro- and nanoporous structures both in the core and on the fiber surfaces originated *via* solvent composition and PS solution concentration tuning. McCann et al. [142] created highly porous fibers consisting of various polymers by electrospinning with a liquid nitrogen bath used to freeze the fibers, inducing a phase separation between the polymer and the solvent. After removing the solvent in vacuum, highly porous fibers were obtained.

Megelski et al. [143] used the phenomenon of separation between a polymer and a nonsolvent along with a high volatility solvent to produce polymeric fibers with a porous micro- and nanostructured surface. These features could be introduced in several different polymeric fibers, and the pores varied from densely packed, well-formed nanopores (20 nm to 350 nm in diameter) to larger, flat pores of approximately 1 μm. For some special cases, water molecules in the air may act as the nonsolvent while electrospinning a non-water-soluble polymer. Casper et al. [144] found that when electrospinning in an atmosphere with more than 30% relative humidity, increasing the humidity caused an increase in the number, diameter, shape, and distribution of pores in the fiber surface.

To take advantage of the phase separation of different polymers, a post-processing step, including solvent extraction, thermal degradation or UV irradiation crosslinking, must be done in order to remove the sacrificial phase, forming pores in the fiber. For example, You et al. [145] fabricated PGA/PLA blend fibers and used trichloromethane to remove the PLA afterwards, so fibers with interconnected pores and a circular shape were obtained.

For inorganic electrospun porous fibers, calcination has often been applied to the electrospun organic/inorganic composite fibers in order to remove the organic phases, while the remaining inorganic materials unite to form porous structures. For example, Kokubo et al. [146] produced multi-core cable-like TiO_2 nanofibers through a calcination process of composite polyvinyl acetate (PVAc)/titania nanofibers by using a hot pressing pretreatment. Additionally, Sun et al. [147] prepared bamboo-like fibers (Fig. 4j) through the following series of steps: (1) preparation of the tetraethyl orthosilicate (TEOS)/polyacrylonitrile (PAN) composite nanofibers by electrospinning; (2) heat treatment of the precursors at 1200 °C in a H_2/Ar (5/95 by volume) atmosphere, leading to ultrafine SiO_2 clusters which then transfer and aggregate into much larger SiO_2 particles lined up uniformly in the core of the nanofibers; (3) removal of the SiO_2 particles in an HF aqueous solution, obtaining the final bamboo-like nanofibers.

3.1.4. Ribbon fibers

In addition to cylindrical nanofibers, electrospinning can also produce fibers with a variety of cross-sectional shapes. Koombhongse et al. [148] reported the fabrication of electrospun ribbon fibers from 10% poly (ether imide) (PEI) in hexafluoro-2-propanol, as shown in Fig. 4k. They proposed a possible formation mechanism of the ribbon fiber as follows: during electrospinning, a thin, mechanically distinct polymer skin on the liquid jet was present. Subsequently, the solvent inside the fiber matrix escaped, at which point atmospheric pressure caused the collapse of the tube formed by the skin as the solvent evaporated. Thus, the circular cross-section transformed into an ellipse and then flattened, forming a ribbon with a cross-sectional perimeter nearly the same as the perimeter of the jet. Apart from PEI, several other polymers have also been electrospun into flat ribbon fibers, including polystyrene (PS) [148,149], PVA [150], polyethylene (PE) [151], silk fibroin [152–154], Ag/$LaFeO_3$/PVP composite [155] and others. However, applications for these flat ribbon fibers have yet to have been developed.

3.1.5. Other fibers

Fibers with other interesting structures can also be produced *via* electrospinning. For example, PCL nanofibers with a nanohybrid shish-kebab structure (Fig. 4l) mimicking natural bone structures or collagen fibrils were reported by Chen [156] and Wang [157] separately. Kessick et al. [158] fabricated microscale polymeric helical structures (Fig. 4m) on a conductive substrate by electrospinning from a two-component solution consisting of nonconductive PEO and conductive poly (aniline sulfonic acid) (PASA). Xin et al. [159] reported an approach to produce buckled polystyrene patterns by electrospinning 25 wt% polystyrene solution at relatively low applied voltage (around 2.4 kV) and short tip-to-collector distance (2–8 cm). Holzmeister et al. [160] obtained fibers with a high frequency of short branches (Fig. 4n), referred to as "barbed nanowires", through the electrospinning of 8–1 wt% aqueous PVA solutions. Additionally, Ostermann et al. [161] found

that single-crystal V_2O_5 nanorods were grown on rutile nanofibers by carefully calcining composite nanofibers consisting of amorphous V_2O_5, amorphous TiO_2, and poly(vinylpyrrolidone), which may be referred to as inorganic "barbed nanowires" (Fig. 4o).

3.2. Structural diversity of electrospun fiber mats

The structure and morphology of the resulting arrangements of electrospun fibers or electrospun fiber mats also demonstrate great diversity, indicated in Fig. 5. This structural diversity is mainly dependent on the collector type, one of the most important parts of electrospinning apparatus, determining the distribution and macro-structures of the electrospun fibers. Additionally, the other aspects of the processing apparatus, such as the electric field strength, the presence of a magnetic field, and the ingredients of the electrospinning solutions, can also be optimized to get the desired fiber mat structure. The collected electrospun fibers or fiber mats can be roughly divided into the following groups: random fibers, aligned fibers, patterned fibers, 3-D fibrous structures, fiber yarn and other miscellaneous structures.

3.2.1. Random fibers

Random fibers (Fig. 5b) were the most common collection form of electrospun fibers. These randomly oriented fibers will be obtained simply by using the traditional electrospinning collector, a grounded conductive plate, because charged polymeric jets will naturally fly along a spiral trajectory during electrospinning (Fig. 2) [30]. The charged polymeric jets consist of a series of electrically driven bending coils with an increasing radius, accompanied by solvent evaporation, jet splitting and other jet instabilities, and finally solidifying into randomly oriented continuous thin fibers on the grounded plate.

3.2.2. Aligned fibers

In some applications, including electronics [162], ultrasensitive sensors [163] and biomedicine [61,164,165], fibers need to be collected into well-aligned structures. To obtain aligned electrospun fibers, several techniques were developed via changing the trajectory and inhibiting bending instabilities of the charged jet during electrospinning, including improvements to the collectors which could generate additional mechanical force fields, introduction of additional electric fields or magnetic fields and implementation of near-field electrospinning. Based on these techniques, electrospun fibers as aligned structures within a certain region were collected. Liu et al. [166] summarized some of the methods for controlling electrospun nanofiber alignment (Fig. 5b), including using mechanical forces generated with a rotating mandrel, creating electrostatic forces with a pair of parallel metallic plates, using a metallic ring with a metallic pin in the center or an array of metallic beads, and generating magnetic forces with a pair of permanent magnets. For parallel plates, Beachley et al. [110] contributed some improvements (Fig. 3i). Namely, they utilized parallel, automated tracks to orient and collect nanofibers from an electrospinning jet. In addition to the methods above for producing aligned electrospun fibers, recent studies have highlighted the use of near-field electrospinning [41,42] as a promising tool for precisely controlling the orientation of electrospun fibers. Bisht et al. [42] reported the use of a viscoelastic polymer solution and a very low voltage of 200 V in order to reduce bending instabilities and to increase control over the resulting polymer jet during near-field electrospinning. In some situations, the aligned fibers can be turned into another structures. Surrao et al. [167] produced aligned, self-crimping fibers (Fig. 5c) from electrospun aligned poly(l-lactide-co-ε-caprolactone) fibers *via* a post-processing method of adjusting the operating temperature above the polymer's glass-transition temperature. Beaded fibers (Fig. 5d), which were mentioned above, can also be electrospun and collected as aligned structures [168].

3.2.3. Nanofiber yarns

Electrospun nanofiber yarns (Fig. 5e) may be regarded as special 3-D electrospun fibrous structures. The fabrication of these electrospun nanofiber yarns is primarily carried out using either a water bath grounded collector [111,112,169] or a rotating drum [170–173], and then, the as-spun nanofibers are stretched manually or wound around a rotating grounded drum. For example, Smit et al. [111] used a grounded water reservoir collector to collect electrospun fibers, then drew the resulting non-woven web of fibers across the water before collecting the resulting yarn. Teo et al. [112] improved this nanofiber yarn collecting system by adding a water vortex which helped the yarn formation and facilitated yarn collection. In this way, the fibers are automatically stretched by water flow and form continuous fiber bundles at bottom of the vortex.

3.2.4. Patterned fibers

Recently, researchers have demonstrated that patterned materials or materials with ordered microstructures possessed specific functions which were useful in numerous applications such as in cell-substrate interactions. These specific micropatterns have proven to be useful in promoting favorable biological responses, including enhanced protein adsorption, cell attachment and proliferation in tissue regeneration [174–176]. Therefore, designing and controlling the microstructures and patterns of electrospun fiber mats results in more meaningful and significant applications of electrospinning to biomedical technologies and other fields [177–179]. Currently, patterned electrospun fiber mats (as shown in Fig. 5f) are primarily fabricated by using electroconductive template collectors with different kinds of designed micro-/macropatterns [180,181]. Electrical forces are considered to be key factors for determining the deposition and the arrangement of fibers during this process [181].

The localized nanofiber dissolution method reported by Jia et al. [115] represents an alternate way to fabricate electrospun fiber mesh with versatile patterns (Fig. 5g). In this method, a piezoelectric jet system is needed to print solvent droplets directly onto the nanofiber mesh *via* electrical charge-generated pressure, resulting in patterned electrospun fibrous mesh after the dissolution of the fiber matrix by a solvent. In order to optimize the printing conditions, two major criteria should be considered: (1) the solvent drops should be big enough to efficiently dissolve the desired area of fibers, and (2) the excessive diffusion of solvents as a result of evaporation should be minimized to maintain a high resolution, implying that the solvent must be chosen carefully.

There are also other techniques available for fabricating patterned electrospun fiber mats. For example, low voltage near-field electrospinning is a useful tool for obtaining certain patterned fibers [42], as was described in Section 2.3. Alternatively, Yan et al. [182] reported a honeycomb-patterned nanofibrous structure (Fig. 5h) with a pore diameter ranging from a micrometer to over 200 μm and with depths as greater than 150 μm, all of which were self-assembled from a charged electrospun polymer nanofiber in a wet state on the substrate by appropriately controlling the electrospinning conditions. This self-assembly of electrospun nanofibers are driven by the competitive actions of surface tension and electrostatic repulsion. Additionally, the "nano-fiber/nets" consisted of common electrospun nanofibers and ultrafine nano-nets, may be considered as a special fibrous pattern [183]. Ding et al. [184] reported a novel 2-D "fishnet-like" nanoweb (Fig. 4i) in a 3-D fibrous mat as a result of using poly (acrylic acid) or nylon-6. The authors hypothesized that the formation of the nanowebs was dependent on the splitting of defect films, which occurred only under certain

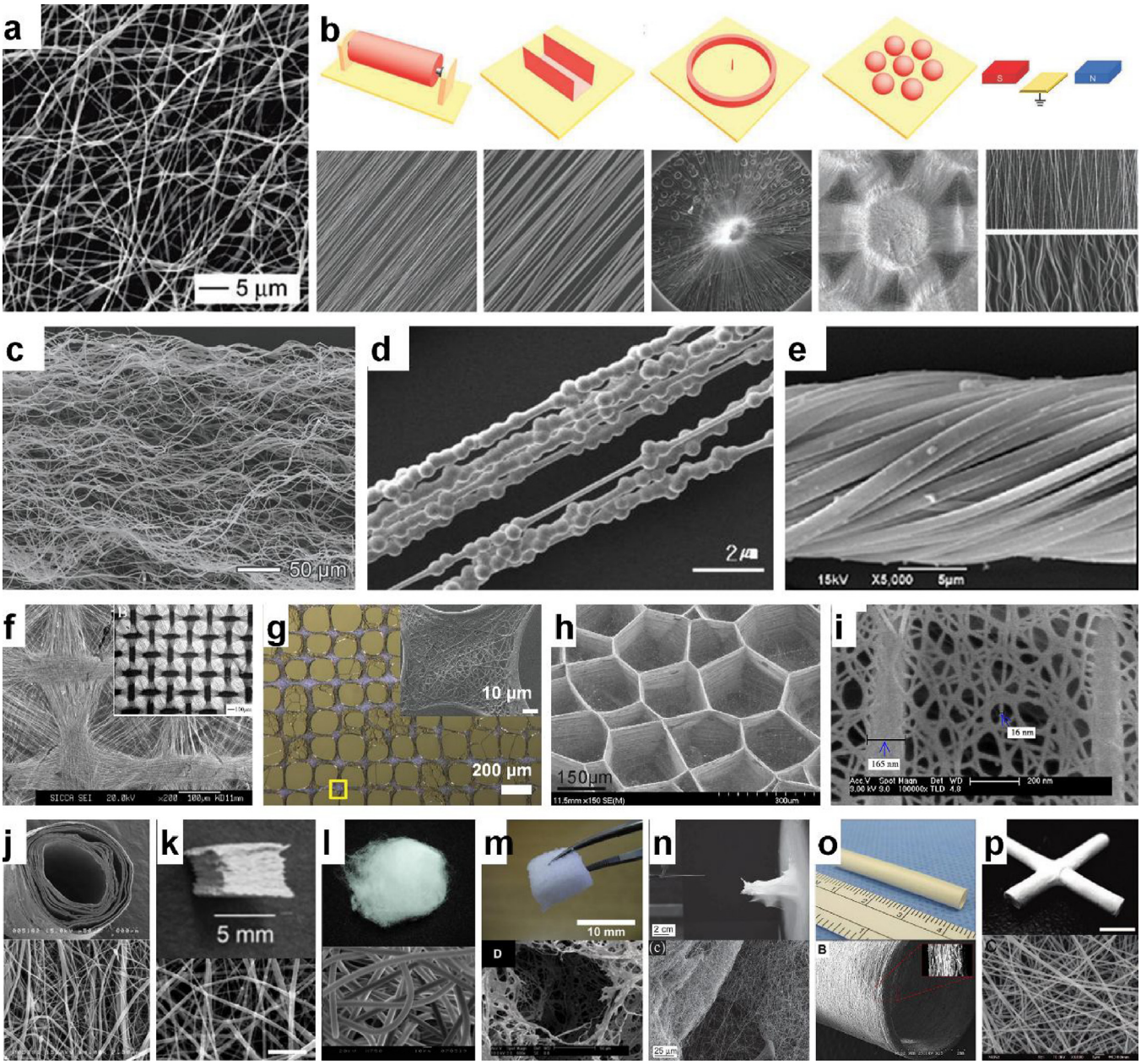

Fig. 5. Structural diversity of the arrangements of electrospun fibers. a) random electrospun fibers [312]; b) different aligned electrospun fiber collectors and SEM images of corresponding aligned fibers [166]; c) aligned self-crimping fibers [167]; d) aligned beaded fibers [168]; e) electrospun fiber yarn [11]; f–i) patterned fiber mats, f) patterned fibers fabricated by using a patterned fiber collector [181]; g) stereomicroscopy images of fibrous patterns with localized nanofiber dissolution method [115]; h) honeycomb-patterned nanofibers from self-assembly of electrospun nanofibers driven by surface tension and electrostatic repulsion [182]; i) nanofiber spider webs [184]; j–p) the macroscopic photos and corresponding microscopic SEM images of different 3-D electrospun nanofibrous macrostructures, j) the fibrous tube fabricated from electrospun fiber mats by manual [189]; k) 3D fibrous stacks [191]; l) 3D fibrous structure from expansion of electrospun microfibers [193]; m) macroporous and nanofibrous hyaluronic acid/collagen hybrid scaffold fabricated by concurrent electrospinning and deposition/leaching of salt particles [192]; n) 3D fibrous structure fabricated by electrospinning the blend solution of alginate/PEO/F127 [52]; o) the fibrous tube produced by using a rolling stick collector [190]; p) the crossed fibrous tube produced by using the perpendicular collecting stick [102].

Sources: e) [11],Copyright 2013; m) [192], Copyright 2008; o) [190], Copyright 2015. Reproduced with permission from Elsevier Ltd; i) [184], Copyright 2006. Reproduced with permission from IOP Publishing; b) [166], Copyright 2012; f) [181], Copyright 2007; g) [115], Copyright 2014; j) [189], Copyright 2008; k) [191], Copyright 2011; l) [193], Copyright 2010; n) [52], Copyright 2012. Reproduced with permission from John Wiley & SonsInc; p) [102], Copyright 2008; a) [312], Copyright 2009; c) [167], Copyright 2010; d) [168], Copyright 2006; h) [182], Copyright 2011. Reproduced with permission from the American Chemical Society.

conditions including a high applied voltage, a low relative humidity and a fast phase separation between the polymers and the solvents.

3.2.5. 3-D nanofibrous macrostructures

In practical applications, electrospun fibers are often used as 2-D materials. However, for some applications such as tissue engineering, the 2-D electrospun fiber mats may not fully meet the needs of the user. According to the basic principles of tissue engineering, designing and manufacturing an artificially engineered scaffold construct for cell seeding and culturing is one of the core technologies. Compared with 2-D scaffolds, 3-D scaffolds provide better links between cells, and generate microenvironments which are more like realistic *in vivo* physiological conditions, since 3-D scaffolds offered another dimension for cell–cell interactions, cell migration and cell morphogenesis, all of which are important in regulating cell cycles and tissue functions [185]. Therefore, it is nec-

essary to fabricate 3-D fibrous structures from electrospun fibers. Although challenges still exist in the fabrication of 3-D electrospun fibrous structures, some progress has been made in recent years [186–188].

According to the review by Sun et al. [11], there are four main strategies for the fabrication of 3-D electrospun fibrous macrostructures as shown in Fig. 5(j–p) [52,189–193]: (1) increasing spinning time; (2) assembly by post-processing of 2-D electrospun fiber mats (*e.g.,* folding, layer-by-layer electrospinning, sintering, mechanical expansion); (3) direct assembly by an auxiliary factor (*e.g.,* a 3-D template, liquid collector); and (4) self-assembly.

4. Biomedical applications of electrospun polymeric fibers

Owing to the structural diversity, high surface area and adjustable porosity of the electrospun fibrous systems, they can be widely used in many different fields. In particular in the biomedical field, for example, the intrinsic properties such as structural diversity and high surface area, are advantageous for the loading and subsequent release of different drugs in drug delivery. The adjustable porosity and the ability of electrospun fibers to mimic the fibrillar nature of the extracellular matrix (ECM) allow its use as promising 2-D or 3-D scaffolds for cell support and growth in tissue engineering. In addition, the high surface area and adjustable porosity of the electrospun ultrafine fibers also provide more surface area for immobilization of functional groups in diagnostics and other applications. So far, a great deal of effort has been devoted to achieving the successful biomedical application of electrospun fibers to a wide range of devices and systems, comprehensively reviewed in this section.

4.1. Drug delivery

Due to the structure of electrospun fibers, and especially as a result of the diversity in individual fiber structures, electrospun fibers possess features such as a flexibility in morphological design, a high surface-area-to-volume ratio, and a similarity to the ECM. These characteristics make electrospun fibers advantageous [194] in drug delivery, as demonstrated by the following aspects: (1) the diversity of polymers available enables researchers to accommodate compatibility with physico-chemically distinct agents [195]; (2) a high drug loading (up to 60%) and an encapsulation efficiency (up to 100%) are possible [196–198]; (3) the ability to control drug release is inherent in the system; (4) the electrospinning process is simple and cost-effective; and (5) the extensive, in depth research regarding the theories of electrospinning and the applications of electrospun fibers provides a solid foundation for future system development, which enables the development of mature commercial products based on electrospun fibers.

4.1.1. Controlled release mechanism of electrospun fibers

4.1.1.1. Controlled release of a single drug. Several methods can be used to achieve a sustained release of a single drug by electrospun fibers, including matching drugs with suitable polymers, using core-shell electrospun fibers or layered electrospun fiber mats as drug carriers, or by encapsulating drug-loaded particles into electrospun fibers.

The choice of polymer is an important factor for achieving a sustained release of drugs from electrospun fibers. Fortunately, a large amount of easily available polymers can be utilized for electrospinning, as mentioned in Section 2.2. Chou et al. [194] summarized the effects of different polymers for electrospinning on the drug loading capacity and drug release time.

After successful loading, drugs need to cross the barriers created by the fiber matrix and then diffuse further into the release medium. This is the drug diffusion path, which offers a mechanism for controlling drug release. For biodegradable polymers, the release of drugs is mainly dependent on the degradation process of the polymer fibers because the degradation of the polymer matrix results in variations in the electrospun fiber morphology, changing the drug diffusion pathway and affecting the drug release. Furthermore, drugs in the degraded regions of the fiber matrix may also dissolve directly into the release medium. For non-degradable polymers that do not swell, the drug diffusion path would not change because there is no variation in fiber morphology over time. In this situation, the conditions controlling the release of the drugs are primarily other factors such as drug solubility, drug partitioning in the polymer and the drug diffusivity in the polymer. Therefore, in general, the release of drugs from the fiber matrix may be affected by fiber morphology, hydrophilicity of the fiber matrix, degradability of fiber matrix, drug partitioning and drug diffusivity in the polymers or the drug solubility in the medium.

In early studies, researchers simply blended drugs with polymers to electrospin into drug-loaded fiber mats. For example, Kim et al. [199] successfully incorporated a hydrophilic antibiotic drug (MefoxinR, cefoxitin sodium) into a poly PLGA-based electrospun nanofiber mat to achieve a controlled release of drugs over the course of 1 h. The researchers observed no loss in structure or bioactivity, and furthermore, they determined that the addition of an amphiphilic block copolymer (PEG-b-PLA) reduced the cumulative amount of released drug during the earlier release time, prolonging the drug release period up to 1 week. Yohe et al. [200] used the compound poly (glycerol monostearate-co-ε-caprolactone) as a hydrophobic polymer dopant with PCL to fabricate superhydrophobic electrospun fibrous mesh, resulting in a mesh with a high apparent contact angle. The air in the porous electrospun mesh may also act as a barrier component, further controlling the drug release rate.

In addition to polymer material selection, the choices available for the loading drugs are also wide ranging and versatile. Heunis et al. [201] summarized the types of drugs that were successfully encapsulated into electrospun fibers, including antibiotics, plasmid DNA, growth factors, antimicrobial components (*e.g.,* silver nanoparticles), proteins, bacteria and phages. However, the fact that a great variety of drugs can be chosen may bring another problem, in that the physical and chemical characteristics as well as the hydrophobicity of different drugs will affect the controlled release process. For example, Carson et al. [202] reported that the release of azidothymidine, maraviroc, raltegravir, and tenofovir disoproxil fumarate was much faster than tenovir in equivalent PCL/PLGA fiber formulations, suggesting that even subtle differences in the chemical structures of drugs would affect release rates. Generally, using electrospun fibers as a drug delivery system requires a careful match between the drug and the polymer.

In addition to matching the drugs with the right materials, changing the drug diffusion pathway is another effective way to control the release of drugs. Based on this approach, electrospun fibers with different structures can be fabricated to control drug release *via* tuning electrospinning parameters. One technique is to employ coaxial electrospinning for the fabrication of core-shell electrospun fibers as a drug delivery system. When drugs are loaded into the core layers of these fibers, the outer shell serves as an effective barrier for preventing the penetration of water molecules and the diffusion of drugs [203]. Specifically, the thickness, composition and permeability of the outer shell impacts the release of drugs in the core region of the fibers [204]. Additionally, emulsion electrospinning were also used to prepare core-shell fibers for controlling drug release [127].

An electrospun mesh with sandwich-like layers [205,206] was also used to change the drug diffusion pathway. Falde et al. [205] fabricated a drug-loaded layered electrospun mesh (Fig. 6a) with

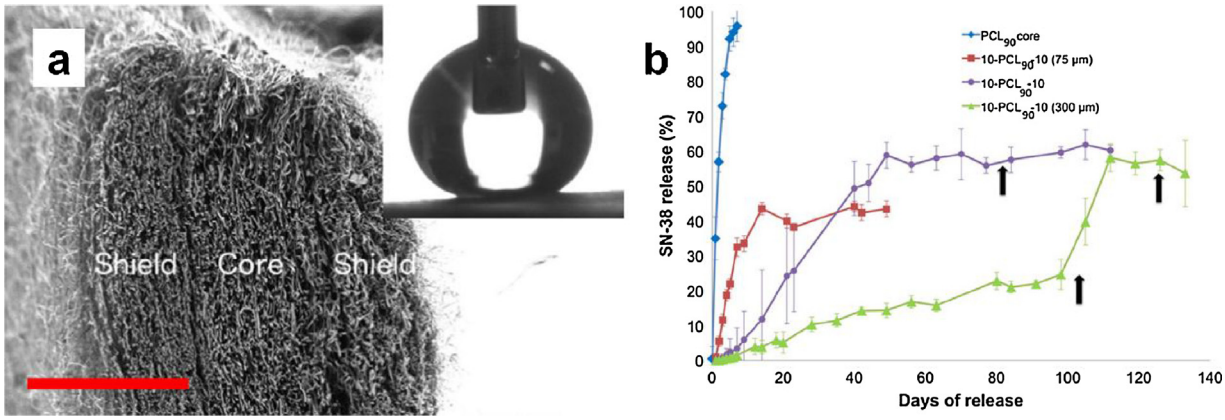

Fig. 6. a) The SEM image of layered superhydrophobic meshes (inserted picture shows the water contact angle with 151.1°), in which the core layer was SN-38-loaded PCL electrospun fiber mats and the two shield layer was PGC—C18 fiber mats, scale bar = 500 μm; b) SN-38, loaded in the 90-μm thick PCL core, release into static PBS with varying shield layer thickness (75 μm, 150 μm, 300 μm).

Sources: [205], Copyright 2015. Reproduced with permission from Elsevier Ltd.

the chemotherapeutic agent SN-38 incorporated into a central "core" layer between two superhydrophobic "shield" layers of electrospun mesh without any drug. They found that the "shield" layers successfully delayed the release of SN-38, and by increasing the thickness of the "shield" layers, one could obviously extend the release time of the drug. As shown in Fig. 6b, with 300 μm thick layers on both sides of the drug-loaded core, there was still a layer of metastable air that could be displaced with an ethanol treatment after 100 days of immersion (indicated by the black arrows), leading to an increase in drug release.

Additionally, the encapsulation of drug-loaded micro-/nanoparticles into electrospun fibers has been reported as an emerging method for controlling drug release. In this system, the combination of micro-/nanoparticles with a large capacity for containing drugs and the electrospun fibers can change the drug diffusion pathway. The drug molecules have to first diffuse out of the particles, then overcome the barrier created by the electrospun fibers, and finally reach the release medium, which may result in a low initial burst followed by a longer-term drug release process. For example, Hu et al. [207] fabricated electrospun composite fibers by incorporating ibuprofen (IBU)-loaded modified mesoporous silica (MMS) nanoparticles into electrospun poly(L-lac-tide) (PLLA) fibers (PLLA-MMS-IBU fibers) to achieve long-term (over 100 days) controlled drug release (Fig. 7a–e). The composite fibrous membranes were also applied in long-term anti-inflammation and anti-adhesion to prevent peritendinous adhesions [208]. Particles were also combined with electrospun fibers in other forms. Mickova et al. [209] reported that they embedded drug-loaded liposomes into electrospun core-shell fibers with PVA as the inner core and PCL as the outer shell, as shown in Fig. 7f, with the potential for this system to be used to control the release of TGF-β, IGF-4, bFGF and other growth factors. Ionescu et al. [210] electrospun drug-loaded microspheres (10 μm to 20 μm in diameter) into sacrificial PEO fibers combined with slow-degrading PCL fibers. After the removal of the sacrificial component, the microspheres remained securely entrapped in the gap of PCL fibers (Fig. 7g). Another system which combined microspheres with electrospun fibers used electrosprayed vascular endothelial growth factor (VEGF)-encapsulating PLGA microparticles with positively charged surfaces onto negatively charged electrospun PLA microfibers, forming an angiogenic microfiber/microparticle composite patch (Fig. 7h) [211]. In addition to the aforementioned polymeric micro-/nanoparticles, some inorganic nanomaterials such as carbon nanotubes [56] or Fe_3O_4 nanoparticles [212], which can adsorb drugs and decrease the diffusion rate of drugs in the polymer matrix, were also encapsulated into the electrospun fibers to control the drug release.

4.1.1.2. Controlled release of multiple drugs. The treatment of some diseases (*e.g.,* combined chemotherapy for a malignant tumor) and the repair of some defective tissues (*e.g.,* regeneration of bone defect) requires a staggered release of various therapeutic drugs or growth factors in order to achieve the best outcome. Therefore, multi-drug loading and the programmable release of each drug species are important goals to achieve in electrospun fibrous drug delivery systems. So far, the most effective ways to realize a controlled independent release of each agent in a fibrous system require loading different drugs in different domains in the individual fiber or within the fiber mats, creating different drug diffusion paths and resulting in different release rates. In other words, differences in the spatial distribution of drugs may achieve variations in release time or may program the release of each drug species. Specifically, several techniques may aid in achieving the goals above, including the following: embedding drugs with different hydrophobicities in the same polymeric nanofiber matrix, incorporating different drug-loaded particles into electrospun fibers, loading different drugs into the inner or outer layer of core-shell fibers, or altering the composition of different drug-loaded fibers.

Embedding drugs with different hydrophobicities in the same polymeric nanofiber matrix is a simple way to realize sequential and distinct release of drugs. For example, Li et al. [213] loaded both hydrophobic dexamethasone (DEX) and hydrophilic green tea polyphenols (GTP) into electrospun PLGA fibers. The hydrophobic DEX molecules inside the fiber matrix only released from the channels formed after the early release of the hydrophilic GTP molecules.

The method of incorporating different drug-loaded particles into electrospun fibers is an effective and relatively simple way to incorporate different drugs into the same fiber matrix (*e.g.,* hydrophilic and hydrophobic drugs in the same fibers). For example, Dong et al. [214] described the successful encapsulation of two distinct compounds as separate domains within a single electrospun fiber, achieved by first directly synthesizing two sets of PVA nanoparticles, one set containing Texas-Red labeled BSA protein and the other set containing Alexafluor 488-labeled epidermal growth factor. These nanoparticles were embedded in a biocompatible polymer (PU or PLGA) through a single-emulsion method. Second, the mixing of these nanoparticle-containing solutions followed by electrospinning of this combination achieved separate drug domains within the fibers. Eunmin et al. further studied the drug release of these particle-loaded fibers [215]. First, they

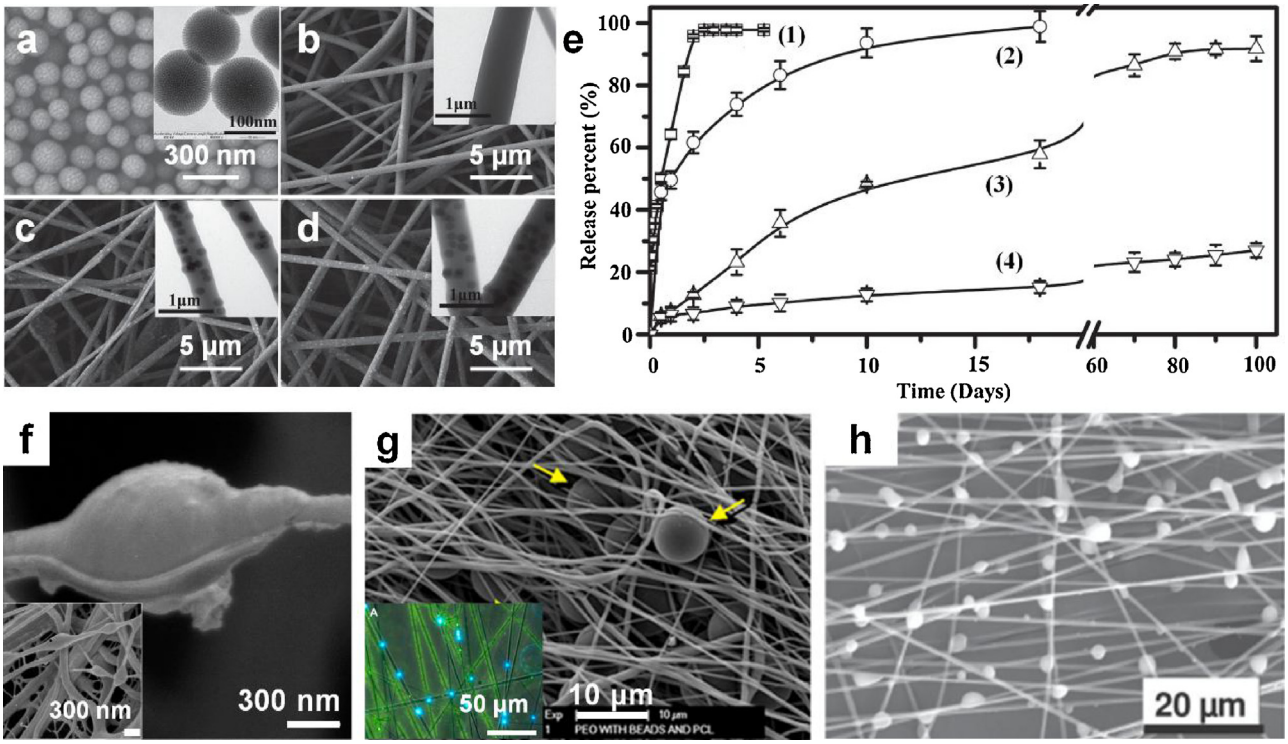

Fig. 7. a–e) Encapsulation of the ibuprofen (IBU)-loaded mesoporous silica nanoparticles (MMSNs) into electrospun PLLA fibers for long-term controlled drug release [207]; SEM images and TEM images (inset) of a) MMS-IBU and b–d) electrospun PLLA-MMS-IBU composite fibers with different drug content; e) *in vitro* IBU release profiles of (1) MMSNs, (2) PLLA-IBU9, (3) PLLA-MMS10-IBU5 and (4) PLLA-MMS15-IBU15; f) SEM images of lipsome-embbed core-shell (PVA-PCL) nanofibers [209]; g) SEM image and fluorescent image (inset) of an anisotropic nanofiber/microsphere composite and in the inset, blue represents microsphere, green represents PCL fibers and black represents PEO fibers [210]; h) the SEM image of an angiogenic microfiber/microparticle composite [211]. (For interpretation of the references to colour in this figure legend, the reader is referred to the web version of this article.)

Sources: a–e) [207], Copyright 2012. Reproduced with permission from John Wiley & Sons Inc; f) [209], Copyright 2012. Reproduced with permission from the American Chemical Society; g) [210], Copyright 2010. Reproduced with permission from Elsevier Ltd; h) [211], Copyright 2011. Reproduced with permission from John Wiley & Sons Inc.

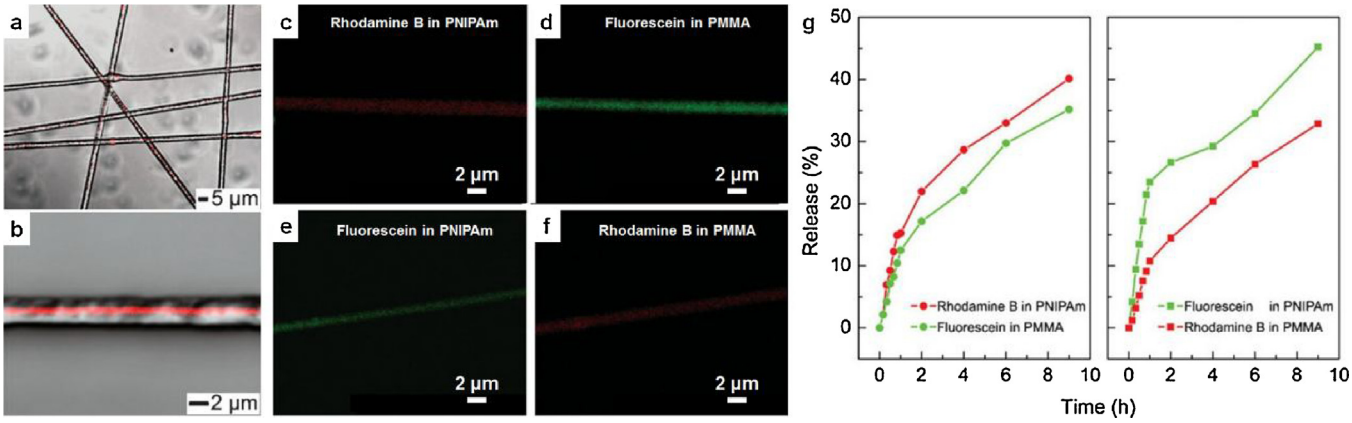

Fig. 8. a–b) CLSM images of colloids-loaded PCL core-shell (inearly arranged colloids-PCL) fibers; c–f) CLSM images of electrospun fibers containing fluorescein or Rhodamin B loaded crosslinked PMMA or PNIPAm colloids; g) release profiles of fluorescein and Rhodamin B from different samples.

Sources: [215], Copyright 2009. Reproduced with permission from John Wiley & Sons Inc.

mixed colloidal particles with PCL and successfully electrospun the mixture into fibers. These electrospun fibers consisted of a linear array of colloidal particles at the core and the PCL as a shell, as shown in Fig. 8a and b. Then, they prepared crosslinked PMMA and poly(N-isopropylacrylamide) (PNIPAM) particles containing the model drugs (fluorescein or Rhodamine B), followed by electrospinning the mixture of these two different particles containing different drugs and the PCL. Finally, they obtained core-shell fibers loaded with two drugs, as shown in Fig. 8(c–f). The two model drugs, as shown in Fig. 8g, followed two distinct release rates due to the differences in swelling behavior of the two colloids, resulting in distinct release pathways for each drug. Furthermore, it is obvious from the release curves that exchanging the carrier of the two drugs would lead to an exchange of the release rates, proving that these particle-containing fibrous drug delivery systems can realize the programmed release of multi-agents.

Further developments of these electrospun micro-/nanoparticle-loaded composite fiber systems include advancements in the way the drugs are loaded. For example, different drugs can be introduced in the particles and the fiber

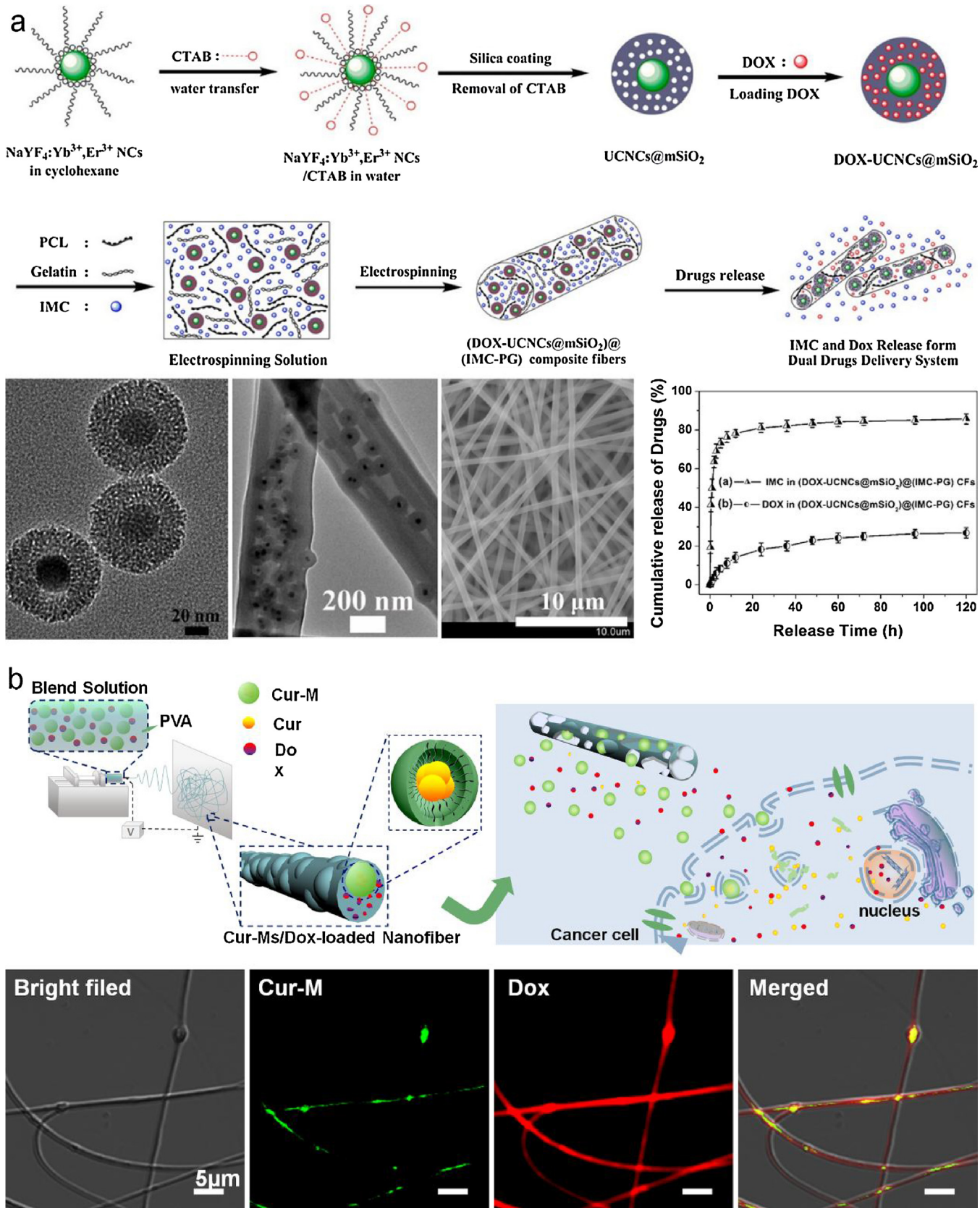

Fig. 9. a) The preparation and characterization of PCL/gelatin composite electrospun fibers containing doxorubicin-loaded silica nanoparticles and indomethacin and the release profiles of the two drugs [217]. b) The Upper panel is the schematic illustrations of the fabrication of the electrospun micelles/drug-loaded nanofibers, the time-programmed release of micelles and Dox from the nanofibers, the delivery of released micelles and Dox into cancer cells. The lower panel is the confocal laser scanning microscopy images of the micelles/drug-loaded nanofibers [218].

Sources: a) [217], Copyright 2013. Reproduced with permission from the American Chemical Society; b) [218], Copyright 2014. Reproduced with permission from John Wiley & Sons Inc.

matrix at the same time [216]. Due to the different release pathways of the drug in the matrix versus the drug in the particles, there should be distinct release profiles. Based on this hypothesis, Hou et al. [217] loaded doxorubicin-loaded silica nanoparticles and indomethacin into PCL/gelatin composite nanofibers and successfully achieved the individual release of the two drugs (Fig. 9a). Our group also incorporated polymeric micelles into electrospun nanofibers to realize time-programmed multi-agent release [218] (Fig. 9b). Because the fiber matrix is PVA, a water-soluble polymer, both the drug and the drug-loaded micelles can simultaneously release from the nanofibers in an aqueous environment. Over time, the drug in the micelles will gradually release. Thus, the electrospun micelle/drug-loaded nanofiber system accommodates multiple drugs safely embedded within the fiber matrix and enables the independent control of each drug release.

In addition to the approaches above, core-shell fibers are another effective method for controlling the release of different drugs, because the shell and core layers of the fiber can encapsulate different drugs. Su et al. [219] used rhodamine B and bovine serum albumin (BSA) as model drugs and compared the release profiles under different situations, including loading both drugs into the same layer (core or shell) and loading different drugs into the two different layers. They found that when either drug was in the shell layer, an obvious initial burst release would occur and the release rate was relatively fast. When a drug was loaded in the core layer, the initial burst release was suppressed and the release rate decreased.

Furthermore, electrospun layered fiber mats can also effectively control the release of a variety of drugs. Okuda et al. [206] reported the fabrication of a multilayered drug-loaded poly(L-lactide-co-ε-caprolactone) (PLCL) nanofiber mesh used for time-programmed dual release (Fig. 10). The top layer of the mesh was the carrier for drug ChroB, the second layer was a barrier mesh, the third layer was carrying another drug (5, 10, 15, 20-tetraphenyl-21H, 23H-porphinetetrasulfonic acid disulfuric acid, TPPS), and the bottom was a basement mesh. There were obvious differences in the release profiles of the two drugs, due in part to the barrier mesh. The chromazurol B (ChroB) from the top layer demonstrated an obvious initial burst release, while the TPPS in the third layer had a weaker initial burst release and a relatively slow release. From Fig. 10e and f, it can also be seen that thinner drug-loaded fibers led to faster drug release rates, while a thicker barrier mesh caused a slower release rate.

4.1.1.3. Stimuli-responsive release of drugs. Recently, more and more researchers have investigated electrospun fibrous drug delivery systems based on stimuli-responsive polymers [220,221]. These fibers respond to external stimulation, accompanied by corresponding changes in the physical and chemical properties of the polymers. In accordance with the different types of stimulation [222], these stimuli-responsive fibers can be divided as follows: physical stimulus-responsive electrospun fibers (*e.g.,* temperature-responsive fibers [223,224], magnetic field-responsive fibers [225–227], light-responsive fibers [228], electro-responsive fibers [229]), chemical stimulus-responsive electrospun fibers (*e.g.,* pH-responsive fibers [230], humidity-responsive fibers [132], gas-responsive fibers [231,232], ethanol-responsive fibers [233], reduction-responsive fibers [234], glucose-responsive [235] and protein-responsive fibers [236]) or multi stimuli-responsive fibers [237–239]. Theoretically, the application of these stimuli-responsive electrospun fibers in a drug delivery system may provide a more precisely controlled drug release, in contrast to the fibrous drug delivery systems above. For example, Kim et al. [227] fabricated dual-responsive electrospun fibers containing both doxorubicin and magnetic nanoparticles within a fiber matrix made from a temperature sensitive polymer, poly(N-isopropylacrylamide). By applying an alternating magnetic field to the fiber mats, the magnetic nanoparticles inside the fiber matrix responded and produced heat periodically, causing the polymer to swell or shrink and effectively controlling the DOX release rate (Fig. 11a–c). Li et al. [224] in our group developed a novel nanogel-in-microfiber drug delivery system (Fig. 11d and e) whose release can be switched on and off in response to a temperature change. Thermo-sensitive poly(N-isopropylacrylamide) (PIPAAm) nanogels were embedded within the shell layer of the electrospun core-shell nanofibers, a material which could shrink or swell in response to a variation in the environmental temperature, resulting in the formation or disappearance of nanochannels between the nanogel and shell matrix. Thus, a variation in shell permeability was created, which served as a valve to control the release of the encapsulated drug in the core layer. From the release profiles (Fig. 11e), it can be found that for the nanogel-in-microfiber device (E2), a more obviously temperature-switched reversible release of the model drug (methyl orange (MO)) was presented, where the MO concentration increased sharply at 40 °C, while increased slightly at 20 °C in all cycles. After three cycles, the cumulative drug release of E2 approached 92.72% ± 5.19%. While for the no nanogel device (E1), a relative slow and sustained release pattern was found owing to the direct diffusion of MO from the hydrophobic PCL shell, and the cumulative drug release of E1 approached only about 40%.

4.1.2. Oral drug delivery

Electrospun nanofibers were also found to be useful in the oral delivery of poorly soluble drugs, since the high surface area to volume ratio enhances the dissolution rate of the nanosized drugs embedded in the nanofibers [240]. Soluble polymers (such as PVA and gelatin) were always employed. Yu et al. [241] developed an oral, fast-dissolving drug delivery membrane (FDM) prepared from electrospun PVP ultrafine fibers loaded with IBU. They found that the fast-dissolving drug delivery membrane with different doping concentrations of the drug had almost the same wetting and disintegrating time at approximately 15 s and 8 s, respectively; and 84.9% and 58.7% of the IBU were released within the first 20 s for FDM with a drug-to-PVP ratio of 1:4 and 1:2, respectively. Li et al. [242] also used PVA as the filament-forming polymer and drug carrier to fabricate a fast-dissolving drug delivery system by electrospinning. Caffeine and riboflavin were used as the model drugs. They found that the PVA/caffeine and PVA/riboflavin nanofibrous mats had almost the same dissolution time (approximately 1.5 s) and wetting time (approximately 4.5 s). The *in vitro* release study showed that the drugs were released in a burst manner (the caffeine to an extent of 100% and the riboflavin to an extent of 40% within 60 s) from the PVA nanofibrous matrices. Nam et al. [243] employed PVA and Soluplus (SP)-based electrospun nanofiber mat for the delivery of Angelica gigas Nakai (AGN) extract to oral cancers. The AGN-loaded PVA/SP electrospun nanofiber (AGN/PVA/SP NF) mat possesses an average diameter of 170 ± 35 nm and an entrapment efficiency of 84.6 ± 18.6%. As compared to the AGN-loaded PVA (AGN/PVA) nanofiber mat, the AGN/PVA/SP nanofiber mat presented instant wetting (within 2 s) and rapid disintegration (within 3 min) properties (Fig. 12a). Aduba Jr. et al. [244] fabricated electrospun gelatin nanofiber scaffolds for oral mucosal drug delivery. They used the photoreactive polyethylene glycol diacrylate as a cross-linker to stabilize the scaffold by forming a semi-interpenetrating network gelatin nanofiber scaffold. The mucin absorption studies suggest that these scaffolds will likely encourage mucoadhesion.

4.1.3. Transdermal drug delivery

Transdermal delivery represents an attractive alternative to the oral delivery of drugs. Because electrospun fibers not only possess a high surface area to volume ratio and a high porosity but also

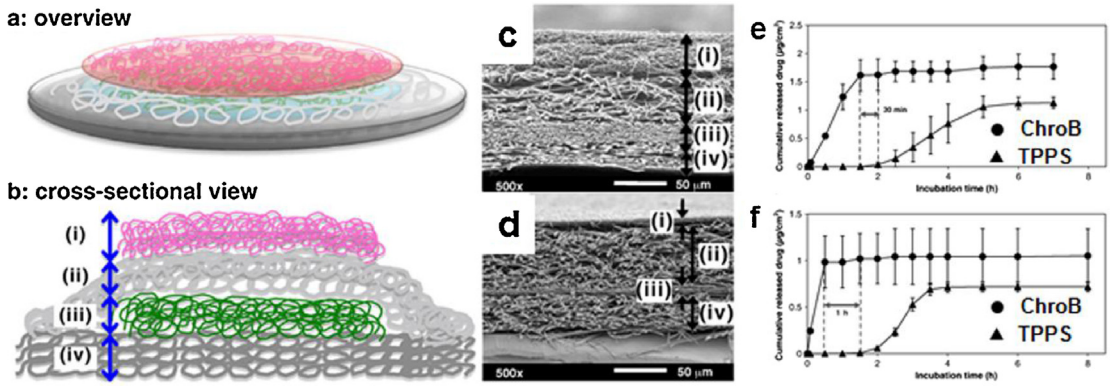

		Composition	Fiber diameter	Mesh thickness
Construct c	First drug loaded mesh	ChroB + PLCL 75:25	490 ± 230 nm	38 ± 7.0 μm
	Barrier mesh	PLCL 75:25	1.3 ± 0.6 μm	58 ± 8.0 μm
	Second drug loaded mesh	TPPS + PLCL 75:25	610 ± 200 nm	19 ± 2.0 μm

		Composition	Fiber diameter	Mesh thickness
Construct d	First drug loaded mesh	ChroB + PLCL 75:25	130 ± 30 nm	6.0 ± 1.0 μm
	Barrier mesh	PLCL 75:25	1.2 ± 0.4 μm	54 ± 5.0 μm
	Second drug loaded mesh	TPPS + PLCL 75:25	150 ± 20 nm	5.0 ± 1.0 μm

Fig. 10. a–b) Schematic diagram of multilayered drug-loaded nanofiber meshes; c–d) cross-sectional SEM observations of multilayered nanofiber meshes with different layer thickness, in which i) stands for ChroB-loaded fiber mat, ii) stands for barrier fiber mat, iii) stands for TPPS-loaded fiber mat, iv) stands for basal fat mat; e) the drug release profiles of samples in c); f) the drug release profiles of samples in d); the table below shows the corresponding thichness of different layers.

Sources: [206], Copyright 2010. Reproduced with permission from Elsevier Ltd.

a large amount of candidate polymers are available, the application of electrospun fiber mats in transdermal drug delivery system appears promising. To date, several groups have fabricated various transdermal drug delivery systems based on electrospun polymeric fibers. For example, Taepaiboon et al. [245] reported the use of electrospun cellulose acetate nanofiber mats as carriers for the transdermal delivery of model vitamins. Madhaiyan et al. [246] used polycaprolactone nanofibers as a carrier to achieve a sustained release of Vitamin B_{12}, a molecule well-suited for transdermal patch applications, as is demonstrated in Fig. 12b. Yun et al. [229] fabricated an electro-responsive transdermal drug delivery system by electrospinning PVA/poly(acrylic acid) (PAA)/multi-walled carbon nanotubes (MWCNTs) nanocomposites. The uniform distribution of the oxyfluorinated MWCNTs in the nanofibers imbued this system with electro-responsive swelling and drug releasing behaviors. Li et al. [213] fabricated electrospun PLGA fibers containing 15 wt% dexamethasone (DEX) and 10 wt% green tea polyphenols (GTP) as an effective transdermal treatment of keloid (Fig. 12c). They fixed the fiber mesh onto the keloid model in the subcutaneous tissue of athymic nude mice by suture. The fiber mesh was sterilized and soaked in physiological saline in advanced. During the treatment, the fiber meshes were wetted by dropping saline into it every other day. After 3 months' treatment, the results of histological analysis showed that most of the hyalinized collagen fibers were disappeared and the loose, thin and small collagen bundles appeared in the keloid, indicating these dual drugs-loaded fiber meshes represented an effective transdermal treatment of keloid. Cheng et al. [247] reported a facile approach for biofunctionalization of PLGA fibrous scaffolds with various molecules, such as PEG polymer (for cell repellent), Arginine-Glycine-Aspartic (RGD) peptide (for cell adhesion) and bFGF growth factor (for cell proliferation) *via* mussel-inspired poly(dopamine) (PDA) coating in aqueous solution, with negligible effects on the scaffold properties (*e.g.*, drug activity and loading ratio). They also demonstrated that the ginsenoside-Rg3-loaded fibrous scaffold modified with bFGF growth factor was able to promote the early-stage wound healing in rabbit ear wounds (bio-signal from bFGF), and inhibit later-stage hypertrophic scars formation (release of Rg3 drug), after implantation for 14 days.

4.1.4. Implantable drug delivery systems

Electrospun fibers have also been widely used in implantable drug delivery systems, especially in anticancer studies. For many of these *in vitro* anticancer studies and anticancer drug screening, electrospun fibers are used as carriers of anticancer drugs or nucleic acids co-cultured with cancer cells; thus, the loading drugs or nucleic acids are released into the culture medium and impact the growth of cancer cells [56,205,248,249]. Regardless of the fact that large differences exist between these experimental studies and practical cancer therapies in a clinic, the drug-loaded nanofibers are useful for drug screening, pre-evaluation of drugs or carriers before *in vivo* experiments or as a platform to investigate the physiological characteristics of tumor cells.

In vivo anticancer implants are actually an effective local drug delivery system. Compared with systemic administration (*e.g.*, intravenous (i.v.) injection), antitumor implants effectively ensure the drug concentration is at a relatively high level near the tumor tissues and reduce the distribution of the drug in surrounding normal tissues, thereby reducing side effects [250–252]. Additionally, implants decrease the drug administration time, which lessens the pain felt by patients [252]. Because electrospun fibers effectively control drug release and are easy to degrade *in vivo*, electrospun drug-loaded fibers are a promising local drug delivery system. So far, several studies regarding electrospun drug-loaded fibers as antitumor implants have been reported [253–256]. The antitumor efficacy of the implants was evaluated mainly according to the tumor size or weight changes and the histological analysis after the treatment, while animal body weight as well as survival rate was always used to evaluate the safety of the implants. The fibrous antitumor implants are used differently according to the

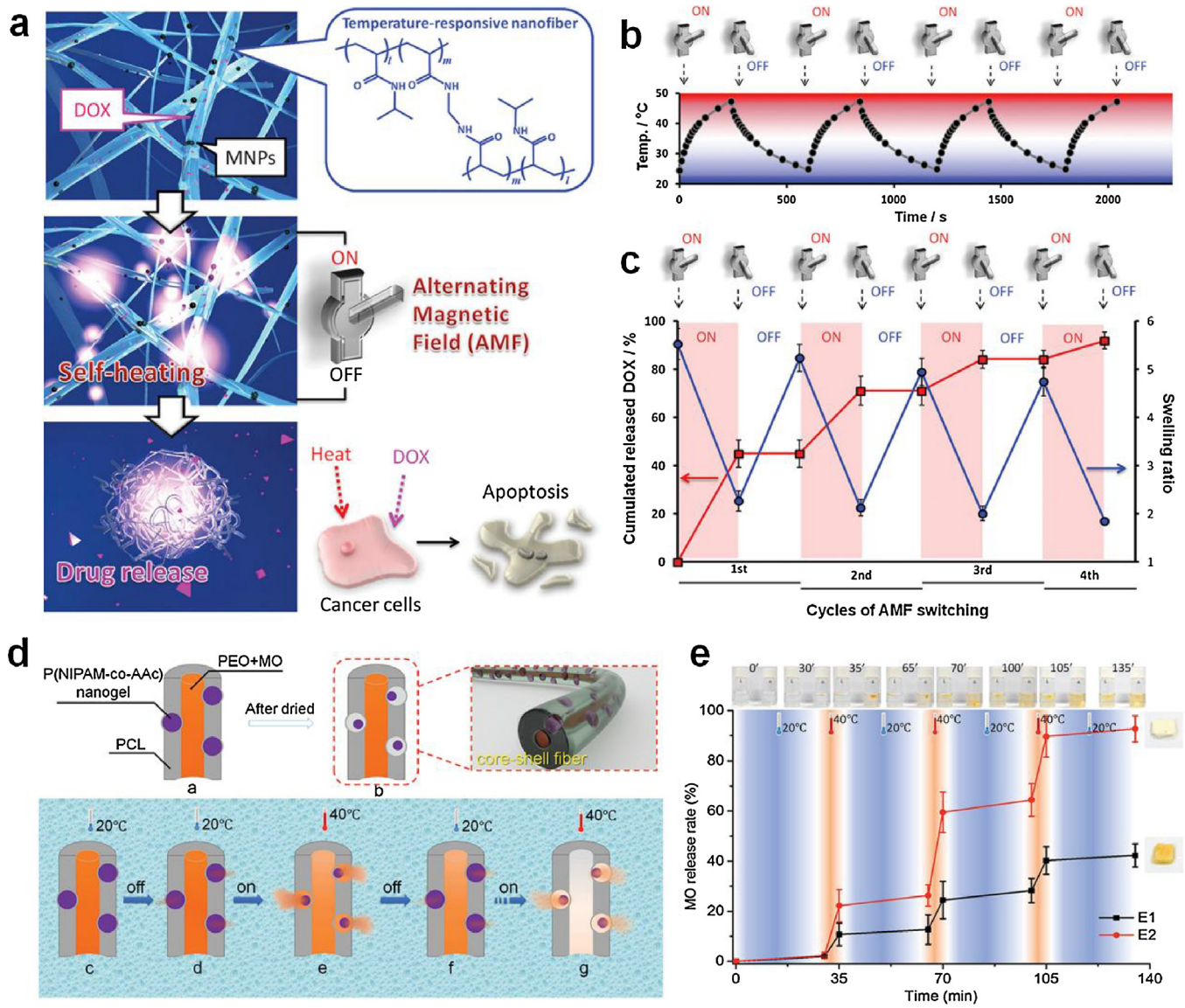

Fig. 11. a–c) A smart hyperthermia nanofiber system [227]. a) The schematic diagram of the drug release mechanism of a smart hyperthermia nanofiber system that utilizes magnetic nanoparticles dispersed in temperature-responsive polymers, incorporating doxorubicin, as responsive to stimulation of alternating magnetic field; b) Temperature changes of the nanofibers under the stimulation of alternating magnetic field; c) the drug release profile and the swelling ratio of the nanofiber system under the stimulation of alternating magnetic field. d, e) a nanogel-in-microfiber device that can thermally switched release drugs in the core [224]. d) The illustration of thermally switched drug release mechanism of electrospun nanogel-in-microfiber device (E2) under lower-to-higher temperature conversion. e) The drug release performances of no nanogel fiber device (E1) and E2 under lower-to-higher temperature conversion for three cycles. Images on top are digital photos of E1 and E2 taken at different time point and images on right are digital photos of E1 and E2 after 135 min of drug release.

Sources: a–c) [227], Copyright 2013, d, e) [224], Copyright 2015. Reproduced with permission from John Wiley & Sons Inc.

specific circumstances of each case. For example, our group [257] developed an implantable, active-targeting micelle-in-nanofiber device (Fig. 12d) in which the Dox-loaded active-targeting micelles were enveloped in the core (PVA) of the core-shell polymeric nanofibers, and the outer shell layer consists of cross-linked gelatin. We implanted this device subcutaneously into 4T1 (murine breast cancer cell) tumor-bearing Balb/c mice near solid tumors in order to test the antitumor effects and found that over the same duration (21 days) for either treatment, the implantable nanofiber device groups displayed comparable tumor growth suppression compared with the intravenously delivered Dox formulations (free Dox and Dox-loaded micelles), even though the intravenously delivered Dox formulations were injected 4 times (total Dox dosage: 8 mg/kg) and the nanofiber devices were implanted only once (2 mg/kg). What's more, for comparison, the intravenously delivered Dox formulations were also injected only once to 4T1 tumor-bearing Balb/c mice at an equivalent Dox dose of 2 mg/kg in the very beginning of the treatment, and we found that after 21 days, the mean tumor volumes of all the intravenously delivered Dox formulations groups were over 1000 mm^3, which were much larger than the nanofiber groups (less than 500 mm^3), suggesting that under the same dosage of Dox (2 mg/kg), implantable nanofiber groups performed much better antitumor effect than the once-injection of free Dox or Dox-loaded micelles groups. In addition, the body weight of mice in the nanofiber devices groups have not change much and even had a slight increase, as compared with control groups (saline group or blank-nanofiber groups), and the mice in the active-targeting micelle-in-nanofiber device group also had a relative higher survival rate (over 33%, after 42 days of treatment), suggesting this active-targeting micelle-in-nanofiber device possesses a low toxicity to the body. Zong et al. [258] established an orthotopic mice model of cervical/vaginal cancers by directly injecting U14 cells

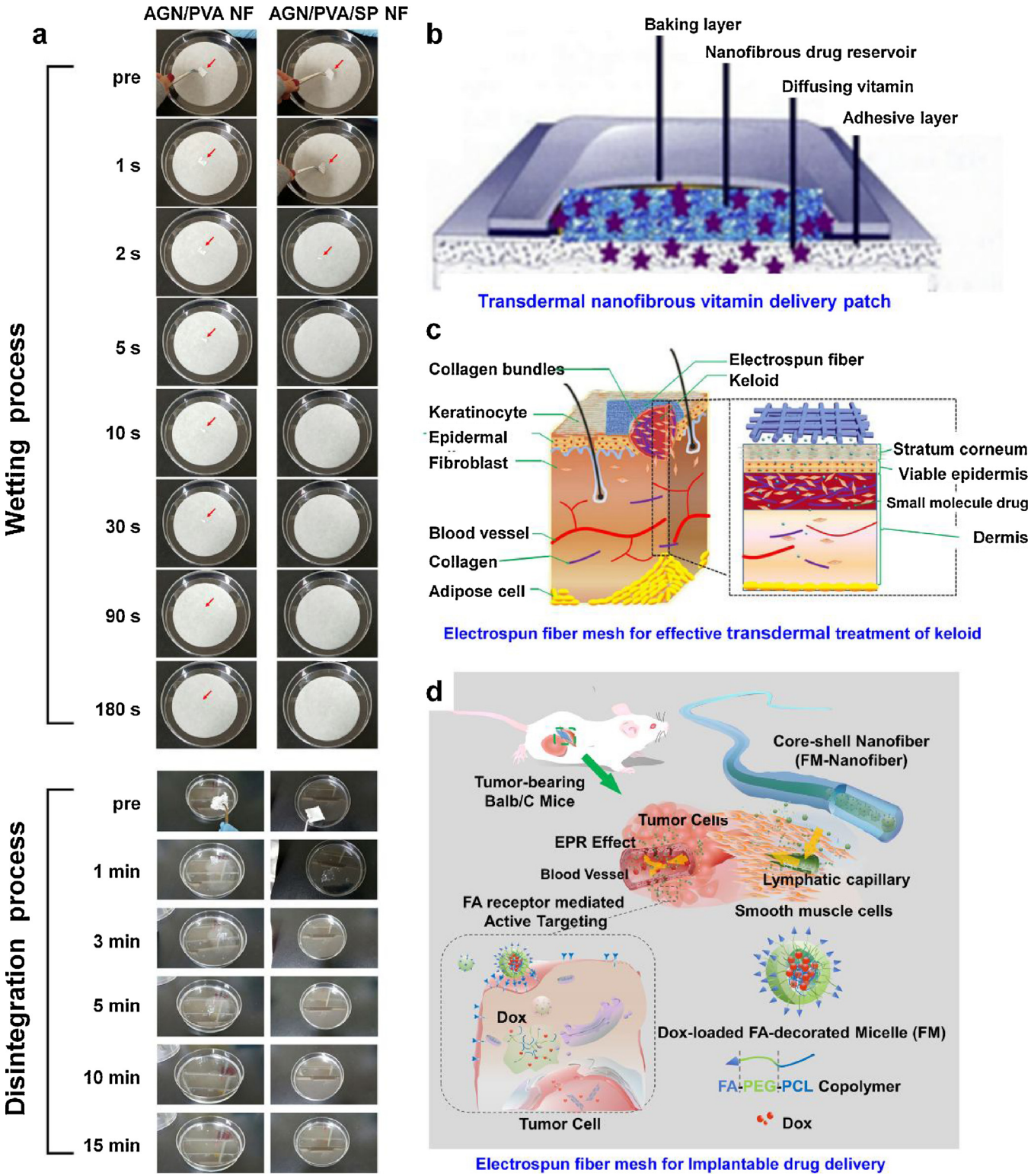

Fig. 12. a) Photographs of the wetting and disintegration process of oral drug delivery membranes. The AGN/PVA/SP NF membrane is fabricated from a PVA and soluplus (SP)-based nanofiber (NF) membrane containing the *Angelica gigas* Nakai (AGN) extract, used for oral cancer therapy. The AGN/PVA NF membrane is made from AGN-loaded PVA nanofibers [243]. b) Electrospun nanofibrous transdermal vitamin B_{12} delivery system [246]. c) Electrospun ultrafine fibrous transdermal dexamethasone and green tea polyphenols system for effective treatment of keloid [213]. d) An implantable active-targeting micelle-in-nanofiber device for cancer therapy [257].

Sources: a) [243], Copyright 2017, b) [246], Copyright 2013. Reproduced with permission from Elsevier Ltd; d) [257], Copyright 2015. Reproduced with permission from the American Chemical Society.

into the vaginal submucosa of female KM mice nearby the cervix in situ. Then they implanted 10% cisplatin-loaded PLA/PEO composite fiber membranes into the vaginal canal of female KM mice to treat the cancers. For comparison, group of the *i.v.* injection of cisplatin was also applied, and repeatedly administrated for three times on day 0, 3, and 6. After 9 days' treatment, the tumor inhibition rate

values of implantable fiber groups and *i.v.* injection groups, calculated according to the tumor weights, were ordered as follows: 70.5% (cisplatin/i.v group (5 mg/kg)) > 68.3% (cisplatin/fiber group (10 mg/kg)) > 61.6% (cisplatin/i.v group (2.5 mg/kg)) > 52.7% (cisplatin/fiber group (5 mg/kg)). However, there was a sharp decline in the body weight of mice receiving cisplatin injection with average weight losses of 30.6% (5 mg/kg) and 12.1% (2.5 mg/kg) on day 9, and only half mice in group of cisplatin/i.v group (5 mg/kg) survived past 9 days. In comparison, there was only a weight loss of 2.8% in the mice of cisplatin/fiber group (5 mg/kg) and all animals survived all along. Taking all these results into consideration, the authors believed that cisplatin-loaded fibers was able to preferred partition of cisplatin in vaginal tract, reasonable distribution in rectum, uterus and tumor, while very low concentration in peripheral organs, achieving a good balance between the safety and anti-tumor efficacy compared to *i.v.* injection of cisplatin. Luo et al. [259] injected hepatoma H22 cells into Kunming mice subcutaneously to form solid tumors and used hydroxycamptothecin (HCPT)-loaded core-sheath PELA (HCPT/PELA) fibers as intratumoral implants against an H22 tumor model. After 14 days' treatment, they found that the tumor sizes of different groups increased as follows: over 500% (both saline group and empty PELA fibers group) > about 420% (free HCPT group) > about 256% (HCPT/PELA fibers group), indicating the HCPT/PELA fibers had better tumor suppression, which may be owing to the sustained release of HCPT from fibers can continuous inhibit the tumor growth. Kaplan et al. [260] established a Lewis lung cancer model subcutaneously in the backs of C57BL/6 female mice. When the tumors reached 300 mm^3, they removed the tumors and threated the mice for preventing local cancer recurrence in different ways: 1) a cisplatin-loaded superhydrophobic electrospun polycaprolactone/poly(glycerol monostearate-co-caprolactone) (PCL/PGC-C18) nanofiber mesh (13.2 mg/kg equivalent dose) implanted at the resection site; 2) implantation of an unloaded superhydrophobic mesh; 3) implantation of an unloaded superhydrophobic mesh and intraperitoneal (i.p.) cisplatin (2 doses × 6.6 mg/kg); or 4) only i.p. cisplatin 2 doses × 6.6 mg/kg. After treatment, the resected control animals without chemotherapy were found to develop local recurrences within a median of 6 days, and both the ways of 3) and 4) did not significantly increase median freedom from local recurrence. While the median freedom from local recurrence was significantly increased for mice treated with cisplatin-loaded meshes compared to those treated with i.p. cisplatin, with median recurrence-free survival to over 23 days. Zhang et al. [261] attached both multi-walled carbon nanotubes and doxorubicin-containing PLLA fiber mats into an established cervical cancer model under the mouse's armpit; then, since the carbon nanotubes were able to effectively generate thermo by absorbing near-infrared radiation (NIR), they performed NIR radiation photothermal therapy combined with chemotherapy to effectively inhibit the growth of the tumor. The NIR radiation could initiate burst release of DOX from the fibers owing to the relatively low glass transition temperature of PLLA, and significantly increase the temperature of fibers-covering tumor site.

In addition to anticancer studies, electrospun fibers have also been used as implantable devices as a potential therapy for gout attacks, anti-viral and antibiotics, as well as surgical applications. For example, Wang et al. [262] developed luteolin-loaded electrospun PCL/gelatin composite fibrous mats and implanted them near the gout sites of the New Zealand rabbits' knees. They found that these implantable devices alleviated acute gouty arthritis and may offer a potential gout therapy for overcoming recurrent attacks. Blakney et al. [195] reviewed the application of electrospun fibers in vaginal anti-HIV drug delivery. According to their oppinions, drug-eluting fibers can be designed to achieve multiple design constraints in a single product for topical HIV prevention, because electrospun fibers are able to deliver diverse agents, incorporate multiple agents *via* composites, and facilitate controlled release for pericoital and sustained (coitally-independent) use, and it is technologically feasible to scale-up. However, challenges of using electrospun fibers still exist, like issues related to vehicle deployment, spreading and retention in the vaginal vault, the unknown safety and toxicity of the interaction of the fibers with the mucosal environment, and difficulties in precisely controlled release of multiple drugs from a single electrospun fiber mat.

The application of electrospun fibers in local and sustained delivery of antibacterial agents is promising for the treatment of recurrent and chronic infections, especially in cases involving antibiotic-resistant bacteria [133,263]. Song et al. [264] fabricated a PLLA electrospun fibrous membrane containing levofloxacin (Lev) and silver loaded mesoporous silica nanoplatform (Lev@MSN@Ag) *via* blending electrospinning for the treatment of drug-resistant bacterial infections. These Lev@MSN@Ag–PLLA electrospun fibrous membrane, with low concentrations of drugs (28 μg/mL Lev and 12 μg/mL Ag), shows superior antibacterial ability against drug-resistant strains (methicillin resistant staphylococcus aureus, MRSA) with a concentration of 5×10^5 CFU/mL in the *in vitro* test. Furtherly, the *in vivo* study demonstrated that these fibers could significantly inhibited bacterial growth and infection over 8 weeks. Ashbaugh et al. [263] developed an electrospun composite coating comprised of PLGA nanofibers embedded in a PCL film for locally co-deliver combinatorial antibiotics (either linezolid (Lin), vancomycin (Van), daptomycin (Dap) or rifampin (Rif)) from the implant surface. The release of each antibiotic would be adjusted by loading each drug into the different polymers or by varying PLGA/PCL polymer ratios. The authors used an *in vivo* (mouse) model of prosthetic joint infection (PJI) to evaluate the PLGA/PCL composite-coated K-wires (an implant) against *S. aureus* (strain Xen36, which possesses a stable bioluminescent construct). Three different combinations of antibiotic-loaded coatings (Van/Van + Rif, Lin/Lin + Rif and Dap/Dap + Rif each) were placed in the right femoral intramedullary canal of mice and *S. aureus* (1×10^3 CFU) was pipetted directly onto the protruding implant in the knee joint before closure. The *in vivo* bioluminescence imaging was applied to noninvasively monitor the bacterial burden and CFU from the homogenized bone/joint tissue samples and from the sonicated implants were assayed on day 14. Results showed that bioluminescence imaging signals from all these three different combinations of antibiotic-loaded coatings approached background levels and had <100 CFU (Van/Van + Rif) or no CFU (Lin/Lin + Rif and Dap/Dap + Rif) in the bone/joint tissue and no CFU detected from the implants, indicating these combinations of antibiotic-loaded coatings were highly effective in preventing infection of the bone/joint tissue.

The electrospun fibers were also employed for preventing tissue adhesions, one of the most common postsurgical complications and compromised the quality of patients' life, occurring simultaneously as the damaged tissue heals and accompanied with inflammation, pain and even dyskinesia in particular circumstances [265]. For example, Bölgen et al. [266] reported an antibiotic embedded electrospun PCL membranes for prevention of abdominal adhesions. The antibiotic (Biteral®) solution was dropped slowly and distributed evenly on the electrospun PCL membrane, then absorbed and embedded by the membrane. The antibiotic embedded PCL membranes were implanted on the right side of the abdominal wall on a rat model, which significantly eliminated postsurgery abdominal adhesions, and improved healing. The prevention of peritendinous adhesions by using electrospun fibers was also reported. Jiang et al. [267] incorporated Celecoxib into PELA fibrous membranes *via* electrospinning and found that these Celecoxib-loaded PELA membranes could down-regulate ERK1/2 and SMAD2/3 phosphorylation, leading to reduced collagen I and collagen III expression, inflammation reaction, and fibroblast and

tenocyte adhesion and proliferation, and achieving a successful prevention of tendon adhesion in the rabbit. Chen et al. [268] used an electrospun chitosan-grafted polycaprolactone (PCL-g-CS) nanofibrous membrane to prevent peritendinous adhesions, in which the chitosan (CS) layer on the PCL-g-CS nanofibers can prevent more non-specific cell adhesion than PCL nanofibers. For animal study, the authors used a 6 mm × 10 mm piece of PCL nanofibrous membrane, PCL-g-CS nanofibrous membrane or Seprafilm™ (a commonly used commercial anti-adhesion product) to wrapped around the tendon repair site in a rabbit flexor digitorum profundus (FDP) tendon model, where the flexor digitorum superficialis tendons were removed and the FDP tendons were divided and cut (just distal to the chiasm and proximal to the vincula), and then repaired with sutures. The *in vivo* peritendinous adhesions was evaluated by direct observation 2, 4 and 8 weeks after surgical exploration of the repair sites, and the results showed that the PCL-g-CS nanofibrous membrane possessed the best peritendinous anti-adhesion effect as compared with both the PCL nanofibrous membrane and the Seprafilm™. Besides the application in tendon anti-adhesions, electrospun fibers were also used prevent failed back surgery syndrome (FBSS) recently. Liu et al. [269] incorporated IBU into electrospun fibrous membranes achieving sustained release of IBU for several weeks, which was useful in preventing both acute and chronic inflammation in rats following laminectomy and membrane implantation. The histological analysis further demonstrated this IBU-loaded electrospun fibrous membrane had an excellent anti-adhesion effect, and can reduce the associated neurological deficits.

4.2. Tissue engineering and regenerative medicine

In addition to the application of electrospun fibers in drug delivery systems, these materials are also widely used as scaffolds for tissue engineering due to their inherent structural features. The continuous thin fibers created by electrospinning have the ability to mimic the ECM because of their large surface areas, complex fibrous interfacial topological structure, ease of functionalization, and controllable mechanical properties, and may be an ideal method for fabricating tissue engineering (TE) scaffolds [270,271]. Currently, research in this area is devoted to cell penetration, the incorporation of growth and differentiating factors, the toxicity of solvents used, overall productivity, and the creation of functional gradients. Progress in the use of electrospinning for TE applications is highlighted below. In tissue repair research, various electrospun fibrous scaffolds which mimic native extracellular matrices should be applied in accordance with the natural organization of cells, including the use of random, aligned and 3-D structural fibers in order to adapt to the demands of tissue repair. For example, as shown in Fig. 13a, Liu et al. [166] summarized typical examples of tissues in the human body whose regeneration would benefit from the use of anisotropic structured electrospun nanofiber scaffolds. Here, we review the application of electrospun fibers in various tissue regeneration fields, including wound dressing, vascular tissue engineering, muscle tissue engineering, neural tissue engineering, bone tissue engineering and others.

4.2.1. Wound dressing

Skin, the largest organ of the human body, is composed of three layers, the epidermis, dermis and hypodermis and behaves as a barrier with protective, immunologic, thermoregulatory and sensory functions [272].

Conventional skin substitutes such as autografts, allografts and xenografts have been employed for skin regeneration. Autografts are the gold standard of skin therapies because they are not subject to rejection, and yet, because of limited availability, the risk of donor site morbidity and scar formation, safer substitutes are needed [273,274]. Allografts and xenogafts are more available alternatives but carry the risk of disease transmission and immunological rejection [64,273,275]. Recent attempts have focused on the development of bioengineered substitutes as a promising therapeutic alternative capable of facilitating skin regeneration and wound healing for the treatment of acute and chronic wounds or burns. Several scaffold types, such as films, sponges, micro- and nanofibers made of natural and synthetic polymers, have been developed to date [276].

The high specific surface area of nanofibers is a significant advantage as it enhances fluid absorption, dermal drug delivery and exhibits better absorption of functional proteins such as albumin, fibronectin and laminin on the surface [277]. Moreover, the high porosity of these electrospun nanofibrous scaffolds facilitates the exchanges of oxygen, water and nutrient as well as the removal of metabolic waste. Additionally, the small-sized pores restrain the penetration of harmful microorganisms [40]. Numerous studies on the application of electrospun nanofibrous scaffolds with various components for skin substitutes and wound dressings have been reported. For example, Powell et al. [278] compared freeze-dried and electrospun collagen scaffolds as skin substitutes and found that the electrospun scaffold skin substitutes possessed optimal cellular organization, potentially reducing wound contraction, as shown in Fig. 13b. Zhang et al. [279] utilized coaxial electrospinning to fabricate individually collagen-coated PCL nanofibers (*i.e.,* Collagen-r-PCL in the form of a core-shell structure) and found that the density of human dermal fibroblasts on the core-shell nanofiber membrane increased linearly by 19.5% (2 days), 22.9% (4 days), and 31.8% (6 days) as compared to PCL nanofibers. Qu et al. [280] developed a system in which collagenase was stored inside PEO electrospun nanofibers and released upon hydration. Through a series of *in vitro* and *in vivo* studies, their findings show that the partial digestion of the wound interface improved wound repair by creating a more compliant and porous microenvironment which expedited cell migration to and/or proliferation at the wound margin. Sun et al. [281] constructed a 3-D fibrous scaffolds for accelerated vascularization by using a photocrosslinkable natural hydrogel based on gelatin methacryloyl (GelMA) *via* electrospinning. They found that the ultraviolet (UV) photocrosslinkable gelatin electrospun hydrogel fibrous membranes, possessing soft adjustable mechanical properties and controllable degradation properties, can support endothelial cells and dermal fibroblasts adhesion, proliferation, and migration into the scaffolds, which facilitates vascularization. After the fibrous scaffold was implanted below the skin flap in a rat model, the skin flap survival rate was higher than the control group, and more microvascular formation was observed, which was potentially beneficial for the flap tissue vascularization.

The morphology of an electrospun fiber mat also affects the growth of seeded fibroblasts. For example, the alignment of the fibers may control cell orientation and strengthen the interaction between the cell body and the fibers in the longitudinal direction [282,283]. Furthermore, Ma et al. [284] developed sandwich-type scaffolds as microskin grafts for use in skin regeneration consisting of radially aligned nanofibers as the bottom layer, nanofiber membranes with square arrayed microwells and nanostructured cues as the top layer, and microskin tissues in the middle. The microskin tissues were confined in the square arrayed wells and simultaneously guided by the nanotopographic cues, facilitating the *in vitro* migration of the cultured NIH 3T3 fibroblasts and primary rat skin cells. These sandwich-type transplants displayed an even distribution of those microskin grafts and improved the "take" rate of the microskin tissues, promoting re-epithelialization on the wound. Additionally, the void region in the scaffolds promoted exudate drainage from the wound. Reis et al. [285] reported a electrospun 3-D fibrous construct with an asymmetrical inner structure

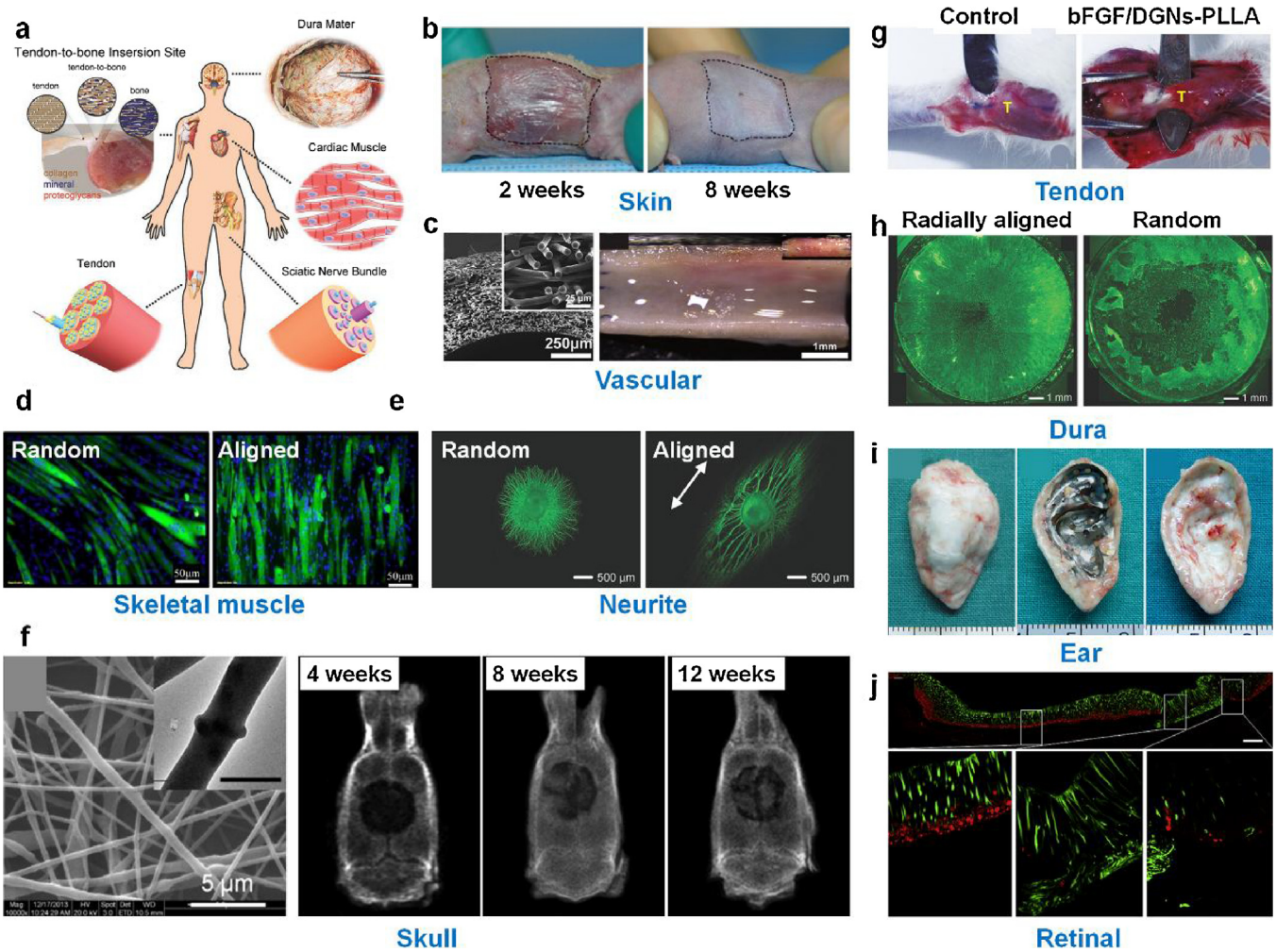

Fig. 13. a) Illustration of typical examples of tissues in the human body whose regeneration would benefit from the use the anisotropic structured electrospun nanofiber scaffolds [166]. b) electrospun nanofiber scaffold for skin regeneration [278]; c) tubular electrospun fibers for artificial blood vessels [293]; d) nanofibers for muscle tissue engineering [303]; e) nanofibers for outgrowth of neurite [312]; f) nanofibers for repair of rat calvarial defect [66]; g) nanofibers for tendon regeneration [322]; h) radially aligned electrospun nanofibers as dural substitutes for wound healing [323]; i) electrospun fibers for engineering ear-shaped cartilage [324]; j) nanofibers for repair of retinal [325].

Sources: j) [325], Copyright 2014; b) [278], Copyright 2007; c) [293], Copyright 2014; d) [303], Copyright 2012; f) [66], Copyright 2014; g) [322], Copyright 2013; i) [324], Copyright 2012. Reproduced with permission from Elsevier Ltd; a) [166], Copyright 2012. Reproduced with permission from John Wiley & Sons Inc; e) [312], Copyright 2009; h) [323], Copyright 2010. Reproduced with permission from the American Chemical Society.

and engineered surfaces for wound healing applications, which possesses thickness of 3.7 ± 0.1 mm and fibrous-based microsized conical protrusions (length: 1000 ± 300 μm; width: 3800 ± 80 μm) at their top side, with a median peak density of 73 peaks per cm^2, while maintaining a non-woven mesh bottom. As this 3-D construct was used as wound dressing, it actively promoted wound healing (90 ± 0.5% of wound closure within 48 h).

Electrospun fibers can also act as assistant materials for wound dressing. For example, Yang et al. [286] built a novel dissolving microneedle (DMN) delivery system on an electrospun pillar array (DEPA), which was able to rapidly implant DMNs into the skin. After the DMNs implanted into the skin, the separation of the DMNs from the fibrous sheet was dependent on both the pillar height and the properties of the fibrous sheet. Zhao et al. [287] developed a cell-on-a-chip model with electrospun fibers to simulate a cutaneous wound *in vitro* and screened the performance of several electrospun fibers as wound dressings. They found that the results acquired by the microchip model corroborates the animal experimental results. This electrospun fiber-based screening method is expected to change the way that scientists screen candidates for wound dressings.

4.2.2. Vascular tissue engineering

Vascular tissue engineering preparation methods using electrospun fibers can be divided into a few categories: (1) as-spun micro-/nanofiber tubes used to directly culture cells, making blood vessels [106,190,288,289]; (2) flat fiber membranes seeded with endothelial cells or smooth muscle cells for a certain time, then rolled into vessels [290,291]; and (3) as-spun micro-/nanofiber tubular scaffolds implanted *in vivo* and used to induce cells from experimental animals to migrate into the scaffolds in order to finally obtain vascular tissue [292,293].

For the first method, in 2008, Zhang et al. [102] fabricated 3-D fibrous tubes composed of ultrafine electrospun fibers with a novel static method as shown in Fig. 4l. By using this technique, integrated macro tubes can be prepared directly. Browning et al. [289] developed a multilayer vascular graft based on collagen-mimetic proteins. They used electrospun polyurethane tubular mesh to reinforce the tubular PEG-Scl2 hydrogel during the formation of the tubular hydrogel, achieving suitable biomechanical properties. This PEG-Scl2 hydrogel, who was able to bind to endothelial cells (ECs) and resist platelet adhesion, was fabricated by conjugating a collagen-mimetic protein derived from group A Streptococcus,

Scl2.28 (Scl2), into a PEG hydrogel. This multilayer vascular scaffold had minimal platelet interactions and could promote the migration of ECs. Ju et al. [106] fabricated a bilayered tubular scaffold with an inner layer composed of small diameter fibers and an outer layer composed of large diameter fibers, and found that this bilayered scaffold permits both EC adhesion on the lumen and SMC infiltration into the outer layer. In addition to the studies discussed above, Uttayarat et al. [288] combined electrospinning and spin-casting techniques to pattern the luminal surface of small-diameter polyurethane (PU) grafts with microfibers and microgrooves. The microgrooves guide endothelial cell orientation along the axis of the blood vessel. The tracks of the circumferentially oriented microfibers were generated by electrospinning PU onto a mandrel rotated at high velocity, whereas the longitudinal tracks of the microgrooves were generated by spin-casting PU over a rotating poly (dimethylsiloxane) (PDMS) mold. They found that the endothelial cells seeded onto the grafts formed confluent monolayers with individual cells exhibiting an elongated morphology parallel to the micropatterns. The cells were phenotypically similar to natural endothelial cells as assessed by the expression of the endothelial cell-specific marker, vascular endothelial cell cadherin. Cell-seeded flat fiber membranes could be rolled into tubular vascular scaffolds. For example, Rayatpisheh et al. [290] combined cell sheet technology and electrospun scaffolds to engineer tubular, aligned, and contractile blood vessels, resulting in rapid circumferential alignment of smooth muscle cells with expression contractile genes immediately and introduction of an analogue to small diameter blood vessel's internal elastic lamina. Lee et al. [291] successfully built a vascular structure by first transfer printing of three different cell layers (human umbilical vein endothelial cells, human aortic smooth muscle cells and human dermal fibroblasts) onto electrospun nanofibers using thermosensitive hydrogels, and then manually rolling the cell-seeded nanofibers into tubular with the diameter and length being approximately 3 mm and 12 mm, respectively. As-spun micro-/nanofiber tubular scaffolds was able to induced cells migrate into the scaffolds after *in vivo* implantation by replacing rat abdominal aorta. For example, as shown in Fig. 13c, Wang et al. [293] replaced rat abdominal aorta with macroporous electrospun PCL vascular scaffold with thicker fibers (5–6 μm) and larger pores (~30 μm), and after 100 days, they found the endothelium coverage was complete and the smooth muscle layer organized with abundant ECM is similar to those in the native arteries. Analysis of the cellularization process revealed that a large number of M2 macrophages were induced by the thicker-fiber scaffolds to infiltrate into the graft wall, which further promoted cellular infiltration and vascularization. Furthermore, this regenerated arteries can act as adrenaline-induced contractile response and acetylcholine-induced relaxation.

4.2.3. Muscle tissue engineering

Human muscle tissues, including skeletal, cardiac, and smooth muscle, not only function as a locomotive apparatus but also deliver the protein breakdown products and maintain the normal functioning of the organs [294–296]. Although the muscle tissues have an inherent capacity for regeneration following injury, severe trauma (*e.g.,* volumetric muscle loss), tumor ablation or heart disease, may overwhelm these natural muscle repair mechanisms. Thus, muscle tissue engineering have been focused in recent years [297–299]. ECM-like electrospun fibers are suitable for muscle cell adhesion and proliferation and the fiber alignment is one of the most important parameters for muscle tissue engineering [300]. Compared to scaffolds with randomly arranged fibers, scaffolds with highly aligned (anisotropic), or unidirectionally oriented fibers have been repeatedly demonstrated to enhance myoblast adherence, proliferation, myotube formation and muscle cell alignment. Additionally, the porosity of a fibrous scaffold and the extent of cell infiltration affects the muscle cell growth. For example, water-soluble polymers co-spun with PCL could be easily removed following scaffold fabrication, resulting in spaces that act as pathways for improving cell infiltration [301]. Along with the fiber structure (the topographic cues), sensitivity of cells to other physical stimuli can be incorporated into the nanofibers. For example, electrically conductive materials were incorporated within aligned electrospun PCL [302–304], polyurethane [305] and PCL/polyaniline (PANi) [303] scaffolds (Fig. 13d), leading to a more efficient electrical stimulation in the developing cultures and further improving myotube maturity. Mechanical stimulation and substrate stiffness are other factors that have been previously demonstrated to influence skeletal muscle development. Elastomeric polyurethane scaffolds prepared with optimal stiffness and cyclical mechanical strain during culturing led to the development of more mature, striated myotubes than with fiber alignment alone [305]. In addition, the muscle tissue engineering, especially the field of cardiac tissue engineering, has continuously moved from 2-D culture systems to 3-D culture systems which are more representative of living systems [299]. Some other techniques (such as micropatterning [297] and microfluidics [298]) have been combined with electrospinning to build novel and functional 3-D scaffolds for muscle tissue engineering. For example, Fleischer et al. [306] reported a bottom-up approach to assemble a modular tissue consisting of multiple tissue layers with distinct structures and functions. One layer was designed to support cardiac cells and promote their organization into a contracting tissue. On this layer, they created microgrooves (width of 115 ± 5 μm, ridge width of 120 ± 2 μm, and height of 110 ± 10 μm) on the thin albumin electrospun fiber layer *via* laser-patterning for increasing the surface area of the fibrous scaffold and mimicking native anisotropy of the natural ECM. Microholes (40 ± 0.8 μm in diameter) were also created on the ridges of the fibrous layer to increase the mass transfer between different layers. Another layer enables the organization of endothelial cells into blood vessels, which were patterned with microtunnels (450 μm) to form a predefined vasculature, and cage-like structures between the microtunnels to accommodate controlled-release systems to continuously supply signals for vascularization. The PLGA microparticles enabling a long-term VEGF release were deposited into the cages, while endothelial cells were seeded onto the microtunnels. Furthermore, the third kind of layers with cage-like structures contain drug-loaded PLGA microparticles enabling the controlled release of different biofactors (e.g. DEX, an anti-inflammatory agent) affecting the engineered tissue or the host. Before transplantation, the tissue and microparticulate layers were integrated to form thick 3D cardiac patches by an ECM-based biological glue. Finally, the patches were transplanted in rats. After 2 weeks, they found that patches without the VEGF remained white, while the VEGF-loaded patches were filled with blood vessels. The histological analysis and immunostaining the extracts for smooth muscle cells, which stabilize blood vessels, further demonstrated that the ability of the VEGF microparticulate layer to improve blood vessel infiltration into the cardiac patch.

4.2.4. Neural tissue engineering

The use of electrospun fibrous scaffolds as substrates for neural tissue engineering has also been investigated by many researchers [307–309]. *In vitro* and *in vivo* experiments of substrates using polymer films versus electrospun fibers determined that the electrospun fiber-based substrates had a higher efficacy in enhancing nerve regeneration. *In vitro*, patterns of neurite cell outgrowth from the primary dorsal root ganglia (DRG) seeded on a scaffold of electrospun nanofibers with various order, structures, and surface properties were seen. As shown in Fig. 13e, neurite outgrowth occurred radially without specific directionality on randomly oriented nanofibers, while the cells preferentially extended along the

longitudinal axis of the fiber on aligned fibers [310–312]. *In vivo*, axonal extension within electrospun fibrous nerve conduits and partial functional reconnection have been demonstrated [313,314]. The electrospun fibers were also used in generation and transplantation of reprogrammed human neurons in the brain. For example, Carlson et al. [315] developed a 3-D microtopographic scaffolds, using tunable electrospun microfibrous polymeric substrates, for promoting *in situ* stem cell neuronal reprogramming, neural network establishment and support neuronal engraftment into the brain. They found that the transplantation of scaffold-supported neuronal networks into mouse brain striatum successfully improved survival ~38-fold at the injection site, as comparing to injected isolated cells, and allowed the delivery of multiple neuronal subtypes. All the above findings suggested that electrospun fibers with various controlled and designed structures are potential candidates for neural regeneration [316,317].

4.2.5. Bone tissue engineering

In the bone reconstruction field, electrospun nanofibers have also attracted considerable attention, which has primarily been aimed at identifying suitable material compositions for electrospinning [318]. Bone-associated cells and their progenitor/stem cells show initial responses similar to those in other tissues, which are often anchorage-dependent. The nanofibrous substratum may provide favorable conditions for cell anchorage and growth. In tandem with initial cell responses, further osteoblastic differentiation and mineralization have also reportedly been well regulated on nanofibrous surfaces as compared to a dense substrate of polymers [319]. Although studies on the *in vivo* feasibility of electrospun nanofibers in bone reconstruction and tissue engineering are in the early stages, recent reports using electrospun nanofibers with new compositions targeted for bone growth as well as some processing tools for designing 3-D scaffolds have highlighted the potential use of electrospun materials in bone tissue engineering. To broaden the application of electrospun nanofiber in bone tissue engineering, our group has developed various electrospun nanofiber scaffolds to promote either *in vitro* or *in vivo* osteogenesis, including the following: beaded nanofibers with surface nanoroughness for modulating and facilitating cellular behaviors [130,131], electrically conductive electrospun aligned PLA/MWCNTs nanofibers with a synergistic combination of topographic cues and electrical stimulation for osteoblast outgrowth [61], a 3-D nano/micro alternating multilayered scaffold loaded with rBMSCs and BMP-2 [320], and nanoparticle-embedded electrospun nanofibers for the efficient repair of critical-sized rat calvarial defects (Fig. 13f) [66].

4.2.6. Other applications

In addition to aforementioned applications of electrospun fibers, there are many other potential applications in tissue engineering. For example, Jiang and Li et al. [321] developed aligned PCL–PEG nanofibers in porous chitosan scaffolds in order to improve the orientation of collagen fibers in regenerated periodontium. Liu et al. [322] formulated dextran glassy nanoparticles (DGNs) loaded with basic fibroblast growth factor (bFGF) and encapsulated these nanoparticles into poly-L-lactic acid (PLLA) copolymer fibers in order to secure the bioactivity of bFGF in a sustained manner, thus promoting cell proliferation and tendon healing both *in vitro* and *in vivo* (Fig. 13g). Xie et al. [164] demonstrated the fabrication of "aligned-to-random" electrospun nanofiber scaffolds that mimic the structural organization of collagen fibers at the tendon-to-bone insertion site. Tendon fibroblasts cultured on such a scaffold exhibited highly organized and haphazardly oriented morphologies on the aligned and random portions, respectively. They also prepared scaffolds based on radially aligned electrospun nanofibers, which showed great potential as artificial dural substitutes (Fig. 13h) [323]. This scaffold was able to direct and enhance the cell migration from the periphery to the center and induce faster cellular migration and population than random nanofibers. The authors also found that dural fibroblast cells, which cultured on the scaffolds of radially aligned fibers, expressed extracellular matrix like type I collagen in a high degree of organization. Xue et al. successfully used electrospun gelatin/polycaprolactone fibrous membranes to build an ear-shaped cartilage (Fig. 13i) [324]. Liu et al. [325] developed electrospun fibrous scaffolds with 200 nm fiber topography enhanced retinal pigment epithelial culture (Fig. 13j), which showed subretinal biocompatibility. Jungebluth et al. [326] used electrospun polyethylene terephthalate (PET) fibrous tubular scaffold (with inner diameter of 2–3 mm and wall thickness of 0.5-1.0 mm) as a model of the artificial tracheal tissue engineering scaffold. They used a tissue engineering strategy and orthotopic transplantation of this artificial model scaffold together with the natural decellularized donor tracheae to illustrate that their protocol was a reliable and reproducible model which could be used to investigate the critical aspects and pathways of *in situ* tracheal tissue restoration and regeneration. Their protocol also included details about the way to assess the scaffolds' biomechanical properties and cell viability before implantation. Wang et al. [327] fabricated a hierarchical microwell-array scaffold by using electrospun thermoplastic silicone PU nanofibers for cell-transplantation to treat diabetes. During the fabrication process, the electrospun PU nanofibers were deposited onto a conductive PDMS micropillar-array patterned collector. This scaffold effectively allowed for assembling of islets and aggregates of mensenchymal stem cells (MSCs) in high density, which enabled the transplantation of cells with spatial control and improved the transplant's engraftment efficacy *in vivo* for treating diabetes. For the *in vivo* transplantation, a circular microwell scaffold (with diameter of 7 mm) containing 250 islets was transplanted into the streptozotocin (STZ)-induced diabetic mice in the epididymal fat pad (EFP). The EFP is a transplantation site featured with well-perfused fat tissue and convenient accessibility through facile operation procedures. The results of nonfasting blood glucose measurements during 120 days after the transplantation, suggested that the islets-contained microwell scaffold group had well-preserved metabolic function, with no significantly difference from the normal mice group.

4.3. Diagnostics

Due to their high surface area to volume ratio, the contact area between the active sensing regions of a nanofiber mat and the cells or molecules are much higher than that of flat films. Thus, nanofiber mats have also been used to enhance paper-based diagnostics.

4.3.1. Humoral diagnosis of cancer

Electrospun fibers were employed for the detection of tumor markers or circulating tumor cells (CTCs) in the blood and in other body fluids of a patient with early-stage cancer [328]. Zhang et al. [329] electrospun titanium butoxide (TBT)/PVP composite fibers onto a silicon substrate and obtained titanium dioxide (TiO_2) nanofibers by a calcination process and by removing organic components. Then, they modified the nanofibers with a biotinylated anti-epithelial cell adhesion molecule (anti-EpCAM) and finally captured junction colon cancer cells and gastric cancer cells with the device. Ma et al. [330] fabricated microfibers, nanofibers and nanofibers/microbeads composite materials from PS *via* electrospinning (Fig. 14a), and then anti-EpCAM was used to modify the fibers. The human breast adenocarcinoma cell (MCF7) capture efficiency of these fibers was investigated, with all fibers demonstrating a relatively high capture efficiency. The nanofibers/microbeads composites possessed the highest capture efficiency. Zhao et al. [331] combined biotinylated anti-EpCAM

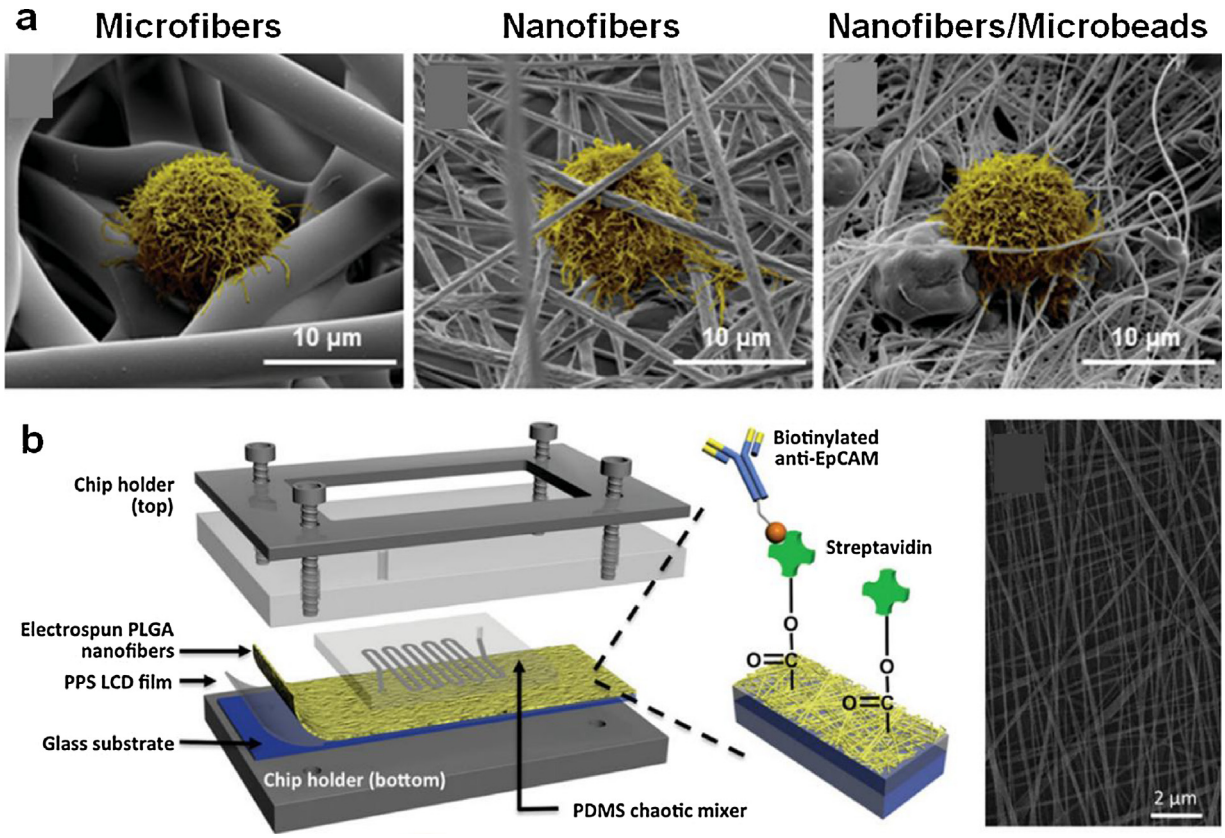

Fig. 14. a) SEM images of captured CTCs by anti-EpCAM modified PS mcirofibers, PS nanofibers and nanofibers/microspheres composites [330]; b) combination of biotinylated anti-EpCAM modified PLGA nanofibers and microfluidics for capturing CTCs [331].
Sources: a) [330],Copyright 2015, b) [331],Copyright 2013. Reproduced with permission from John Wiley & Sons Inc.

modified PLGA nanofibers with a microfluidic technique (Fig. 14b) and successfully captured human breast cancer cells (SK-BR-3) in a PBS and in blood. They used a confocal microscope laser to separate captured cells for further gene sequencing detection. They also used a biotinylated anti-CD146 antibody-modified PLGA nanofiber mat combined with a microfluidic device to successfully capture melanoma circulating tumor cells [332]. Xu et al. [333] covalently conjugated hyaluronic acid onto PEI-modified electrospun PLGA (PLAG-PEI-HA) nanofibers and integrate the nanofibers into a microfluidic chamber. They found that CD44+ carcinoma of various origins (HeLa, KB, A549, and MCF-7 cells) were selectively captured by this PLGA-PEI–HA nanofibers combined microfluidic platform. Notably, the HeLa cells were more efficiently captured by the PLGA-PEI-HA nanofibrous membrane under flowing conditions than in static dish at a density of 20 cells/mL. The captured HeLa cells could grow on the nanofibrous membrane in the microchip for days without compromised cell viability.

In addition to the detection of CTCs, the electrospun fibrous membranes have also been used for the detection of tumor-associated factors and genes, such as the p53 gene [334] or the K-RAS gene [335].

4.3.2. Diagnostics for other diseases

Reinholt et al. [336] used PLA nanofibers functionalized by anti-*E. coli* antibodies for the detection of *Escherichia coli* O157:H7. Choi et al. [337] fabricated hollow tungsten trioxide (WO_3) hemitubes using electrospun fibers as sacrificial templates combined with a physical vapor deposition (PVD) method, used for the detection of hydrogen sulfide molecules and acetone molecules in exhaled breath for the potential diagnosis of halitosis and diabetes, respectively. In later work, these researchers developed stannic oxide (SnO_2) nanofibers functionalized with reduced graphene oxide nanosheets, which were used as highly sensitive sensors for the detection of acetone and hydrogen sulfide levels in exhaled human breath [338]. Lee et al. [339] used an aptamer-immobilized electrospun polystyrene–poly(styrene-co-maleic anhydride) (PS–PSMA) nanofiber as a new aptasensor platform for protein detection, and they found that the aptamer-on-nanofiber-based biosensor demonstrated a 2500-fold higher sensitivity than a traditional 96-microwell plate format.

4.4. Other applications in medicine

4.4.1. Mimicking the tumor microenvironment

A deep understanding of tumor growth and its growth environment helps improve the administration of drugs and the testing of new medicines. Therefore, various materials and methods have been used in order to mimic tumor microenvironments and to build *in vitro* tumor models [340–342]. With structures similar to the ECM, electrospun fibers have also been used in this type of study. Hartman et al. [343] built a 3-D growth microenvironment for tumor cells based on electrospun PCL fibers and a bioactive peptide derived from domain IV of perlecan heparan sulfate proteoglycan; this microenvironment can maintain the migration process of prostate cancer cells. Fischer et al. [344] used electrospun PCL fibers with different molecular weights and mouse fibrosis lung extract to build a 3-D microenvironment, which was then used to explore the pathogenesis of congenital pulmonary interstitial fibrosis. Considering most preclinical drug screening systems fail to predict whether a given drug candidate will work in clinical trials, which was possibly due to the fact that cells are plated on culture dishes devoid of signaling cues present *in vivo*, thus, San-

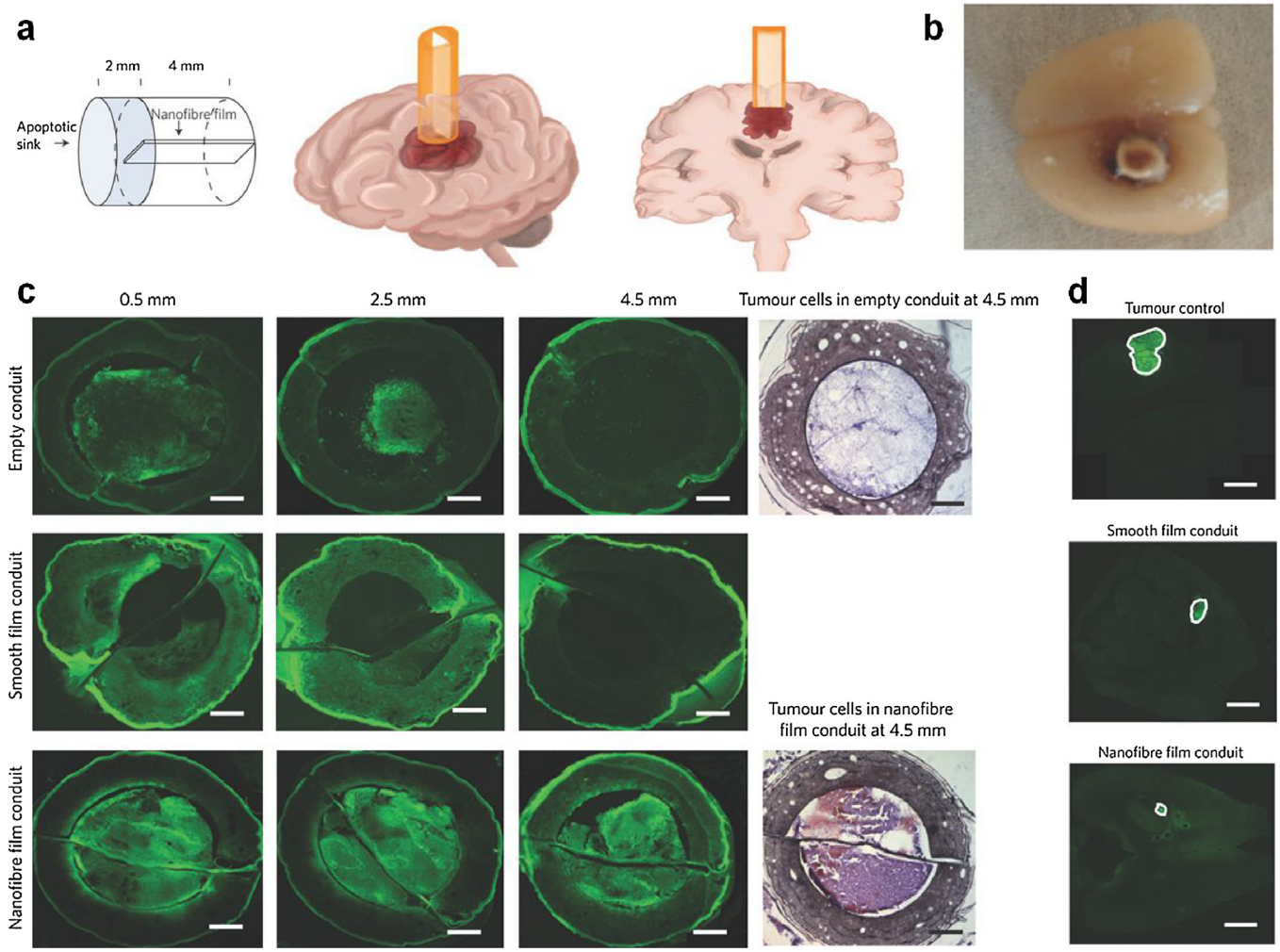

Fig. 15. a) Representation of the tumor guide containing a nanofiber film inserted into a rat brain [351]. Three-dimensional view (left) and coronal view (right) of the brain and conduit; b) digital image of extracted brain containing a conduit from the top view; after 7 days' implantation, c) fluorescence images showing the presence of tumor cells throughout the cross-section of all the conduits (empty, smooth film and aligned nanofiber film) at various distances, 0.5 mm, 2.5 mm and 4.5 mm, respectively, from the interface of the tumor in the brain, scale bar = 400 μm; d) fluorescence images showing the tumor core in the brain for the tumor control, the smooth film conduit and the nanofiber film conduit.

Sources: a) [351], Copyright 2014. Reproduced with permission from Nature Publishing Group.

toro et al. [345] cultured Ewing sarcoma (ES) cells onto electrospun PCL 3-D scaffolds within a flow perfusion bioreactor, where the flow-derived shear stress could provide a physiologically relevant mechanical stimulation. They found that cells exposed to flow perfusion produced more insulin-like growth factor-1 (IGF1) ligand, showing shear stress-dependent sensitivity to IGF-1 receptor targeted drugs as compared with static conditions. Furthermore, the flow perfusion increased nutrient supply throughout the scaffold, which enriched ES culture over static conditions.

Additionally, directional electrospun fibers have been used in many cases. In one example, aligned electrospun fibers were used to study the migration of glioma cells [346–349] or breast cancer cells [350] and their invasion and metastasis ability *in vitro*. Interestingly, a few researchers also explored the novel treatment way to tumors using aligned electrospun fibers. For example, Jain et al. [351] systematically investigated the apoptosis of glioblastoma tumor induced by conduit made from electrospun aligned fibers (Fig. 15). In this study, they induced directional migration of tumor cells through the aligned fibers to a gel pool that would induce apoptosis of cancer cells. It can be seen in Fig. 15c, after 7 days, the amount of tumor cells in the aligned nanofiber film conduits was the highest among all the groups, and the corresponding internal glioma in the animal brain was the smallest, which suggested that this conduit with aligned fibers could promote the migration of glioma cells from the glioma tumor. This method using fibrous antitumor implants or conduit is innovative, and the antitumor effect is remarkable, which may open up a new way for the application of electrospun fibers in the treatment of cancer.

4.4.2. Immobilization of enzyme

The high specific surface area and porosity of the electrospun fibers also help in effectively alleviating the diffusion resistance of a substrate, thus greatly improving the catalytic ability of an enzyme. Enzymes are catalysts with features of high specificity and high catalytic efficiency, which are applicable in a wide range of disciplines, including biomedicine, food engineering and other fields. However, an enzyme may not be stable in a highly acidic, alkaline or other harsh environment, and these instabilities negatively affect performance. One method for addressing these problems is to fix the enzyme onto a carrier [352]. The performance of an immobilized enzyme is highly dependent on the structure and performance of the support material, such that the selection of the carrier material is particularly important [353]. Compared with nanoparticles and carbon nanotubes, electrospun nanofibers can be easily processed

into various fiber membranes (*e.g.,* non-woven fiber membranes, and fiber bundles), conducive for enhancing the recoverability and durability of an immobilized enzyme.

4.4.3. Protection and filtration

Electrospun fibers were also utilized in protection and filtration applications. For example, Selvam et al. [354] incorporated silver nanoparticles into poly(acrylonitrile) electrospun nanofibers for bacterial filtration. Guo et al. [355] prepared poly(butylene terephthalate) electrospun/melt-blown composite mats for white blood cell (WBC) filtration, reducing the number of WBCs in the donors' blood to 10^4/L following filtration. Furthermore, electrospun fiber mats have also been used as, for example, high-efficiency transparent air filters [356] and protective masks [357].

5. Conclusions and future challenges

Electrospinning technology has been widely used to fabricate polymer fibers with various hierarchical structures from 1-D to 2-D to 3-D, accomplished by changing electrospinning setups and processing factors. The fiber matrix can be made of any number of diverse polymer materials, with the fiber diameter ranging from nano- to micro- meter and the fiber morphologies readily tunable. These electrospun fibers have been employed for drug delivery, tissue engineering, disease diagnostics and many other applications. Precise drug release and programmed drug release profiles can be achieved as a result of the well-defined multilevel structure of the fibers. The polymer fibers are ideal tissue engineering scaffolds because of their nanofibrous structure, which has a high surface to volume ratio and an ability to mimic the ECM of living cells. However, some challenges of using electrospun fibers for biomedical application still exist. More sophisticated electrospinning techniques need to be developed in accordance with the requirements of biomedical applications. For drug delivery *(e.g.,* cancer therapy) applications, joint, interdisciplinary investigations from material scientists and biologists are needed to further develop multileveled fibers. The microfluidic-assisted electrospinning approach, which can more precisely control the composition of the electrospinning solution, may be a good strategy for producing those multileveled fibers. For tissue engineering, a key factor is accurately controlling the fiber deposition, preferably on a nanometer scale, in order to more precisely mimic an ECM. Additionally, it is critical to understand the cellular reaction to electrospun materials with different compositions, fiber orientations and microstructures. These goals can be easier to achieve by combining the use of electrospinning, microfluidic spinning and 3D printing to construct the 3D scaffolds consisting of diverse fiber sizes, depositions and orientations similar to *in vivo* like ECM [358]. What' more, a database may need to be developed to record the interactions between different cells and different fiber scaffolds for better analysis and understanding their mutual influence and providing useful guidelines to fabricate desired scaffolds. For diagnostics, more sensitive materials should be employed during electrospinning, or surface modification of the fibers by functional groups will be required [359], such as plasma treatment, polydopamine treatment and layer-by-layer technique. Furthermore, the mass production of electrospun nanofibers is a necessity for this technology to increase commercial value, which may be hopefully realized through the needleless electrospinning [360]. Actually, the commercialization of electrospinning technique and the eletrospun fiber products was achieved in some degree [361]. In 1980s, Donaldson Co., Inc was the first to commercialize electrospun fiber technology in the in the US, followed by DuPont (micro-denier fibers). In 1991, companies from the nonwovens sector within the fiber technology industry were the first to produce commercialized filtration products based on electrospinning. Now, the air and water filtration products are still the main focus of business and industrial attentions, compared with other electrospun fibers-based products (such as protective clothing, armor, composite reinforcement, photovoltaic and energy storage devices). While the commercialization of biomedical applications of electrospun fibers (*e.g.,* engineered skin and tissue anti-adhesion membrane) is also gathering interests. However, before the extensive commercialization of these electrospun fibers in biomedical fields, more extensive *in vivo* studies, even clinical trials are still needed to be done to evaluate the real influence of electrospun nano-/microfibers in healthcare and biomedical engineering. In conclusion, hierarchically structured polymer fibers have great potential for use in biomedical applications, and it is believed that they will be used in the human body with further refinements to electrospinning technology.

Acknowledgments

This work was partially supported by National Natural Science Foundation of China (Nos. 51373138, 21574105, 51703189, 51725303), the Sichuan Province Youth Science and Technology Innovation Team (Grant No.2016TD0026) and the Fundamental Research Funds for the Central Universities (No. 2682017CX040).

References

[1] Zhao N, Wang Z, Cai C, Shen H, Liang FY, Wang D, et al. Bioinspired materials: from low to high dimensional structure. Adv Mater 2014;26:6994–7017.
[2] Zan GT, Wu QS. Biomimetic and bioinspired synthesis of nanomaterials/nanostructures. Adv Mater 2016;28:2099–147.
[3] Liu Y, Luo D, Wang T. Hierarchical structures of bone and bioinspired bone tissue engineering. Small 2016;12:4611–32.
[4] Mitragotri S, Lahann J. Physical approaches to biomaterial design. Nat Mater 2009;8:15–23.
[5] Hu XL, Hu JM, Tian J, Ge ZS, Zhang GY, Luo KF, et al. Polyprodrug amphiphiles: hierarchical assemblies for shape-regulated cellular internalization, trafficking, and drug delivery. J Am Chem Soc 2013;135:17617–29.
[6] Mai YY, Eisenberg A. Self-assembly of block copolymers. Chem Soc Rev 2012;41:5969–85.
[7] Su B, Wu YC, Jiang L. The art of aligning one-dimensional (1D) nanostructures. Chem Soc Rev 2012;41:7832–56.
[8] Yao X, Song YL, Jiang L. Applications of bio-inspired special wettable surfaces. Adv Mater 2011;23:719–34.
[9] Sun TL, Feng L, Gao XF, Jiang L. Bioinspired surfaces with special wettability. Acc Chem Res 2005;38:644–52.
[10] Xia F, Jiang L. Bio-inspired, smart, multiscale interfacial materials. Adv Mater 2008;20:2842–58.
[11] Sun B, Long YZ, Zhang HD, Li MM, Duvail JL, Jiang XY, et al. Advances in three-dimensional nanofibrous macrostructures via electrospinning. Prog Polym Sci 2014;39:862–90.
[12] Zeng W, Shu L, Li Q, Chen S, Wang F, Tao XM. Fiber-based wearable electronics: a review of materials, fabrication, devices, and applications. Adv Mater 2014;26:5310–36.
[13] Wang XD, Wolfbeis OS. Fiber-optic chemical sensors and biosensors. Anal Chem 2016;88:203–27.
[14] Senthamizhan A, Balusamy B, Uyar T. Glucose sensors based on electrospun nanofibers: a review. Anal Bioanal Chem 2016;408:1285–306.
[15] Anis SF, Khalil A, Saepurahman Singaravel G, Hashaikeh R. A review on the fabrication of zeolite and mesoporous inorganic nanofibers formation for catalytic applications. Microporous Mesoporous Mater 2016;236:176–92.
[16] Li XY, Chen YM, Huang HT, Mai YW, Zhou LM. Electrospun carbon-based nanostructured electrodes for advanced energy storage-a review. Energy Storage Mater 2016;5:58–92.
[17] Jung JW, Lee CL, Yu S, Kim ID. Electrospun nanofibers as a platform for advanced secondary batteries: a comprehensive review. J Mater Chem A 2016;4:703–50.
[18] Wu HB, Zhang GQ, Yu L, Lou XW. One-dimensional metal oxide-carbon hybrid nanostructures for electrochemical energy storage. Nanoscale Horiz 2016;1:27–40.
[19] Wang XF, Yu JY, Sun G, Ding B. Electrospun nanofibrous materials: a versatile medium for effective oil/water separation. Mater Today 2016;19:403–14.
[20] Zhu MM, Han JQ, Wang F, Shao W, Xiong RH, Zhang QL, et al. Electrospun nanofibers membranes for effective air filtration. Macromol Mater Eng 2017;302(1600353):1–27.
[21] Kadam VV, Wang LJ, Padhye R. Electrospun nanofibre materials to filter air pollutants-a review. J Ind Text 2016;0:1–28, http://dx.doi.org/10.1177/1528083716676812.

[22] Wu J, Wang N, Zhao Y, Jiang L. Electrospinning of multilevel structured functional micro-/nanofibers and their applications. J Mater Chem A 2013;1:7290–305.
[23] Kenry Lim CT. Nanofiber technology: current status and emerging developments. Prog Polym Sci 2017;70:1–17.
[24] Zhao YS, Fu H, Peng A, Ma Y, Liao Q, Yao J. Construction and optoelectronic properties of organic one-dimensional nanostructures. Acc Chem Res 2010;43:409–18.
[25] Lu X, Wang C, Wei Y. One-dimensional composite nanomaterials: synthesis by electrospinning and their applications. Small 2009;5:2349–70.
[26] Zang L, Che Y, Moore JS. One-dimensional self-assembly of planar π-conjugated molecules: adaptable building blocks for organic nanodevices. Acc Chem Res 2008;41:1596–608.
[27] Hu JT, Odom TW, Lieber CM. Chemistry and physics in one dimension: synthesis and properties of nanowires and nanotubes. Acc Chem Res 1999;32:435–45.
[28] Xue JJ, Xie JW, Liu WY, Xia YN. Electrospun nanofibers: new concepts, materials, and applications. Acc Chem Res 2017;50:1976–87.
[29] Hunley MT, Long TE. Electrospinning functional nanoscale fibers: a perspective for the future. Polym Int 2008;57:385–9.
[30] Reneker DH, Yarin AL. Electrospinning jets and polymer nanofibers. Polymer 2008;49:2387–425.
[31] Lannutti J, Reneker D, Ma T, Tomasko D, Farson D. Electrospinning for tissue engineering scaffolds. Mater Sci Eng C 2007;27:504–9.
[32] Peng S, Jin G, Li LL, Li K, Srinivasan M, Ramakrishna S, et al. Multi-functional electrospun nanofibres for advances in tissue regeneration, energy conversion & storage, and water treatment. Chem Soc Rev 2016;45:1225–41.
[33] Li D, Xia YN. Electrospinning of nanofibers: reinventing the wheel. Adv Mater 2004;16:1151–70.
[34] Bailey AG. Electrostatic spraying of liquids. New York: John Wiley & Sons; 1988, 197 pp.
[35] Rutledge GC, Fridrikh SV. Formation of fibers by electrospinning. Adv Drug Deliv Rev 2007;59:1384–91.
[36] Reneker DH, Yarin AL, Fong H, Koombhongse S. Bending instability of electrically charged liquid jets of polymer solutions in electrospinning. J Appl Phys 2000;87:4531–47.
[37] Yarin AL, Kataphinan W, Reneker DH. Branching in electrospinning of nanofibers. J Appl Phys 2005;98(064501):1–12.
[38] Hohman MM, Shin M, Rutledge G, Brenner MP. Electrospinning and electrically forced jets. I. Stability theory. Phys Fluids 2001;13:2201–20.
[39] Xin Y, Reneker DH. Garland formation process in electrospinning. Polymer 2012;53:3629–35.
[40] Ramakrishna S, Fujihara K, Teo WE, Lim TC, Ma Z. An introduction to electrospinning and nanofibers. Singapore: World Scientific Publishing Co Pte Ltd; 2005, 396 pp.
[41] Ru CH, Chen J, Shao ZS, Pang M, Luo J. A novel mathematical model for controllable near-field electrospinning. AIP Adv 2014;4(017108):1–11.
[42] Bisht GS, Canton G, Mirsepassi A, Kulinsky L, Oh S, Dunn-Rankin D, et al. Controlled continuous patterning of polymeric nanofibers on three-dimensional substrates using low-voltage near-field electrospinning. Nano Lett 2011;11:1831–7.
[43] Beachley V, Wen X. Effect of electrospinning parameters on the nanofiber diameter and length. Mater Sci Eng C 2009;29:663–8.
[44] Theron SA, Zussman E, Yarin AL. Experimental investigation of the governing parameters in the electrospinning of polymer solutions. Polymer 2004;45:2017–30.
[45] Deitzel JM, Kleinmeyer J, Harris D, Tan NCB. The effect of processing variables on the morphology of electrospun nanofibers and textiles. Polymer 2001;42:261–72.
[46] Peng HS, Zhou SB, Guo T, Li YS, Li XH, Wang JX, et al. In vitro degradation and release profiles for electrospun polymeric fibers containing paracetanol. Colloids Surf B 2008;66:206–12.
[47] Zhou SB, Peng HS, Yu XJ, Zheng XT, Cui WG, Zhang ZR, et al. Preparation and characterization of a novel electrospun spider silk fibroin/poly(d,l-lactide) composite fiber. J Phys Chem B 2008;112:11209–16.
[48] Peng HS, Zhou SB, Jiang J, Guo T, Zheng XT, Yu XJ. Pressure-induced crystal memory effect of spider silk proteins. J Phys Chem B 2009;113:4636–41.
[49] Wu LL, Li H, Li S, Li XR, Yuan XY, Li XL, et al. Composite fibrous membranes of PLGA and chitosan prepared by coelectrospinning and coaxial electrospinning. J Biomed Mater Res A 2009;92:563–74.
[50] Yang Y, Zhu XL, Cui WG, Li XH, Jin Y. Electrospun Composite mats of poly[(d,l-lactide)-co-glycolide] and collagen with high porosity as potential scaffolds for skin tissue engineering. Macromol Mater Eng 2009;294:611–9.
[51] Gautam S, Dinda AK, Mishra NC. Fabrication and characterization of PCL/gelatin composite nanofibrous scaffold for tissue engineering applications by electrospinning method. Mater Sci Eng C 2013;33:1228–35.
[52] Bonino CA, Efimenko K, Jeong SI, Krebs MD, Alsberg E, Khan SA. Three-dimensional electrospun alginate nanofiber mats via tailored charge repulsions. Small 2012;8:1928–36.
[53] Duan B, Yuan XY, Zhu Y, Zhang YY, Li XL, Zhang Y, et al. A nanofibrous composite membrane of PLGA-chitosan/PVA prepared by electrospinning. Eur Polym J 2006;42:2013–22.
[54] Islam MS, Karim MR. Fabrication and characterization of poly(vinyl alcohol)/alginate blend nanofibers by electrospinning method. Colloids Surf A 2010;366:135–40.
[55] Lee KH, Kim HY, Khil MS, Ra YM, Lee DR. Characterization of nano-structured poly(ε-caprolactone) nonwoven mats via electrospinning. Polymer 2003;44:1287–94.
[56] Shao SJ, Li L, Yang G, Li JR, Luo C, Gong T, et al. Controlled green tea polyphenols release from electrospun PCL/MWCNTs composite nanofibers. Int J Pharm 2011;421:310–20.
[57] Cipitria A, Skelton A, Dargaville TR, Dalton PD, Hutmacher DW. Design, fabrication and characterization of PCL electrospun scaffolds-a review. J Mater Chem 2011;21:9419–53.
[58] Croisier F, Duwez AS, Jérôme C, Léonard AF, van der Werf KO, Dijkstra PJ, et al. Mechanical testing of electrospun PCL fibers. Acta Biomater 2012;8:218–24.
[59] Gong T, Li W, Chen H, Wang L, Shao S, Zhou S. Remotely actuated shape memory effect of electrospun composite nanofibers. Acta Biomater 2012;8:1248–59.
[60] Casasola R, Thomas NL, Trybala A, Georgiadou S. Electrospun poly lactic acid (PLA) fibres: effect of different solvent systems on fibre morphology and diameter. Polymer 2014;55:4728–37.
[61] Shao SJ, Zhou SB, Li L, Li JR, Luo C, Wang JX, et al. Osteoblast function on electrically conductive electrospun PLA/MWCNTs nanofibers. Biomaterials 2011;32:2821–33.
[62] Blackwood KA, McKean R, Canton I, Freeman CO, Franklin KL, Cole D, et al. Development of biodegradable electrospun scaffolds for dermal replacement. Biomaterials 2008;29:3091–104.
[63] Zhu XL, Cui WG, Li XH, Jin Y. Electrospun fibrous mats with high porosity as potential scaffolds for skin tissue engineering. Biomacromolecules 2008;9:1795–801.
[64] Kumbar SG, Nukavarapu SP, James R, Nair LS, Laurencin CT. Electrospun poly(lactic acid-co-glycolic acid) scaffolds for skin tissue engineering. Biomaterials 2008;29:4100–7.
[65] Kim SJ, Jang DH, Park WH, Min BM. Fabrication and characterization of 3-dimensional PLGA nanofiber/microfiber composite scaffolds. Polymer 2010;51:1320–7.
[66] Li L, Zhou GL, Wang Y, Yang G, Ding S, Zhou SB. Controlled dual delivery of BMP-2 and dexamethasone by nanoparticle-embedded electrospun nanofibers for the efficient repair of critical-sized rat calvarial defect. Biomaterials 2015;37:218–29.
[67] Wannatong L, Sirivat A, Supaphol P. Effects of solvents on electrospun polymeric fibers: preliminary study on polystyrene. Polym Int 2004;53:1851–9.
[68] Uyar T, Havelund R, Hacaloglu J, Besenbacher F, Kingshott P. Functional electrospun polystyrene nanofibers incorporating α-, β-, and γ-cyclodextrins: comparison of molecular filter performance. ACS Nano 2010;4:5121–30.
[69] Lu P, Xia YN. Maneuvering the internal porosity and surface morphology of electrospun polystyrene yarns by controlling the solvent and relative humidity. Langmuir 2013;29:7070–8.
[70] Su QX, Zhao AJ, Peng HS, Zhou SB. Preparation and characterization of biodegradable electrospun polyanhydride nano/microfibers. J Nanosci Nanotechnol 2010;10:6369–75.
[71] Bergmeister H, Seyidova N, Schreiber C, Strobl M, Grasl C, Walter I, et al. Biodegradable, thermoplastic polyurethane grafts for small diameter vascular replacements. Acta Biomater 2015;11:104–13.
[72] Demir MM, Yilgor I, Yilgor E, Erman B. Electrospinning of polyurethane fibers. Polymer 2002;43:3303–9.
[73] Yano T, Higaki Y, Tao D, Murakami D, Kobayashi M, Ohta N, et al. Orientation of poly(vinyl alcohol) nanofiber and crystallites in non-woven electrospun nanofiber mats under uniaxial stretching. Polymer 2012;53:4702–8.
[74] Zhang CX, Yuan XY, Wu LL, Han Y, Sheng J. Study on morphology of electrospun poly(vinyl alcohol) mats. Eur Polym J 2005;41:423–32.
[75] Jin WJ, Lee HK, Jeong EH, Park WH, Youk JH. Preparation of polymer nanofibers containing silver nanoparticles by using poly(n-vinylpyrrolidone). Macromol Rapid Commun 2005;26:1903–7.
[76] Bai J, Li YX, Zhang CQ, Liang XF, Yang QB. Preparing AgBr nanoparticles in poly(vinyl pyrrolidone) (PVP) nanofibers. Colloids Surf A 2008;329:165–8.
[77] Fong H, Chun I, Reneker DH. Beaded nanofibers formed during electrospinning. Polymer 1999;40:4585–92.
[78] Rho KS, Jeong L, Lee G, Seo B, Park YJ, Hong SD, et al. Electrospinning of collagen nanofibers: effects on the behavior of normal human keratinocytes and early-stage wound healing. Biomaterials 2006;27:1452–61.
[79] Ayres C, Bowlin GL, Henderson SC, Taylor L, Shultz J, Alexander J, et al. Modulation of anisotropy in electrospun tissue-engineering scaffolds: analysis of fiber alignment by the fast Fourier transform. Biomaterials 2006;27:5524–34.
[80] Ostrovidov S, Shi X, Zhang L, Liang X, Kim SB, Fujie T, et al. Myotube formation on gelatin nanofibers-multi-walled carbon nanotubes hybrid scaffolds. Biomaterials 2014;35:6268–77.
[81] Min BM, Lee G, Kim SH, Nam YS, Lee TS, Park WH. Electrospinning of silk fibroin nanofibers and its effect on the adhesion and spreading of normal human keratinocytes and fibroblasts in vitro. Biomaterials 2004;25:1289–97.
[82] Stephens JS, Fahnestock SR, Farmer RS, Kiick KL, Chase DB, Rabolt JF. Effects of electrospinning and solution casting protocols on the secondary structure of a genetically engineered dragline spider silk analogue investigated via fourier transform raman spectroscopy. Biomacromolecules 2005;6:1405–13.

[83] Desai K, Kit K, Li J, Zivanovic S. Morphological and surface properties of electrospun chitosan nanofibers. Biomacromolecules 2008;9:1000–6.
[84] Kim GH, Park KE. Alginate-nanofibers fabricated by an electrohydrodynamic process. Polym Eng Sci 2009;49:2242–8.
[85] Pu CC, He JX, Cui SZ, Gao WD. Double-nozzle air-jet electrospinning for nanofiber fabrication. J Appl Polym Sci 2014;131(40040):1–12.
[86] Yang EL, Shi JJ, Xue Y. Influence of electric field interference on double nozzles electrospinning. J Appl Polym Sci 2010;166:3688–92.
[87] Theron SA, Yarin AL, Zussman E, Kroll E. Multiple jets in electrospinning: experiment and modeling. Polymer 2005;46:2889–99.
[88] Han D, Steckl AJ. Triaxial electrospun nanofiber membranes for controlled dual release of functional molecules. ACS Appl Mater Interfaces 2013;5:8241–5.
[89] Chen HY, Wang N, Di JC, Zhao Y, Song YL, Jiang L. Nanowire-in-microtube structured core/shell fibers via multifluidic coaxial electrospinning. Langmuir 2010;26:11291–6.
[90] Li D, McCann JT, Xia YN. Use of Electrospinning to directly fabricate hollow nanofibers with functionalized inner and outer surfaces. Small 2005;1:83–6.
[91] Li D, Xia YN. Direct Fabrication of Composite and ceramic hollow nanofibers by electrospinning. Nano Lett 2004;4:933–8.
[92] Yu DG, Yang C, Jin M, Williams GR, Zou H, Wang X, et al. Medicated Janus fibers fabricated using a Teflon-coated side-by-side spinneret. Colloids Surf B 2016;138:110–6.
[93] Wang N, Chen HY, Lin L, Zhao Y, Cao XY, Song YL, Jiang L. Multicomponent phase change microfibers prepared by temperature control multifluidic electrospinning. Macromol Rapid Commun 2010;31:1622–7.
[94] Zhou FL, Gong RH, Porat I. Polymeric nanofibers via flat spinneret electrospinning. Polym Eng Sci 2009;49:2475–81.
[95] Wang X, Niu H, Lin T, Wang XG. Needleless electrospinning of nanofibers with a conical wire coil. Polym Eng Sci 2009;49:1582–6.
[96] Wang X, Niu HT, Wang XG, Lin T. Needleless electrospinning of uniform nanofibers using spiral coil spinnerets. J Nanomater 2012;2012(785920):1–9.
[97] Lu B, Wang Y, Liu Y, Duan H, Zhou J, Zhang Z, et al. Superhigh-throughput needleless electrospinning using a rotary cone as spinneret. Small 2010;6:1612–6.
[98] Alamein MA, Liu Q, Stephens S, Skabo S, Warnke F, Bourke R, et al. Nanospiderwebs: artificial 3d extracellular matrix from nanofibers by novel clinical grade electrospinning for Stem Cell Delivery. Adv Healthc Mater 2013;2:702–17.
[99] Niu HT, Lin T, Wang XG. Needleless electrospinning. I. A comparison of cylinder and disk nozzles. J Appl Polym Sci 2009;114:3524–30.
[100] Yang RR, He JH, Xu L, Yu JY. Bubble-electrospinning for fabricating nanofibers. Polymer 2009;50:5846–50.
[101] Liu Y, He JH, Yu JY. Bubble-electrospinning: a novel method for making nanofibers. J Phys Conf Ser 2008;96(12001):1–4.
[102] Zhang DM, Chang J. Electrospinning of three-dimensional nanofibrous tubes with controllable architectures. Nano Lett 2008;8:3283–7.
[103] Hejazi F, Mirzadeh H, Contessi N, Tanzi MC, Faré S. Novel class of collector in electrospinning device for the fabrication of 3D nanofibrous structure for large defect load-bearing tissue engineering application. J Biomed Mater Res A 2017;105:1535–48.
[104] Li D, Wang Y, Xia YN. Electrospinning nanofibers as uniaxially aligned arrays and layer-by-layer stacked films. Adv Mater 2004;16:361–6.
[105] Dalton PD, Klee D, Möller M. Electrospinning with dual collection rings. Polymer 2005;46:611–4.
[106] Ju YM, Choi JS, Atala A, Yoo JJ, Lee SJ. Bilayered scaffold for engineering cellularized blood vessels. Biomaterials 2010;31:4313–21.
[107] Pan H, Li LM, Hu L, Cui XJ. Continuous aligned polymer fibers produced by a modified electrospinning method. Polymer 2006;47:4901–4.
[108] Katta P, Alessandro M, Ramsier RD, Chase GG. Continuous electrospinning of aligned polymer nanofibers onto a wire drum collector. Nano Lett 2004;4:2215–8.
[109] Zussman E, Theron A, Yarin AL. Formation of nanofiber crossbars in electrospinning. Appl Phys Lett 2003;82:973–5.
[110] Beachley V, Katsanevakis E, Zhang N, Wen XJ. A novel method to precisely assemble loose nanofiber structures for regenerative medicine applications. Adv Healthc Mater 2013;2:343–51.
[111] Smit E, Bűttner U, Sanderson RD. Continuous yarns from electrospun fibers. Polymer 2005;46:2419–23.
[112] Teo WE, Gopal R, Ramaseshan R, Fujihara K, Ramakrishna S. A dynamic liquid support system for continuous electrospun yarn fabrication. Polymer 2007;48:3400–5.
[113] Zhang X, Gao XH, Jiang L, Qin JH. Flexible generation of gradient electrospinning nanofibers using a microfluidic assisted approach. Langmuir 2012;28:10026–32.
[114] Park SH, Kim TG, Kim HC, Yang DY, Park TG. Development of dual scale scaffolds via direct polymer melt deposition and electrospinning for applications in tissue regeneration. Acta Biomater 2008;4:1198–207.
[115] Jia C, Yu D, Lamarre M, Leopold PL, Teng YD, Wang HJ. Patterned electrospun nanofiber matrices via localized dissolution: potential for guided tissue formation. Adv Mater 2014;26:8192–7.
[116] Loscertales IG, Barrero A, Guerrero I, Cortijo R, Marquez M, Gañán-Calvo AM. Micro/nano encapsulation via electrified coaxial liquid jets. Science 2002;295:1695–8.
[117] Sun Z, Zussman E, Yarin AL, Wendorff JH, Greiner A. Compound core-shell polymer nanofibers by co-electrospinning. Adv Mater 2003;15:1929–32.
[118] Yu JH, Fridrikh SV, Rutledge GC. Production of submicrometer diameter fibers by two-fluid electrospinning. Adv Mater 2004;16:1562–6.
[119] Jiang H, Hu Y, Li Y, Zhao P, Zhu K, Chen W. A facile technique to prepare biodegradable coaxial electrospun nanofibers for controlled release of bioactive agents. J Control Release 2005;108:237–43.
[120] Jin HJ, Fridrikh SV, Rutledge GC, Kaplan DL. Electrospinning bombyx mori silk with poly(ethylene oxide). Biomacromolecules 2002;3:1233–9.
[121] Wang M, Yu JH, Kaplan DL, Rutledge GC. Production of submicron diameter silk fibers under benign processing conditions by two-fluid electrospinning. Macromolecules 2006;39:1102–7.
[122] Zhao Y, Cao XY, Jiang L. Bio-mimic multichannel microtubes by a facile method. J Am Chem Soc 2007;129:764–5.
[123] Roh KH, Martin DC, Lahann J. Biphasic Janus particles with nanoscale anisotropy. Nat Mater 2005;4:759–63.
[124] Madhugiri S, Dalton A, Gutierrez J, Ferraris JP, Balkus Jr KJ. Electrospun MEH-PPV/SBA-15 composite nanofibers using a dual syringe method. J Am Chem Soc 2003;125:14531–8.
[125] Li XQ, Su Y, Liu SP, Tan LJ, Mo XM, Ramakrishna S. Encapsulation of proteins in poly(l-lactide-co-caprolactone) fibers by emulsion electrospinning. Colloids Surf B 2010;75:418–24.
[126] Hong YL, Chen XS, Jing XB, Fan HS, Gu ZW, Zhang XD. Fabrication and drug delivery of ultrathin mesoporous bioactive glass hollow fibers. Adv Funct Mater 2010;20:1503–10.
[127] Qi HX, Hu P, Xu J, Wang AJ. Encapsulation of drug reservoirs in fibers by emulsion electrospinning: morphology characterization and preliminary release assessment. Biomacromolecules 2006;7:2327–30.
[128] Xu XL, Zhuang XL, Chen XS, Wang XR, Yang LX, Jing XB. Preparation of core-sheath composite nanofibers by emulsion electrospinning. Macromol Rapid Commun 2006;27:1637–42.
[129] Shin YM, Hohman MM, Brenner MP, Rutledge GC. Experimental characterization of electrospinning: the electrically forced jet and instabilities. Polymer 2001;42:09955–67.
[130] Luo C, Li L, Li JR, Yang G, Ding S, Zhi W, et al. Modulating cellular behaviors through surface nanoroughness. J Mater Chem 2012;22:15654–64.
[131] Ding S, Li JR, Luo C, Li L, Yang G, Zhou SB. Synergistic effect of released dexamethasone and surface nanoroughness on mesenchymal stem cell differentiation. Biomater Sci 2013;1:1091–100.
[132] Tian XL, Bai H, Zheng YM, Jiang L. Bio-inspired heterostructured bead-on-string fibers that respond to environmental wetting. Adv Funct Mater 2011;21:1398–402.
[133] Luo D, Zhang X, Shahid S, Cattell MJ, Gould DJ, Sukhorukov GB. Electrospun poly(lactic acid) fibers containing novel chlorhexidine particles with sustained antibacterial activity. Biomater Sci 2017;5:111–9.
[134] Zhang CL, Yu SH. Nanoparticles meet electrospinning: recent advances and future prospects. Chem Soc Rev 2014;43:4423–48.
[135] Friedemann K, Corrales T, Kappl M, Landfester K, Crespy D. Facile and large-scale fabrication of anisometric particles from fibers synthesized by colloid-electrospinning. Small 2012;8:144–53.
[136] Crespy D, Friedemann K, Popa AM. Colloid-electrospinning: fabrication of multicompartment nanofibers by the electrospinning of organic or/and inorganic dispersions and emulsions. Macromol Rapid Commun 2012;33:1978–95.
[137] Jin Y, Yang DY, Kang DY, Jiang XY. Fabrication of necklace-like structures via electrospinning. Langmuir 2010;26:1186–90.
[138] Yuan W, Zhang KQ. Structural evolution of electrospun composite fibers from the blend of polyvinyl alcohol and polymer nanoparticles. Langmuir 2012;28:15418–24.
[139] Dayal P, Liu J, Kumar S, Kyu T. Experimental and theoretical investigations of porous structure formation in electrospun fibers. Macromolecules 2007;40:7689–94.
[140] Bognitzki M, Czado W, Frese T, Schaper A, Hellwig M, Steinhart M, et al. Nanostructured fibers via electrospinning. Adv Mater 2001;13:70–2.
[141] Lin JY, Ding B, Yu JY, Hsieh Y. Direct fabrication of highly nanoporous polystyrene fibers via electrospinning. ACS Appl Mater Interfaces 2010;2:521–8.
[142] McCann JT, Marquez M, Xia YN. Highly porous fibers by electrospinning into a cryogenic liquid. J Am Chem Soc 2006;128:1436–7.
[143] Megelski S, Stephens JS, Chase DB, Rabolt JF. Micro- and nanostructured surface morphology on electrospun polymer fibers. Macromolecules 2002;35:8456–66.
[144] Casper CL, Stephens JS, Tassi NG, Chase DB, Rabolt JF. Controlling surface morphology of electrospun polystyrene fibers: effect of humidity and molecular weight in the electrospinning process. Macromolecules 2004;37:573–8.
[145] You Y, Youk JH, Lee SW, Min BM, Lee SJ, Park WH. Preparation of porous ultrafine PGA fibers via selective dissolution of electrospun PGA/PLA blend fibers. Mater Lett 2006;60:757–60.
[146] Kokubo H, Ding B, Naka T, Tsuchihira H, Shiratori S. Multi-core cable-like TiO2 nanofibrous membranes for dye-sensitized solar cells. Nanotechnology 2007;18(165604):1–6.
[147] Sun Y, Sills RB, Hu X, Seh ZW, Xiao X, Xu H, et al. A bamboo-inspired nanostructure design for flexible, foldable, and twistable energy storage devices. Nano Lett 2015;15:3899–906.

[148] Koombhongse S, Liu WX, Reneker DH. Flat polymer ribbons and other shapes by electrospinning. J Polym Sci B Polym Phys 2001;39:2598–606.
[149] Rojas OJ, Montero GA, Habibi Y. Electrospun nanocomposites from polystyrene loaded with cellulose nanowhiskers. J Appl Polym Sci 2009;113:927–35.
[150] Koski A, Yim K, Shivkumar S. Effect of molecular weight on fibrous PVA produced by electrospinning. Mater Lett 2004;58:493–7.
[151] Yoshioka T, Dersch R, Tsuji M, Schaper AK. Orientation analysis of individual electrospun PE nanofibers by transmission electron microscopy. Polymer 2010;51:2383–9.
[152] Ner Y, Stuart JA, Whited G, Sotzing GA. Electrospinning nanoribbons of a bioengineered silk-elastin-like protein (SELP) from water. Polymer 2009;50:5828–36.
[153] Zhang KH, Mo XM, Huang C, He CL, Wang HS. Electrospun scaffolds from silk fibroin and their cellular compatibility. J Biomed Mater Res A 2010;93:976–83.
[154] Wang H, Zhang YP, Shao HL, Hu XC. Electrospun ultra-fine silk fibroin fibers from aqueous solutions. J Mater Sci 2005;40:5359–63.
[155] Li SD, Zhao Y, Wang CY, Li DD, Gao K. Fabrication and characterization unique ribbon-like porous Ag/LaFeO3 nanobelts photocatalyst via electrospinning. Mater Lett 2016;170:122–5.
[156] Chen X, Wang WD, Cheng S, Dong B, Li CY. Mimicking bone nanostructure by combining block copolymer self-assembly and 1d crystal nucleation. ACS Nano 2013;7:8251–7.
[157] Wang XF, Salick MR, Wang XD, Cordie T, Han WJ, Peng YY, et al. Poly(ε-caprolactone) nanofibers with a self-induced nanohybrid shish-kebab structure mimicking collagen fibrils. Biomacromolecules 2013;14:3557–69.
[158] Kessick R, Tepper G. Microscale polymeric helical structures produced by electrospinning. Appl Phys Lett 2004;84:4807–9.
[159] Xin Y, Reneker DH. Hierarchical polystyrene patterns produced by electrospinning. Polymer 2012;53:4254–61.
[160] Holzmeister A, Greiner A, Wendorff JH. Barbed nanowires from polymers via electrospinning. Polym Eng Sci 2009;49:148–53.
[161] Ostermann R, Li D, Yin YD, McCann JT, Xia YN. V2O5 Nanorods on TiO2 nanofibers: a new class of hierarchical nanostructures enabled by electrospinning and calcination. Nano Lett 2006;6:1297–302.
[162] Xiang J, Lu W, Hu Y, Wu Y, Yan H, Lieber CM. Ge/Si nanowire heterostructures as high-performance field-effect transistors. Nature 2006;441:489–93.
[163] McAlpine MC, Ahmad H, Wang D, Heath JR. Highly ordered nanowire arrays on plastic substrates for ultrasensitive flexible chemical sensors. Nat Mater 2007;6:379–84.
[164] Xie J, Li X, Lipner J, Manning CN, Schwartz AG, Thomopoulos S, et al. Aligned-to-random nanofiber scaffolds for mimicking the structure of the tendon-to-bone insertion site. Nanoscale 2010;2:923–6.
[165] Li L, Yang G, Li J, Ding S, Zhou SB. Cell behaviors on magnetic electrospun poly-d, l-lactide nanofibers. Mater Sci Eng C 2014;34:252–61.
[166] Liu WY, Thomopoulos S, Xia YN. Electrospun nanofibers for regenerative medicine. Adv Healthc Mater 2012;1:10–25.
[167] Surrao DC, Hayami JWS, Waldman SD, Amsden BG. Self-Crimping, biodegradable, electrospun polymer microfibers. Biomacromolecules 2010;11:3624–9.
[168] Lim JM, Moon JH, Yi GR, Heo CJ, Yang SM. Fabrication of one-dimensional colloidal assemblies from electrospun nanofibers. Langmuir 2006;22:3445–9.
[169] Baji A, Mai YW, Du XS, Wong SC. Improved tensile strength and ferroelectric phase content of self-assembled polyvinylidene fluoride fiber yarns. Macromol Mater Eng 2012;297:209–13.
[170] Wang XF, Zhang K, Zhu MF, Yu H, Zhou Z, Chen YM, et al. Continuous polymer nanofiber yarns prepared by self-bundling electrospinning method. Polymer 2008;49:2755–61.
[171] Ko F, Gogotsi Y, Ali A, Naguib N, Ye H, Yang GL, et al. Electrospinning of continuous carbon nanotube-filled nanofiber yarns. Adv Mater 2003;15:1161–5.
[172] Wang XF, Zhang K, Zhu MF, Hsiao BS, Chu B. Enhanced mechanical performance of self-bundled electrospun fiber yarns via post-treatments. Macromol Rapid Commun 2008;29:826–31.
[173] Penchev H, Paneva D, Manolova N, Rashkov I. Hybrid nanofibrous yarns based on N-carboxyethylchitosan and silver nanoparticles with antibacterial activity prepared by self-bundling electrospinning. Carbohydr Res 2010;345:2374–80.
[174] Li WJ, Danielson KG, Alexander PG, Tuan RS. Biological response of chondrocytes cultured in three-dimensional nanofibrous poly(ε-caprolactone) scaffolds. J Biomed Mater Res A 2003;67A:1105–14.
[175] Li WJ, Laurencin CT, Caterson EJ, Tuan RS, Ko FK. Electrospun nanofibrous structure: a novel scaffold for tissue engineering. J Biomed Mater Res A 2002;60:613–21.
[176] Li WJ, Tuli R, Huang X, Laquerriere P, Tuan RS. Multilineage differentiation of human mesenchymal stem cells in a three-dimensional nanofibrous scaffold. Biomaterials 2005;26:5158–66.
[177] Lee J, Lee SY, Jang J, Jeong YH, Cho DW. Fabrication of patterned nanofibrous mats using direct-write electrospinning. Langmuir 2012;28:7267–75.
[178] Zhao S, Zhou Q, Long YZ, Sun GH, Zhang Y. Nanofibrous patterns by direct electrospinning of nanofibers onto topographically structured non-conductive substrates. Nanoscale 2013;5:4993–5000.
[179] Cho SJ, Kim B, An T, Lim G. Replicable multilayered nanofibrous patterns on a flexible film. Langmuir 2010;26:14395–9.
[180] Park SM, Kim DS. Electrolyte-assisted electrospinning for a self-assembled, free-standing nanofiber membrane on a curved surface. Adv Mater 2015;27:1682–7.
[181] Zhang D, Chang J. Patterning of electrospun fibers using electroconductive templates. Adv Mater 2007;19:3664–7.
[182] Yan GD, Yu J, Qiu YJ, Yi XS, Lu J, Zhou XS, et al. Self-assembly of electrospun polymer nanofibers: a general phenomenon generating honeycomb-patterned nanofibrous structures. Langmuir 2011;27:4285–9.
[183] Wang XF, Ding B, Sun G, Wang MR, Yu JY. Electro-spinning/netting: a strategy for the fabrication of three-dimensional polymer nano-fiber/nets. Prog Mater Sci 2013;58:1173–243.
[184] Ding B, Li CR, Miyauchi Y, Kuwaki O, Shiratori S. Formation of novel 2D polymer nanowebs via electrospinning. Nanotechnology 2006;17:3685–91.
[185] Ng R, Zang R, Yang KK, Liu N, Yang ST. Three-dimensional fibrous scaffolds with microstructures and nanotextures for tissue engineering. RSC Adv 2012;2:10110–24.
[186] Sun B, Jiang XJ, Zhang SC, Zhang JC, Li YF, You QZ, et al. Electrospun anisotropic architectures and porous structures for tissue engineering. J Mater Chem B 2015;3:5389–410.
[187] Su Z, Li J, Ouyang Z, Arras MML, Wei G. Jandt KD. Biomimetic 3D hydroxyapatite architectures with interconnected pores based on electrospun biaxially orientated PCL nanofibers. RSC Adv 2014;4:14833–9.
[188] Blakeney BA, Tambralli A, Anderson JM, Andukuri A, Lim DJ, Dean DR, et al. Cell infiltration and growth in a low density, uncompressed three-dimensional electrospun nanofibrous scaffold. Biomaterials 2011;32:1583–90.
[189] Wang W, Itoh S, Konno K, Kikkawa T, Ichinose S, Sakai K, et al. Effects of Schwann cell alignment along the oriented electrospun chitosan nanofibers on nerve regeneration. J Biomed Mater Res A 2009;91:994–1005.
[190] Ahn H, Ju YM, Takahashi H, Williams DF, Yoo JJ, Lee SJ, et al. Engineered small diameter vascular grafts by combining cell sheet engineering and electrospinning technology. Acta Biomater 2015;16:14–22.
[191] Leung LH, Fan S, Naguib HE. Fabrication of 3D electrospun structures from poly(lactide-co-glycolide acid)-nano-hydroxyapatite composites. J Polym Sci B Polym Phys 2012;50:242–9.
[192] Kim TG, Chung HJ, Park TG. Macroporous and nanofibrous hyaluronic acid/collagen hybrid scaffold fabricated by concurrent electrospinning and deposition/leaching of salt particles. Acta Biomater 2008;4:1611–9.
[193] Shim IK, Jung MR, Kim KH, Seol YJ, Park YJ, Park WH, et al. Novel three-dimensional scaffolds of poly(L-lactic acid) microfibers using electrospinning and mechanical expansion: fabrication and bone regeneration. J Biomed Mater Res B 2010;95B:150–60.
[194] Chou SF, Carson D, Woodrow KA. Current strategies for sustaining drug release from electrospun nanofibers. J Control Release 2015;220(Pt B):584–91.
[195] Blakney AK, Ball C, Krogstad EA, Woodrow KA. Electrospun fibers for vaginal anti-HIV drug delivery. Antiviral Res 2013;100:S9–16.
[196] Blakney AK, Krogstad EA, Jiang YH, Woodrow KA. Delivery of multipurpose prevention drug combinations from electrospun nanofibers using composite microarchitectures. Int J Nanomedicine 2014;9:2967–78.
[197] Ball C, Woodrow KA. Electrospun solid dispersions of maraviroc for rapid intravaginal preexposure prophylaxis of HIV. Antimicrob Agents Chemother 2014;58:4855–65.
[198] Krogstad EA, Woodrow KA. Manufacturing scale-up of electrospun poly(vinyl alcohol) fibers containing tenofovir for vaginal drug delivery. Int J Pharm 2014;475:282–91.
[199] Kim K, Luu YK, Chang C, Fang D, Hsiao BS, Chu B, et al. Incorporation and controlled release of a hydrophilic antibiotic using poly(lactide-co-glycolide)-based electrospun nanofibrous scaffolds. J Control Release 2004;98:47–56.
[200] Yohe ST, Colson YL, Grinstaff MW. Superhydrophobic materials for tunable drug release: using displacement of air to control delivery rates. J Am Chem Soc 2012;134:2016–9.
[201] Heunis TD, Dicks LM. Nanofibers offer alternative ways to the treatment of skin infections. J Biomed Biotechnol 2010;2010(510682):1–10.
[202] Carson D, Jiang Y, Woodrow KA. Tunable release of multiclass anti-HIV drugs that are water soluble and loaded at high drug content in polyester blended electrospun fibers. Pharm Res 2016;133:125–36.
[203] Huang ZM, He CL, Yang AZ, Zhang Y, Han XJ, Yin J, et al. Encapsulating drugs in biodegradable ultrafine fibers through co-axial electrospinning. J Biomed Mater Res A 2006;77:169–79.
[204] Zhang YZ, Wang X, Feng Y, Li J, Lim CT, Ramakrishna S. Coaxial electrospinning of (fluorescein isothiocyanate-conjugated bovine serum albumin)-encapsulated poly(ε-caprolactone) nanofibers for sustained release. Biomacromolecules 2006;7:1049–57.
[205] Falde EJ, Freedman JD, Herrera VL, Yohe ST, Colson YL, Grinstaff MW. Layered superhydrophobic meshes for controlled drug release. J Control Release 2015;214:23–9.
[206] Okuda T, Tominaga K, Kidoaki S. Time-programmed dual release formulation by multilayered drug-loaded nanofiber meshes. J Control Release 2010;143:258–64.
[207] Hu CM, Cui WG. Hierarchical structure of electrospun composite fibers for long-term controlled drug release carriers. Adv Healthc Mater 2012;1:809–14.

[208] Hu CM, Liu S, Zhang Y, Li B, Yang HL, Fan CY, et al. Long-term drug release from electrospun fibers for in vivo inflammation prevention in the prevention of peritendinous adhesions. Acta Biomater 2013;9:7381–8.
[209] Mickova A, Buzgo M, Benada O, Rampichova M, Fisar Z, Filova E, et al. Core/shell nanofibers with embedded liposomes as a drug delivery system. Biomacromolecules 2012;13:952–62.
[210] Ionescu LC, Lee GC, Sennett BJ, Burdick JA, Mauck RL. An anisotropic nanofiber/microsphere composite with controlled release of biomolecules for fibrous tissue engineering. Biomaterials 2010;31:4113–20.
[211] DeVolder RJ, Bae H, Lee J, Kong H. Directed blood vessel growth using an angiogenic microfiber/microparticle composite patch. Adv Mater 2011;23:3139–43.
[212] Tan ST, Wendorff JH, Pietzonka C, Jia ZH, Wang GQ. Biocompatible and biodegradable polymer nanofibers displaying superparamagnetic properties. Chemphyschem 2005;6:1461–5.
[213] Li JR, Fu R, Li L, Yang G, Ding S, Zhong ZD, et al. Co-delivery of dexamethasone and green tea polyphenols using electrospun ultrafine fibers for effective treatment of keloid. Pharm Res 2014;31:1632–43.
[214] Dong B, Smith ME, Wnek GE. Encapsulation of multiple biological compounds within a single electrospun fiber. Small 2009;5:1508–12.
[215] Jo E, Lee S, Kim KT, Won YS, Kim H, Cho EC, et al. Core-sheath nanofibers containing colloidal arrays in the core for programmable multi-agent delivery. Adv Mater 2009;21:968–72.
[216] Friedemann K, Turshatov A, Landfester K, Crespy D. Characterization via two-color sted microscopy of nanostructured materials synthesized by colloid electrospinning. Langmuir 2011;27:7132–9.
[217] Hou ZY, Li XJ, Li CX, Dai YL, Ma PA, Zhang X, et al. Electrospun upconversion composite fibers as dual drugs delivery system with individual release properties. Langmuir 2013;29:9473–82.
[218] Yang G, Wang J, Li L, Ding S, Zhou SB. Electrospun micelles/drug-loaded nanofibers for time-programmed multi-agent release. Macromol Biosci 2014;14:965–76.
[219] Su Y, Su QQ, Liu W, Jin GR, Mo XM, Ramakrishn S. Dual-drug encapsulation and release from core-shell nanofibers. J Biomater Sci Polym Ed 2012;23:861–71.
[220] Chen ML, Li YF, Besenbacher F. Electrospun nanofibers-mediated on-demand drug release. Adv Healthc Mater 2014;3:1721–32.
[221] Weng L, Xie JW. Smart electrospun nanofibers for controlled drug release: recent advances and new perspectives. Curr Pharm Des 2015;21:1944–59.
[222] Huang C, Soenen SJ, Rejman J, Lucas B, Braeckmans K, Demeester J, et al. Stimuli-responsive electrospun fibers and their applications. Chem Soc Rev 2011;40:2417–34.
[223] Lin XL, Tang DY, Cui WW, Cheng Y. Controllable drug release of electrospun thermoresponsive poly(N-isopropylacrylamide)/poly(2-acrylamido-2-methylpropanesulfonic acid) nanofibers. J Biomed Mater Res A 2012;100:1839–45.
[224] Li L, Yang G, Zhou GL, Wang Y, Zheng XT, Zhou SB. Thermally switched release from a nanogel-in-microfiber device. Adv Healthc Mater 2015;4:1658–63.
[225] Sasikala ARK, Unnithan AR, Yun YH, Park CH, Kim CS. An implantable smart magnetic nanofiber device for endoscopic hyperthermia treatment and tumor-triggered controlled drug release. Acta Biomater 2016;31:122–33.
[226] Jedlovszky-Hajdu A, Molnar K, Nagy PM, Sinko K, Zrinyi M. Preparation and properties of a magnetic field responsive three-dimensional electrospun polymer scaffold. Colloids Surf A 2016;503:79–87.
[227] Kim Y, Ebara M, Aoyagi T. A smart hyperthermia nanofiber with switchable drug release for inducing cancer apoptosis. Adv Funct Mater 2013;23:5753–61.
[228] Fu GD, Xu LQ, Yao F, Li GL, Kang ET. Smart nanofibers with a photoresponsive surface for controlled release. ACS Appl Mater Interfaces 2009;1:2424–7.
[229] Yun J, Im JS, Lee YS, Kim HI. Electro-responsive transdermal drug delivery behavior of PVA/PAA/MWCNT nanofibers. Eur Polym J 2011;47:1893–902.
[230] Yuan ZM, Zhao X, Zhao JW, Pan GQ, Qiu WW, Wang XH, et al. Synergistic mediation of tumor signaling pathways in hepatocellular carcinoma therapy via dual-drug-loaded pH-responsive electrospun fibrous scaffolds. J Mater Chem B 2015;3:3436–46.
[231] Li F, Zhang T, Gao X, Wang R, Li BH. Coaxial electrospinning heterojunction SnO2/Au-doped In2O3 core-shell nanofibers for acetone gas sensor. Sens Actuators B 2017;252:822–30.
[232] Ding B, Wang M, Yu J, Sun G. Gas sensors based on electrospun nanofibers. Sensors 2009;9:1609–24.
[233] Zhang Y, Li JP, An G, He XL. Highly porous SnO2 fibers by electrospinning and oxygen plasma etching and its ethanol-sensing properties. Sens Actuators B 2010;144:43–8.
[234] Chen CK, Huang SC. Preparation of reductant-responsive n-maleoyl-functional chitosan/poly(vinyl alcohol) nanofibers for drug delivery. Mol Pharm 2016;13:4152–67.
[235] Balaconis MK, Luo Y, Clark HA. Glucose-sensitive nanofiber scaffolds with an improved sensing design for physiological conditions. Analyst 2015;140:716–23.
[236] Yang DY, Liu X, Jin Y, Zhu Y, Zeng DD, Jiang XY, et al. Electrospinning of poly(dimethylsiloxane)/poly(methyl methacrylate) nanofibrous membrane: fabrication and application in protein microarrays. Biomacromolecules 2009;10:3335–40.
[237] Chen JZ, Zhang SS, Sun FG, Li N, Cui K, He JP, et al. Multi-stimuli responsive supramolecular polymers and their electrospun nanofibers. Polym Chem 2016;7:2947–54.
[238] Wang Y, Kotsuchibashi Y, Uto K, Ebara M, Aoyagi T, Liu Y. Narain R. pH and glucose responsive nanofibers for the reversible capture and release of lectins. Biomater Sci 2015;3:152–62.
[239] Yuan HH, Li BY, Liang K, Lou XX, Zhang YZ. Regulating drug release from pH- and temperature-responsive electrospun CTS-g-PNIPAAm/poly(ethylene oxide) hydrogel nanofibers. Biomed Mater 2014;9(055001):1–10.
[240] Ignatious F, Sun L, Lee CP, Baldoni J. Electrospun nanofibers in oral drug delivery. Pharm Res 2010;27:576–88.
[241] Yu DG, Shen XX, Branford-White C, White K, Zhu LM, Bligh SW. Oral fast-dissolving drug delivery membranes prepared from electrospun polyvinylpyrrolidone ultrafine fibers. Nanotechnology 2009;20(055104):1–9.
[242] Li X, Kanjwal MA, Lin L, Chronakis IS. Electrospun polyvinyl-alcohol nanofibers as oral fast-dissolving delivery system of caffeine and riboflavin. Colloids Surf B 2013;103:182–8.
[243] Nam S, Lee JJ, Lee SY, Jeong JY, Kang WS, Cho HJ. Angelica gigas Nakai extract-loaded fast-dissolving nanofiber based on poly(vinyl alcohol) and Soluplus for oral cancer therapy. Int J Pharm 2017;526:225–34.
[244] Aduba DC, Hammer JA, Yuan Q, Andrew Yeudall WA, Bowlin GL, Yang H. Semi-interpenetrating network (sIPN) gelatin nanofiber scaffolds for oral mucosal drug delivery. Acta Biomater 2013;9:6576–84.
[245] Taepaiboon P, Rungsardthong U, Supaphol P. Vitamin-loaded electrospun cellulose acetate nanofiber mats as transdermal and dermal therapeutic agents of vitamin A acid and vitamin E. Eur J Pharm Biopharm 2007;67:387–97.
[246] Madhaiyan K, Sridhar R, Sundarrajan S, Venugopal JR, Ramakrishna S. Vitamin B12 loaded polycaprolactone nanofibers: a novel transdermal route for the water soluble energy supplement delivery. Int J Pharm 2013;444:70–6.
[247] Cheng LY, Sun XM, Zhao X, Wang L, Yu J, Pan GQ, et al. Surface biofunctional drug-loaded electrospun fibrous scaffolds for comprehensive repairing hypertrophic scars. Biomaterials 2016;83:169–81.
[248] Yan EY, Fan YM, Sun ZY, Gao JW, Hao XY, Pei SC, et al. Biocompatible core-shell electrospun nanofibers as potential application for chemotherapy against ovary cancer. Mater Sci Eng C 2014;41:217–23.
[249] Park Y, Kang E, Kwon O, Hwang T, Park H, Lee JM, et al. Ionically crosslinked Ad/chitosan nanocomplexes processed by electrospinning for targeted cancer gene therapy. J Control Release 2010;148:75–82.
[250] Ho EA, Soo PL, Allen C, Piquette-Miller M. Impact of intraperitoneal, sustained delivery of paclitaxel on the expression of P-glycoprotein in ovarian tumors. J Control Release 2007;117:20–7.
[251] Wolinsky JB, Colson YL, Grinstaff MW. Local drug delivery strategies for cancer treatment: gels, nanoparticles, polymeric films, rods, and wafers. J Control Release 2012;159:14–26.
[252] De Souza R, Zahedi P, Allen CJ, Piquette-Miller M. Polymeric drug delivery systems for localized cancer chemotherapy. Drug Deliv 2010;17:365–75.
[253] Ranganath SH, Wang CH. Biodegradable microfiber implants delivering paclitaxel for post-surgical chemotherapy against malignant glioma. Biomaterials 2008;29:2996–3003.
[254] Bagó JR, Pegna GJ, Okolie O, Mohiti-Asli M, Loboa EG, Hingtgen SD. Electrospun nanofibrous scaffolds increase the efficacy of stem cell-mediated therapy of surgically resected glioblastoma. Biomaterials 2016;90:116–25.
[255] Monterrubio C, Pascual-Pasto G, Cano F, Vila-Ubach M, Manzanares A, Schaiquevich P, et al. SN-38-loaded nanofiber matrices for local control of pediatric solid tumors after subtotal resection surgery. Biomaterials 2016;79:69–78.
[256] Ranganath SH, Fu Y, Arifin DY, Kee I, Zheng L, Lee HS, et al. The use of submicron/nanoscale PLGA implants to deliver paclitaxel with enhanced pharmacokinetics and therapeutic efficacy in intracranial glioblastoma in mice. Biomaterials 2010;31:5199–207.
[257] Yang G, Wang J, Wang Y, Li L, Guo X, Zhou SB. An implantable active-targeting micelle-in-nanofiber device for efficient and safe cancer therapy. ACS Nano 2015;9:1161–74.
[258] Zong S, Wang X, Yang YP, Wu WB, Li HJ, Ma Y, et al. The use of cisplatin-loaded mucoadhesive nanofibers for local chemotherapy of cervical cancers in mice. Eur J Pharm Biopharm 2015;93:127–35.
[259] Luo XM, Xie CY, Wang H, Liu CY, Yan SL, Li XH. Antitumor activities of emulsion electrospun fibers with core loading of hydroxycamptothecin via intratumoral implantation. Int J Pharm 2012;425:19–28.
[260] Kaplan JA, Liu R, Freedman JD, Padera R, Schwartz J, Colson YL, et al. Prevention of lung cancer recurrence using cisplatin-loaded superhydrophobic nanofiber meshes. Biomaterials 2016;76:273–81.
[261] Zhang Z, Liu S, Xiong H, Jing X, Xie Z, Chen X, et al. Electrospun PLA/MWCNTs composite nanofibers for combined chemo- and photothermal therapy. Acta Biomater 2015;26:115–23.
[262] Wang Y, Luo C, Yang G, Wei X, Liu D, Zhou SB. A luteolin-loaded electrospun fibrous implantable device for potential therapy of gout attacks. Macromol Biosci 2016;16:1598–609.
[263] Ashbaugh AG, Jiang X, Zheng J, Tsai AS, Kim W, Thompson JM, et al. Polymeric nanofiber coating with tunable combinatorial antibiotic delivery prevents biofilm-associated infection in vivo. Proc Natl Acad Sci USA 2016;113:E6919–28.

[264] Song ZL, Ma YJ, Xia GG, Wang Y, Kapadia W, Sun ZY, et al. In vitro and in vivo combined antibacterial effect of levofloxacin/silver co-loaded electrospun fibrous membranes. J Mater Chem B 2017;5:7632–43.
[265] Wu W, Cheng RY, Das Neves J, Tang JC, Xiao JY, Ni Q, et al. Advances in biomaterials for preventing tissue adhesion. J Control Release 2017;261:318–36.
[266] Bölgen N, Vargel I, Korkusuz P, Menceloğlu YZ, Pişkin E. In vivo performance of antibiotic embedded electrospun PCL membranes for prevention of abdominal adhesions. J Biomed Mater Res 2007;81:530–43.
[267] Jiang SC, Zhao X, Chen S, Pan GQ, Song JL, He N, et al. Down-regulating ERK1/2 and SMAD2/3 phosphorylation by physical barrier of celecoxib-loaded electrospun fibrous membranes prevents tendon adhesions. Biomaterials 2014;35:9920–9.
[268] Chen SH, Chen CH, Fong YT, Chen JP. Prevention of peritendinous adhesions with electrospun chitosan-grafted polycaprolactone nanofibrous membranes. Acta Biomater 2014;10:4971–82.
[269] Liu S, Pan GQ, Liu GW, Neves JD, Song S, Chen S, et al. Electrospun fibrous membranes featuring sustained release of ibuprofen reduce adhesion and improve neurological function following lumbar laminectomy. J Control Release 2017;264:1–13.
[270] Jiang T, Carbone EJ, Lo KWH, Laurencin CT. Electrospinning of polymer nanofibers for tissue regeneration. Prog Polym Sci 2015;46:1–24.
[271] Agarwal S, Wendorff JH, Greiner A. Progress in the field of electrospinning for tissue engineering applications. Adv Mater 2009;21:3343–51.
[272] Norouzi M, Boroujeni SM, Omidvarkordshouli N, Soleimani M. Advances in skin regeneration: application of electrospun scaffolds. Adv Healthc Mater 2015;4:1114–33.
[273] Kuppan P, Vasanthan KS, Sundaramurthi D, Krishnan UM, Sethuraman S. Development of poly(3-hydroxybutyrate-co-3-hydroxyvalerate) fibers for skin tissue engineering: effects of topography, mechanical, and chemical stimuli. Biomacromolecules 2011;12:3156–65.
[274] Lin HY, Chen HH, Chang SH, Ni TS. Pectin-chitosan-PVA nanofibrous scaffold made by electrospinning and its potential use as a skin tissue scaffold. J Biomater Sci Polym Ed 2013;24:470–84.
[275] Krishnan R, Rajeswari R, Venugopal J, Sundarrajan S, Sridhar R, Shayanti M, et al. Polysaccharide nanofibrous scaffolds as a model for in vitro skin tissue regeneration. J Mater Sci Mater Med 2012;23:1511–9.
[276] Sundaramurthi D, Krishnan UM, Sethuraman S. Electrospun nanofibers as scaffolds for skin tissue engineering. Polym Rev 2014;54:348–76.
[277] Babaeijandaghi F, Shabani I, Seyedjafari E, Naraghi ZS, Vasei M, Haddadi-Asl V, et al. Accelerated epidermal regeneration and improved dermal reconstruction achieved by polyethersulfone nanofibers. Tissue Eng Part A 2010;16:3527–36.
[278] Powell HM, Supp DM, Boyce ST. Influence of electrospun collagen on wound contraction of engineered skin substitutes. Biomaterials 2008;29:834–43.
[279] Zhang YZ, Venugopal J, Huang ZM, Lim CT, Ramakrishna S. Characterization of the surface biocompatibility of the electrospun pcl-collagen nanofibers using fibroblasts. Biomacromolecules 2005;6:2583–9.
[280] Qu F, Pintauro MP, Haughan JE, Henning EA, Esterhai JL, Schaer TP, et al. Repair of dense connective tissues via biomaterial-mediated matrix reprogramming of the wound interface. Biomaterials 2015;39:85–94.
[281] Sun XM, Lang Q, Zhang HB, Cheng LY, Zhang Y, Pan GQ, et al. Electrospun Sphotocrosslinkable hydrogel fibrous scaffolds for rapid in vivo vascularized skin flap regeneration. Adv Funct Mater 2017;27(1604617):1–12.
[282] Zhong S, Teo WE, Zhu X, Beuerman RW, Ramakrishna S, Yung LY. An aligned nanofibrous collagen scaffold by electrospinning and its effects on in vitro fibroblast culture. J Biomed Mater Res A 2006;79:456–63.
[283] Kurpinski KT, Stephenson JT, Janairo RR, Lee H, Li S. The effect of fiber alignment and heparin coating on cell infiltration into nanofibrous PLLA scaffolds. Biomaterials 2010;31:3536–42.
[284] Ma B, Xie JW, Jiang J, Wu J. Sandwich-type fiber scaffolds with square arrayed microwells and nanostructured cues as microskin grafts for skin regeneration. Biomaterials 2014;35:630–41.
[285] Reis TC, Castleberry S, Rego AM, Aguiar-Ricardo A, Hammond PT. Three-dimensional multilayered fibrous constructs for wound healing applications. Biomater Sci 2016;4:319–30.
[286] Yang H, Kim S, Huh I, Kim S, Lahiji SF, Kim M, et al. Rapid implantation of dissolving microneedles on an electrospun pillar array. Biomaterials 2015;64:70–7.
[287] Zhao QL, Wang SW, Xie YY, Zheng WF, Wang Z, Xiao L, et al. A rapid screening method for wound dressing by cell-on-a-chip device. Adv Healthc Mater 2012;1:560–6.
[288] Uttayarat P, Perets A, Li M, Pimton P, Stachelek SJ, Alferiev I, et al. Micropatterning of three-dimensional electrospun polyurethane vascular grafts. Acta Biomater 2010;6:4229–37.
[289] Browning MB, Dempsey D, Guiza V, Becerra S, Rivera J, Russell B, et al. Multilayer vascular grafts based on collagen-mimetic proteins. Acta Biomater 2012;8:1010–21.
[290] Rayatpisheh S, Heath DE, Shakouri A, Rujitanaroj PO, Chew SY, Chan-Park MB. Combining cell sheet technology and electrospun scaffolding for engineered tubular, aligned, and contractile blood vessels. Biomaterials 2014;35:2713–9.
[291] Lee YB, Jun I, Bak S, Shin YM, Lim Y, Park H, et al. Reconstruction of vascular structure with multicellular components using cell transfer printing methods. Adv Healthc Mater 2014;3:1465–74.
[292] Wang ZH, Zheng WT, Wu YF, Wang JN, Zhang XY, Wang K, et al. Differences in the performance of PCL-based vascular grafts as abdominal aorta substitutes in healthy and diabetic rats. Biomater Sci 2016;4:1485–92.
[293] Wang ZH, Cui Y, Wang JN, Yang XH, Wu YF, Wang K, et al. The effect of thick fibers and large pores of electrospun poly(ε-caprolactone) vascular grafts on macrophage polarization and arterial regeneration. Biomaterials 2014;35:5700–10.
[294] Brozovich FV, Nicholson CJ, Degen CV, Gao YZ, Aggarwal M, Morgan KG. Mechanisms of vascular smooth muscle contraction and the basis for pharmacologic treatment of smooth muscle disorders. Pharmacol Rev 2016;68:476–532.
[295] Shimizu N, Maruyama T, Yoshikawa N, Matsumiya R, Ma Y, Ito N, et al. A muscle-liver-fat signalling axis is essential for central control of adaptive adipose remodelling. Nat Commun 2015;6(6693):1–14.
[296] Senyo SE, Lee RT, Kühn B. Cardiac regeneration based on mechanisms of cardiomyocyte proliferation and differentiation. Stem Cell Res 2014;13(3 Pt B):532–41.
[297] Jana S, Levengood SKL, Zhang MQ. Anisotropic materials for skeletal-muscle-tissue engineering. Adv Mater 2016;28:10588–612.
[298] Visone R, Gilardi M, Marsano A, Rasponi M, Bersini S, Moretti M. Cardiac meets skeletal: what's new in microfluidic models for muscle tissue engineering. Molecules 2016;21(1128):1–21.
[299] Emmert MY, Hitchcock RW, Hoerstrup SP. Cell therapy, 3D culture systems and tissue engineering for cardiac regeneration. Adv Drug Deliv Rev 2014;69–70:254–69.
[300] Wolf MT, Dearth CL, Sonnenberg SB, Loboa EG, Badylak SF. Naturally derived and synthetic scaffolds for skeletal muscle reconstruction. Adv Drug Deliv Rev 2015;84:208–21.
[301] Baker BM, Gee AO, Metter RB, Nathan AS, Marklein RA, Burdick JA, et al. The potential to improve cell infiltration in composite fiber-aligned electrospun scaffolds by the selective removal of sacrificial fibers. Biomaterials 2008;29:2348–58.
[302] McKeon-Fischer KD, Flagg DH, Freeman JW. Coaxial electrospun poly(ε-caprolactone), multiwalled carbon nanotubes, and polyacrylic acid/polyvinyl alcohol scaffold for skeletal muscle tissue engineering. J Biomed Mater Res A 2011;99:493–9.
[303] Chen MC, Sun YC, Chen YH. Electrically conductive nanofibers with highly oriented structures and their potential application in skeletal muscle tissue engineering. Acta Biomater 2013;9:5562–72.
[304] Ku SH, Lee SH, Park CB. Synergic effects of nanofiber alignment and electroactivity on myoblast differentiation. Biomaterials 2012;33:6098–104.
[305] Liao IC, Liu JB, Bursac N, Leong KW. Effect of Electromechanical stimulation on the maturation of myotubes on aligned electrospun fibers. Cell Mol Bioeng 2008;1:133–45.
[306] Fleischer S, Shapira A, Feiner R, Dvir T. Modular assembly of thick multifunctional cardiac patches. Proc Natl Acad Sci USA 2017;114:1898–903.
[307] Yang F, Xu CY, Kotaki M, Wang S, Ramakrishna S. Characterization of neural stem cells on electrospun poly(L-lactic acid) nanofibrous scaffold. J Biomater Sci Polym Ed 2004;15:1483–97.
[308] Suwantong O, Waleetorncheepsawat S, Sanchavanakit N, Pavasant P, Cheepsunthorn P, Bunaprasert T, et al. In vitro biocompatibility of electrospun poly(3-hydroxybutyrate) and poly(3-hydroxybutyrate-co-3-hydroxyvalerate) fiber mats. Int J Biol Macromol 2007;40:217–23.
[309] Cao H, Liu T, Chew SY. The application of nanofibrous scaffolds in neural tissue engineering. Adv Drug Deliv Rev 2009;61:1055–64.
[310] Li XR, Li MY, Sun J, Zhuang Y, Shi JJ, Guan DW, et al. Radially aligned electrospun fibers with continuous gradient of SDF1(for the guidance of neural stem cells. Small 2016;12:5009–18.
[311] Xie JW, MacEwan MR, Liu WY, Jesuraj N, Li XR, Hunter D, et al. Nerve guidance conduits based on double-layered scaffolds of electrospun nanofibers for repairing the peripheral nervous system. ACS Appl Mater Interfaces 2014;6:9472–80.
[312] Xie JW, MacEwan MR, Li XR, Sakiyama-Elbert SE, Xia YN. Neurite outgrowth on nanofiber scaffolds with different orders, structures, and surface properties. ACS Nano 2009;3:1151–9.
[313] Panseri S, Cunha C, Lowery J, Del Carro U, Taraballi F, Amadio S, et al. Electrospun micro- and nanofiber tubes for functional nervous regeneration in sciatic nerve transections. BMC Biotechnol 2008;8(39):1–12.
[314] Meiners S, Ahmed I, Ponery AS, Amor N, Harris SL, Ayres V, et al. Engineering electrospun nanofibrillar surfaces for spinal cord repair: a discussion. Polym Int 2007;56:1340–8.
[315] Carlson AL, Bennett NK, Francis NL, Halikere A, Clarke S, Moore JC, et al. Generation and transplantation of reprogrammed human neurons in the brain using 3D microtopographic scaffolds. Nat Commun 2016;7(10862):1–10.
[316] Wang W, Itoh S, Matsuda A, Ichinose S, Shinomiya K, Hata Y, et al. Influences of mechanical properties and permeability on chitosan nano/microfiber mesh tubes as a scaffold for nerve regeneration. J Biomed Mater Res A 2008;84:557–66.
[317] Corey JM, Gertz CC, Wang B, Birrell LK, Johnson SL, Martin DC, et al. The design of electrospun PLLA nanofiber scaffolds compatible with serum-free growth of primary motor and sensory neurons. Acta Biomater 2008;4:863–75.

[318] Jang JH, Castano O, Kim HW. Electrospun materials as potential platforms for bone tissue engineering. Adv Drug Deliv Rev 2009;61:1065–83.
[319] Woo KM, Jun JH, Chen VJ, Seo J, Baek JH, Ryoo HM, et al. Nano-fibrous scaffolding promotes osteoblast differentiation and biomineralization. Biomaterials 2007;28:335–43.
[320] Ding S, Li L, Liu X, Yang G, Zhou GL, Zhou SB. A nano-micro alternating multilayer scaffold loading with rBMSCs and BMP-2 for bone tissue engineering. Colloids Surf B 2015;133:286–95.
[321] Jiang W, Li L, Zhang D, Huang S, Jing Z, Wu Y, et al. Incorporation of aligned PCL-PEG nanofibers into porous chitosan scaffolds improved the orientation of collagen fibers in regenerated periodontium. Acta Biomater 2015;25:240–52.
[322] Liu S, Qin MJ, Hu CM, Wu F, Cui WG, Jin T, et al. Tendon healing and anti-adhesion properties of electrospun fibrous membranes containing bFGF loaded nanoparticles. Biomaterials 2013;34:4690–701.
[323] Xie JW, MacEwan MR, Ray WZ, Liu WY, Siewe DY, Xia YN. Radially aligned, electrospun nanofibers as dural substitutes for wound closure and tissue regeneration applications. ACS Nano 2010;4:5027–36.
[324] Xue JX, Feng B, Zheng R, Lu Y, Zhou GD, Liu W, et al. Engineering ear-shaped cartilage using electrospun fibrous membranes of gelatin/polycaprolactone. Biomaterials 2013;34:2624–31.
[325] Liu ZP, Yu N, Holz FG, Yang F, Stanzel BV. Enhancement of retinal pigment epithelial culture characteristics and subretinal space tolerance of scaffolds with 200 nm fiber topography. Biomaterials 2014;35:2837–50.
[326] Jungebluth P, Haag JC, Sjöqvist S, Gustafsson Y, Rodríguez AB, Del Gaudio C, et al. Tracheal tissue engineering in rats. Nat Protoc 2014;9:2164–79.
[327] Wang K, Wang X, Han CS, Hou WD, Wang JY, Chen LY, et al. From micro to macro: the hierarchical design in a micropatterned scaffold for cell assembling and transplantation. Adv Mater 2017;29(1604600):1–7.
[328] Chen Z, Chen ZF, Zhang AL, Hu JM, Wang XM, Yang ZG. Electrospun nanofibers for cancer diagnosis and therapy. Biomater Sci 2016;4:922–32.
[329] Zhang NG, Deng YL, Tai QD, Cheng B, Zhao LB, Shen QL, et al. Electrospun TiO2 nanofiber-based cell capture assay for detecting circulating tumor cells from colorectal and gastric cancer patients. Adv Mater 2012;24:2756–60.
[330] Ma L, Yang G, Wang N, Zhang PC, Guo FY, Meng JX, et al. Trap effect of three-dimensional fibers network for high efficient cancer-cell capture. Adv Healthc Mater 2015;4:838–43.
[331] Zhao LB, Lu YT, Li FQ, Wu K, Hou S, Yu JH, et al. High-purity prostate circulating tumor cell isolation by a polymer nanofiber-embedded microchip for whole exome sequencing. Adv Mater 2013;25:2897–902.
[332] Hou S, Zhao L, Shen Q, Yu J, Ng C, Kong X, et al. Polymer nanofiber-embedded microchips for detection, isolation, and molecular analysis of single circulating melanoma cells. Angew Chem Int Ed 2013;52:3379–83.
[333] Xu GW, Tan YL, Xu TG, Yin D, Wang MY, Shen MW, et al. Hyaluronic acid-functionalized electrospun PLGA nanofibers embedded in a microfluidic chip for cancer cell capture and culture. Biomater Sci 2017;5:752–61.
[334] Wang XY, Wang XB, Wang XN, Chen FT, Zhu KH, Xu Q, et al. Novel electrochemical biosensor based on functional composite nanofibers for sensitive detection of p53 tumor suppressor gene. Anal Chim Acta 2013;765:63–9.
[335] Wang XY, Shu GF, Gao CC, Yang Y, Xu Q, Tang M. Electrochemical biosensor based on functional composite nanofibers for detection of K-ras gene via multiple signal amplification strategy. Anal Biochem 2014;466:51–8.
[336] Reinholt SJ, Sonnenfeldt A, Naik A, Frey MW, Baeumner AJ. Developing new materials for paper-based diagnostics using electrospun nanofibers. Anal Bioanal Chem 2014;406:3297–304.
[337] Choi S, Lee I, Jang B, Youn D, Ryu W, Park CO, et al. Selective diagnosis of diabetes using pt-functionalized WO3 hemitube networks as a sensing layer of acetone in exhaled breath. Anal Chem 2013;85:1792–6.
[338] Choi SJ, Jang BH, Lee SJ, Min BK, Rothschild A, Kim ID. Selective detection of acetone and hydrogen sulfide for the diagnosis of diabetes and halitosis using SnO2 nanofibers functionalized with reduced graphene oxide nanosheets. ACS Appl Mater Interfaces 2014;6:2588–97.
[339] Lee SJ, Tatavarty R, Gu MB. Electrospun polystyrene-poly(styrene-co-maleic anhydride) nanofiber as a new aptasensor platform. Biosens Bioelectron 2012;38:302–7.
[340] Thoma CR, Zimmermann M, Agarkova I, Kelm JM, Krek W. 3D cell culture systems modeling tumor growth determinants in cancer target discovery. Adv Drug Deliv Rev 2014;69–70:29–41.
[341] Rijal G, Li W. 3D scaffolds in breast cancer research. Biomaterials 2016;81:135–56.
[342] Liu Z, Vunjak-Novakovic G. Modeling tumor microenvironments using custom-designed biomaterial scaffolds. Curr Opin Chem Eng 2016;11:94–105.
[343] Hartman O, Zhang C, Adams EL, Farach-Carson MC, Petrelli NJ, Chase BD, et al. Biofunctionalization of electrospun PCL-based scaffolds with perlecan domain IV peptide to create a 3-D pharmacokinetic cancer model. Biomaterials 2010;31:5700–18.
[344] Fischer SN, Johnson JK, Baran CP, Newland CA, Marsh CB, Lannutti JJ. Organ-derived coatings on electrospun nanofibers as ex vivo microenvironments. Biomaterials 2011;32:538–46.
[345] Santoro M, Lamhamedi-Cherradi S, Menegaz BA, Ludwig JA, Mikos AG. Flow perfusion effects on three-dimensional culture and drug sensitivity of Ewing sarcoma. Proc Natl Acad Sci USA 2015;112:10304–9.
[346] Agudelo-Garcia PA, De Jesus JK, Williams SP, Nowicki MO, Chiocca EA, Liyanarachchi S, et al. Glioma cell migration on three-dimensional nanofiber scaffolds is regulated by substrate topography and abolished by inhibition of STAT3 signaling. Neoplasia 2011;13:822–31.
[347] Grodecki J, Short AR, Winter JO, Rao SS, Winter JO, Otero JJ, et al. Glioma-astrocyte interactions on white matter tract-mimetic aligned electrospun nanofibers. Biotechnol Prog 2015;31:1406–15.
[348] Rao SS, Nelson MT, Xue R, DeJesus JK, Viapiano MS, Lannutti JJ, et al. Mimicking white matter tract topography using core–shell electrospun nanofibers to examine migration of malignant brain tumors. Biomaterials 2013;34:5181–90.
[349] Sharma P, Sheets K, Elankumaran S, Nain AS. The mechanistic influence of aligned nanofibers on cell shape, migration and blebbing dynamics of glioma cells. Integr Biol 2013;5:1036–44.
[350] Nelson MT, Short A, Cole SL, Gross AC, Winter J, Eubank TD, et al. Preferential, enhanced breast cancer cell migration on biomimetic electrospun nanofiber 'cell highways'. BMC Cancer 2014;14(825):1–16.
[351] Jain A, Betancur M, Patel GD, Valmikinathan CM, Mukhatyar VJ, Vakharia A, et al. Guiding intracortical brain tumour cells to an extracortical cytotoxic hydrogel using aligned polymeric nanofibres. Nat Mater 2014;13:308–16.
[352] Bhardwaj N, Kundu SC. Electrospinning A fascinating fiber fabrication technique. Biotechnol Adv 2010;28:325–47.
[353] Ye P, Xu Z, Che AF, Wu J, Seta P. Chitosan-tethered poly(acrylonitrile-maleic acid) hollow fiber membrane for lipase immobilization. Biomaterials 2005;26:6394–403.
[354] Selvam AK, Nallathambi G. Polyacrylonitrile/silver nanoparticle electrospun nanocomposite matrix for bacterial filtration. Fiber Polym 2015;16:1327–35.
[355] Guo SS, Ke QF, Wang H, Jin XY, Li Y. Poly(butylene terephthalate) electrospun/melt-blown composite mats for white blood cell filtration. J Appl Polym Sci 2013;128:3652–9.
[356] Xu J, Liu C, Hsu P, Liu K, Zhang R, Liu Y, et al. Roll-to-roll transfer of electrospun nanofiber film for high-efficiency transparent air filter. Nano Lett 2016;16:1270–5.
[357] Tong HW, Kwok SKC, Kwok HC. Protective masks with coating comprising different electrospun fibers interweaved with each other, formulations forming the same, and method of producing thereof. US 14/964593 2015.
[358] Cheng J, Jun Y, Qin JH, Lee SH. Electrospinning versus microfluidic spinning of functional fibers for biomedical applications. Biomaterials 2017;114:121–43.
[359] Duque Sánchez L, Brack N, Postma A, Pigram PJ, Meagher L. Surface modification of electrospun fibres for biomedical applications: a focus on radical polymerization methods. Biomaterials 2016;106:24–45.
[360] Jirsak O, Petrik S. Recent advances in nanofibre technology: needleless electrospinning. Int J Nanotechnol 2012;9:836–45.
[361] Brown TD, Dalton PD, Hutmacher DW. Melt electrospinning today: an opportune time for an emerging polymer process. Prog Polym Sci 2016;56:116–66.